Review

Surface Functionalization of Nanocarriers with Anti-EGFR Ligands for Cancer Active Targeting

Alessandra Spada and Sandrine Gerber-Lemaire *

Group for Functionalized Biomaterials, Institute of Chemical Sciences and Engineering, Ecole Polytechnique Fédérale de Lausanne, 1015 Lausanne, Switzerland; alessandra.spada@epfl.ch
* Correspondence: sandrine.gerber@epfl.ch

Abstract: Active cancer targeting consists of the selective recognition of overexpressed biomarkers on cancer cell surfaces or within the tumor microenvironment, enabled by ligands conjugated to drug carriers. Nanoparticle (NP)-based systems are highly relevant for such an approach due to their large surface area which is amenable to a variety of chemical modifications. Over the past decades, several studies have debated the efficiency of passive targeting, highlighting active targeting as a more specific and selective approach. The choice of conjugation chemistry for attaching ligands to nanocarriers is critical to ensure a stable and robust system. Among the panel of cancer biomarkers, the epidermal growth factor receptor (EGFR) stands as one of the most frequently overexpressed receptors in different cancer types. The design and development of nanocarriers with surface-bound anti-EGFR ligands are vital for targeted therapy, relying on their facilitated capture by EGFR-overexpressing tumor cells and enabling receptor-mediated endocytosis to improve drug accumulation within the tumor microenvironment. In this review, we examine several examples of the most recent and significant anti-EGFR nanocarriers and explore the various conjugation strategies for NP functionalization with anti-EGFR biomolecules and small molecular ligands. In addition, we also describe some of the most common characterization techniques to confirm and analyze the conjugation patterns.

Keywords: active targeting; EGFR; biomolecules; targeting ligands; targeted therapy; nanomedicine; cancer targeting

1. Introduction

Cancer mortality is reduced when cases are detected and treated at an early stage of development. However, even though much progress has been made in the management of patients, there are still issues that need to be addressed to improve cancer early diagnosis and provide innovative therapeutic modalities [1]. Conventional imaging techniques and cancer treatments lack sensitivity for early detection and show poor specificity, causing adverse side effects. In order to overcome some of their limitations, nanomedicine has emerged as a promising alternative in the past decades [2].

Nanoparticles (NPs) have attracted interest due to their unique features. They are very small colloidal systems, with sizes in the nanometer range, whose morphology and properties depend on their compositions. NPs utilized for therapeutic and diagnostic applications can be classified into several categories, including polymeric, inorganic and lipid-based NPs. Polymeric NPs encompass systems such as polymersomes [3], dendrimers [4] and nanomicelles [5]. Inorganic NPs include mesoporous silica NPs [6], iron oxide NPs [7], gold NPs [8] and quantum dots [9]. Lipid-based NPs primarily consist of liposomes [10] and lipid NPs

(LNPs) [11]. Polymeric NPs typically exhibit mean diameters ranging from 100 to 300 nm. They offer advantages such as precise control over particle characteristics, easy surface functionalization, controlled release capabilities, and protection of drug and payloads from environmental degradation. However, they are prone to aggregation and may induce toxicity in certain cases [12]. Inorganic NPs present high variability in size, structure and geometry [13], with specific electrical, magnetic and optical properties, making them highly suitable for theranostic applications [14]. Nonetheless, they can exhibit toxicity if not coated with biocompatible layers [15]. Lipid-based NPs provide benefits such as enhanced solubility and bioavailability of hydrophobic payloads, controlled release, and biocompatibility [11,16]. Conversely, their drug loading efficiency is lower compared to other types of NPs [17]. NPs are characterized by a high surface-to-volume ratio that generally allows high loading of therapeutic agents and/or imaging probes [18]. To be used in biomedical applications, nanomaterials need to be biocompatible, well characterized and stable in vivo [19]. As compared to traditional chemotherapeutic agents, NPs can encapsulate hydrophobic molecules, increasing their solubility, biocompatibility and retention time at tumor sites [20]. They are capable of co-delivering drug resistance inhibitors while enabling controlled and sustained drug release [21], and circumvent the drug efflux mechanisms, leading to decreased multidrug resistance (MDR) [22]. The surface characteristics of NPs determine their bioavailability and half-life [23]. For example, one of the main obstacles of NP delivery is the opsonization (coating of the NPs by non-specific proteins that leads to immune recognition), sequestration by the reticuloendothelial system (RES) and clearance by the immune system [24]. Smaller NPs (<200 nm) have been reported to escape the RES more efficiently [25–28]. In addition, NPs coated with hydrophilic materials, such as polyethylene glycol (PEG), have been shown to reduce opsonization, thus increasing their circulation time and improving their penetration and accumulation in tumors [28,29]. To improve the targeting of loaded therapeutic agents, enhance efficiency and minimize adverse side effects, dynamically responsive nano-drug delivery systems (DRNSs) have been explored as advanced tools capable of directional drug release with self-regulation and self-feedback mechanisms in response to specific stimuli [30].

The ability of NPs to target malignant cells and tumor tissues results from either passive or active targeting, or a combination of both [31]. The main driving force for passive targeting is the so-called enhanced permeation and retention effect (EPR) [32,33], caused by the leaky tumor vasculature, first reported by Matsumura and Maeda in 1986 [34]. The tumor vascularization presents large pores in the vascular wall and the NPs tend to leak from the blood vessels and accumulate within tumor tissues. At the same time, poor tumor lymphatic drainage increases the retention of the NPs [33]. In the EPR effect, these unique anatomical-pathophysiological features of tumor vasculature allow the transport and internalization of NPs into tumor tissues [35]. Several studies demonstrated the relation between the EPR effect and the size of the NPs: smaller NPs have shown better penetrability into tumor tissues [36,37].

However, there are several limitations with regard to passive targeting, including non-specific NP distribution, non-universal existence of the EPR effect and different permeability of blood vessels across various tumors. In the past decades, the efficiency of passive targeting has been debated, since the model was proved to be oversimplified [38], accounting for only 0.7% of the uptake by tumor tissues, due to non-specific uptake by healthy organs [39,40].

Active targeting is intended to increase the concentration of nanocarriers and their bioavailability at tumor sites [41]. This strategy relies on the specific recognition of biomarkers which are homogeneously overexpressed by cancer cells or cancer associated cells [42]. It mostly addresses tumor cells, but can also be directed toward neighboring angiogenic

endothelial cells, or toward the mildly acidic tumor microenvironment. Therefore, as opposed to passive targeting, active targeting requires the grafting of biomarker-specific ligands to the surface of the nanocarriers, thus increasing the selective recognition of tumor cells (Figure 1) [43].
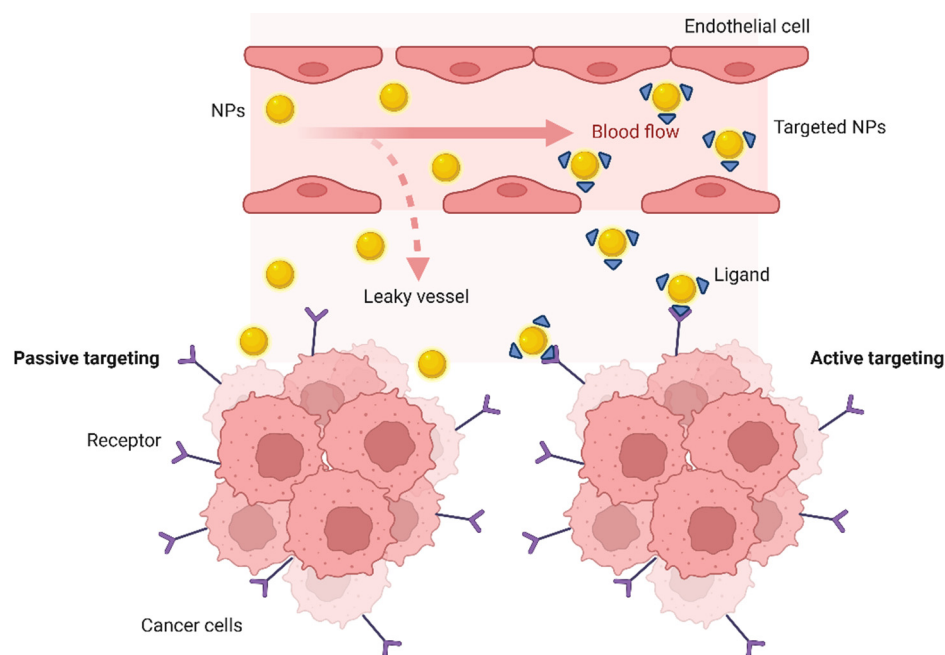

Figure 1. Schematic representation of active targeting vs. passive targeting of cancer cells by nano-delivery systems. In passive targeting, the size and surface properties of nanocarriers facilitate their accumulation within tumor tissues through the EPR effect, resulting from the leaky vasculature of tumors. Conversely, active targeting involves the conjugation of specific ligands to the NP surface, enabling targeted delivery to cancer cells by binding to overexpressed receptors or markers on their surface. Created with BioRender.com.

Several receptors are overexpressed or specifically expressed in different types of cancer, such as folate receptors, integrins, transferrin receptors, G protein-coupled receptors, sigma receptors, fibroblast growth factors and epidermal growth factor receptor (EGFR) [44]. In particular, EGFR is overexpressed in several types of cancer, including non-small cell lung, bladder, gastric, kidney, ovarian, colorectal, breast, pancreatic cancers and squamous-cell carcinoma of head and neck cancers [45–47]. For this reason, nano delivery systems decorated with EGFR-targeting ligands have gained increasing attention as potential tools to achieve enhanced specificity through receptor-mediated endocytosis. In addition, there has been a number of significant studies highlighting the benefits of the combination between EGFR targeting and other treatment modalities, including immunotherapy [48,49]. For example, a bispecific antibody (BsAb) that simultaneously targets both EGFR and programmed cell death protein 1 (PD1), a protein that is involved in immune checkpoint blockade, has been investigated as a novel and promising strategy to effectively treat cancers [50,51]. In addition to the EGFR targeting, the BsAb exhibits a potent antibody-dependent cellular cytotoxicity (ADCC) activity and activates antitumor immunity through blockade of PD1/PD-L1 interaction. Moreover, it was demonstrated that the BsAb is more potent than the individual monoclonal antibodies (mAbs) and their combination at targeting and inhibiting tumor growth. Liposomal nanohybrid cerasomes decorated with anti-EGFR mAb and PD-L1 mAb were explored for targeted tumor imaging and photodynamic therapy (PDT) [52]. The experiments showed that PDT with the EGFR-targeted system combined with PD-L1 mAb treatment strategy was more effective against

tumors in comparison with the simultaneous non-targeted delivery of PDT with liposomal nanohybrid cerasomes and PD-L1 mAb treatment. In another study, simultaneous targeting of EGFR and CD73, an emerging checkpoint for cancer immunotherapy, was investigated as a new therapeutic approach for breast cancer [53]. The combined treatment showed a significant effect in inhibiting the growth and spread of the tumors.

The choice of the conjugation strategy for the grafting of ligands to nanocarriers is a key parameter to ensure their stability and reliability, and is dictated by diverse factors, such as the physicochemical parameters of the nanocarriers (including size, composition, surface charge), the type and composition of the selected ligands. Covalent conjugation refers to the use of direct or spaced covalent bonds, while non-covalent immobilization relies on surface adsorption through electrostatic interactions, hydrophobic interactions, hydrogen bonding and similar types of weaker forces (Figure 2) [54]. Covalent bonds are more stable and resistant, but they often require the introduction of chemical modifications on both the surface of the nanocarriers and ligands. Thus, NPs need to be precisely engineered for the presentation of surface functional groups (thiols, carboxylic acids, amines) that can be exploited as chemical handles for further post-functionalization. While being easy to produce, non-covalent systems are often reversible and suffer from low stability in physiological environments [55].
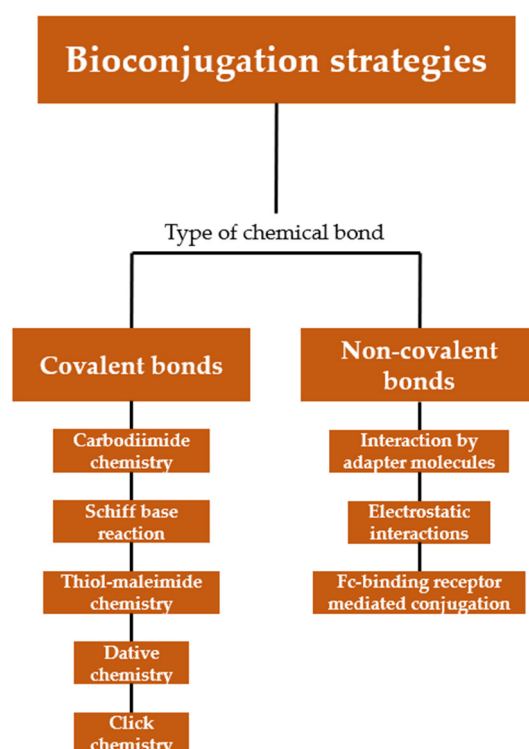

Figure 2. Classification of bioconjugation strategies based on covalent and non-covalent strategies.

Previous reviews described the large number of biological ligands which were identified for facilitating active targeting [31,41,43,56–58]. However, only few reports focused on the conjugation chemistry and the means of characterization of the functionalized NPs.

We herein highlight the most recent and significant anti-EGFR functionalized nanocarriers with a focus on the last five years of the literature. Part of the review also presents the characterization techniques that are commonly used to assess the presence of ligands on the NP surface.

2. Epidermal Growth Factor Receptor

EGFR, also known as ErbB1 or HER1, is a 170 kDa glycoprotein composed of 1186 amino acid residues, and was discovered by Nobel Prize-winning Cohen and colleagues in 1978 [59]. It belongs to the human epidermal growth factor receptor (HER) family of four closely related receptor tyrosine kinases (RTKs). The other components of the family, ubiquitously expressed in epithelial, cardiac, neuronal and mesenchymal cells, are HER2 (ErbB2), HER (ErbB3), and HER4 (ErbB4). The HER family plays vital roles in the modulation of processes in healthy cells, including cell proliferation, motility, survival and differentiation [60], ensuring that the kinetics of these phenomena correspond to the tissues' requirement for homeostasis. It was shown that any dysregulation of these processes leads to cancer development, making therefore EGFR one of the main anticancer targets [61].

As all other members of the HER family, EGFR is a transmembrane protein, consisting of an extracellular domain (ECD), where the ligand binding site resides, a transmembrane domain (TMD), and an intracellular tyrosine kinase domain, which houses the catalytic activity of the receptor [62]. The ECD of EGFR is composed of two homologous domains, DI and DIII, involved in the ligand binding, and DII and DIV, that form disulfide bonds [63]. In an inactive state, the ECD has a tethered configuration, presenting intra-molecular bondages blocking the dimerization arm. Upon ligand binding to the ECD, the cytoplasmatic domain undergoes dimerization and phosphorylation, with the kinase activation being allowed by the configurational changes [64]. The EGFR activation leads to a cascade of subsequent downstream signal transduction pathways, resulting in the mitogenic and anti-apoptotic signal cascades [65]. Among those, the most important are the phosphatidylinositol-3-kinase (PI3K) signaling network, responsible for tumor growth, the RAS/MAPK pathway and the JAK2/STAT pathway (Figure 3) [66].
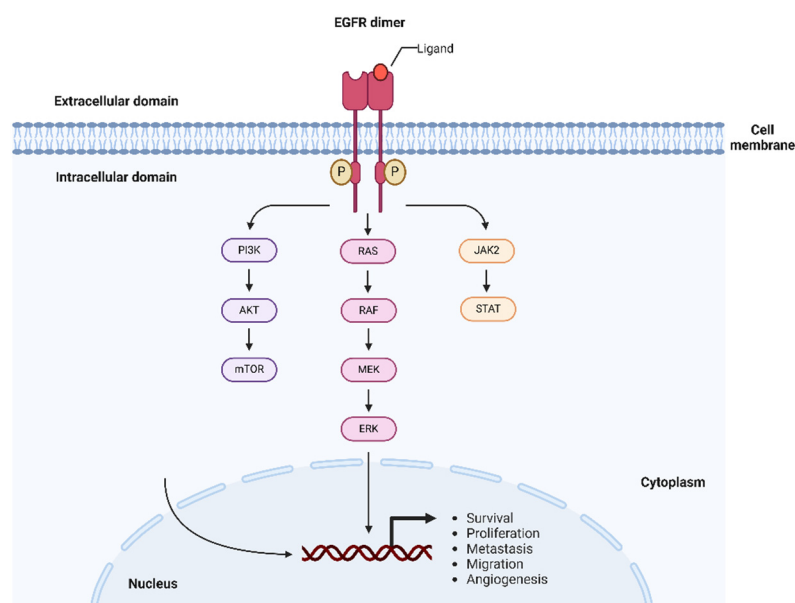

Figure 3. An overview of the EGFR signaling pathway. Upon binding of specific ligands, EGFR undergoes dimerization and phosphorylation, leading to the activation of downstream signaling cascades and resulting in enhanced tumor growth, invasion and metastasis. Some of the main activated pathways include PI3K/AKT, RAS/MAPK, and JAK/STAT, which cross-regulate and interact, contributing to cell proliferation, migration and survival. Created with BioRender.com.

It was established that the EGFR pathway can be activated by several mechanisms, including receptor mutation in specific domains, overexpression, inefficient inactivation or augmented ligand production [67]. Some of these processes, such as genetic alterations

and increased ligand production, occur simultaneously due to autocrine or paracrine loops [68,69]. Furthermore, EGFR genetic mutations lead to abnormal EGFR trafficking, contributing to increased signaling and tumor growth. In normal cells, the number of EGFR is estimated to be around 40,000–100,000 receptors per cell [70], whereas in cancer cells this number rises to more than 10^6 receptors per cell [71]. Several studies established the interconnection between EGFR phosphorylation and carcinogenic events, such as smoke inhalation, exposure to ultraviolet radiation and bacterial infections. Consequently, malignant tumors are more likely to develop in tissues where the receptor is found [65]. EGFR overexpression was observed in a variety of human solid tumors, such as kidney, pancreas, breast, ovary, bladder, colorectal, head and neck and lung cancers [72]. The EGFR levels can be assessed through receptor quantification at the DNA, RNA or protein level, or through investigation of the degree of signaling by studying the activation of the receptor or the downstream markers [72]. For these purposes, different techniques are used, such as DNA analysis, northern blotting or quantitative reverse transcription polymerase chain reaction (rtPCR), immunohistochemistry (IHC), western blot analysis and enzyme immunoassay.

Due to its central roles in a wide range of key cellular processes, EGFR was selected in many targeting and inhibition strategies [73]. The most clinically advanced EGFR inhibitors include mAbs blocking the EGFR's ECD, and small-molecular inhibitors of the intracellular tyrosine kinase domain [74]. To date, fourteen EGFR-targeting agents have been approved for cancer treatments. The Food and Drug Administration agency (FDA) approved several anti-EGFR mAbs, among which cetuximab (2004), panitumumab (2006), necitumumab (2015), amivantamab (2021) (The Antibody Society. Therapeutic monoclonal antibodies approved or in review in the EU or US; www.antibodysociety.org/resources/approved-antibodies; accessed on 25 November 2024). Many other candidates are undergoing clinical studies, such as nimotuzumab, ZZ06, JMT101, SCT200, HLX07 (clinicaltrials.gov), mAb806 [75]. By binding to the ECD and preventing the dimerization processes, these agents are designed to selectively target and kill tumor cells. Tyrosine kinase inhibitors (TKIs), such as erlotinib, gefitinib, lapatinib and icotinib (first-generation), afatinib, neratinibs and dacomitinib (second-generation), or osimertinib (third-generation), target the intracellular tyrosine kinase domain, competing with ATP for binding, and blocking the proliferation signaling [76]. Among the TKIs, gefitinib, erlotinib, lapatinib, afatinib, brigatinib, osimertinib, dacomitinib, vandetanib have received FDA approval for clinical use in cancer therapy [77]. However, the clinical application of EGFR-targeting ligands remains hindered by substantial challenges. A major limitation is the development of resistance to treatment, which impedes the optimal efficacy of EGFR inhibitors. While some patients develop de novo resistance to EGFR inhibition and fail to respond to therapy, others who initially responded to therapy eventually develop acquired resistance [78]. Tumor cells can develop resistance to EGFR inhibitors through various mechanisms, including the acquisition of secondary mutations in the EGFR gene. Additionally, they may activate alternative signaling pathways that circumvent EGFR dependency to sustain cell proliferation or upregulate other receptor tyrosine kinases to compensate for EGFR inhibition [79]. Intratumoral heterogeneity is another well-recognized contributor to resistance against targeted therapies and is considered a major factor in treatment failure [80]. Heterogeneity of the EGFR protein expression has been observed in clinical samples from multiple cancer types [81–84]. Furthermore, the clinical use of EGFR inhibitors is often limited by adverse side effects, such as skin rashes, diarrhea and hepatotoxicity [85]. Future directions and emerging strategies to bridge the gap between EGFR-targeted therapy research and its clinical translation include the development of next-generation inhibitors, designed to overcome resistance mutations, the implementation of combination therapies, that address

both genetic and non-genetic mechanisms of resistance, and the identification of predictive biomarkers, essential for guiding patient selection, optimizing treatment strategies and improving the overall efficacy of EGFR-targeted therapy [86,87].

In addition to its relevance as a therapeutic target, EGFR stands among the most targeted receptors for cancer active targeting [58]. This review focuses on anti-EGFR targeting ligands-functionalized NPs, which are therefore specific to EGFR-overexpressing tumors.

3. EGFR-Targeting Ligands

This section focuses on the description of different nanocarriers functionalized with the main anti-EGFR ligands, such as peptides, proteins, polysaccharides, nucleic acids and small molecules. Each family of anti-EGFR targeting agents is described, highlighting their performance and limitations.

3.1. Epidermal Growth Factor

Epidermal growth factor (EGF) is a small protein, constituted by only 53 amino acids with a molecular weight of approximately 6 kDa. Present in different mammalian species, it was first isolated from parotid gland of male mice and subsequently, human EGF (hEGF) was purified from human urine [88]. hEGF is known as "urogastrone" for its ability to inhibit gastric acid secretion in humans [89,90]. The protein structure presents six cysteine residues able to form three internal disulfide bonds, that can be used for further NP conjugation [91]. The EGF protein possesses a very high affinity for EGFR, with a dissociation constant (Kd) of 2 nM. In 1986, Cohen et al. established that the protein directly stimulated the proliferation of epidermal cells, and that the stimulatory action did not depend on other systemic or hormonal influences [92]. In addition, hEGF has various effects on cell regeneration, including migration of keratinocytes, formation of granulation tissues and stimulation of fibroblast motility, which play major roles in wound healing processes [93,94]. EGF exerts its effects in the target cells by binding to the plasma membrane located EGFR [95].

The advantages of using the EGF protein as targeting agent include: (i) smaller sizes compared to other targeting ligands such as full antibodies (Abs, 6 kDa vs. 150 kDa, respectively); (ii) lower cytotoxicity being one of the native ligands of EGFR [96]; (iii) ease of conjugation to nanocarriers thanks to the presence of disulfide bonds and hydrophobic regions in its structure [97]; (iv) stability at physiological conditions and neutral pH due to an isoelectric point (pI) of around 4.5, making it negatively charged at neutral pHs [98]. On the other hand, EGF production is expensive, less convenient to obtain from human resources, and can cause antigenicity issues when obtained from murine sources.

Zhang et al. demonstrated the importance of the ligand orientation when conjugating EGF to the surface of NPs, in order to minimize interference in the EGF-EGFR interaction [99]. EGF was conjugated to NPs' surface through covalent functionalization via amide bond using the primary amino groups of EGF. However, the presence of three amino groups (N-terminus, Lys48 and Lys28) in the EGF structure did not allow for site-directed chemical coupling. Furthermore, Lys48 and Lys28 are located close to the region where the protein interacts with its receptor. The conjugation was therefore limited to the N-terminus of EGF, by producing three lysine-free EGF, modifying lysine (K) with arginine (R) or serine (S) using gene recombination technology. Among the tested formulations (RS-, SR-EGF-GNPs conjugates), the second one showed enhanced biological activities and growth inhibition in EGFR-overexpressing skin cancer cell line A431. This effect was demonstrated to be due not only to the orientation control, but also to increased binding activities of this mutant EGF to EGFR.

Castilho et al. developed a treatment modality for triple-negative breast cancer, using bifunctional theranostic nanoprobes (BN) for PDT on human breast carcinoma and normal human cells [100]. BNs were modified with EGF targeting ligand and chlorin e6 (Ce6). Conjugation to AuNPs led to 10-fold increased efficacy of the nanoplatform compared with free Ce6. The conjugates induced triple negative breast cancer (TNBC) cell death by increasing reactive oxygen species (ROS) levels, while they did not impact normal cells from human breast epithelium.

Salama et al. engineered EGF-ligated polyethylene glycol-coated TiO_2 NPs (EGF-TiO_2 PEG NPs) to overcome the low cellular uptake and cell-proliferating ability of TiO_2 NPs for PDT and photodynamic diagnosis (PDD) [101]. On A431 epidermal cancer cell line, the binding of EGF-TiO_2 PEG NPs to EGFR induced receptor-mediated endocytosis, leading to increased NP cellular uptake, decreased localization of EGFR on the cell surface, and decreased signaling for cell proliferation compared with unconjugated NPs (Figure 4).
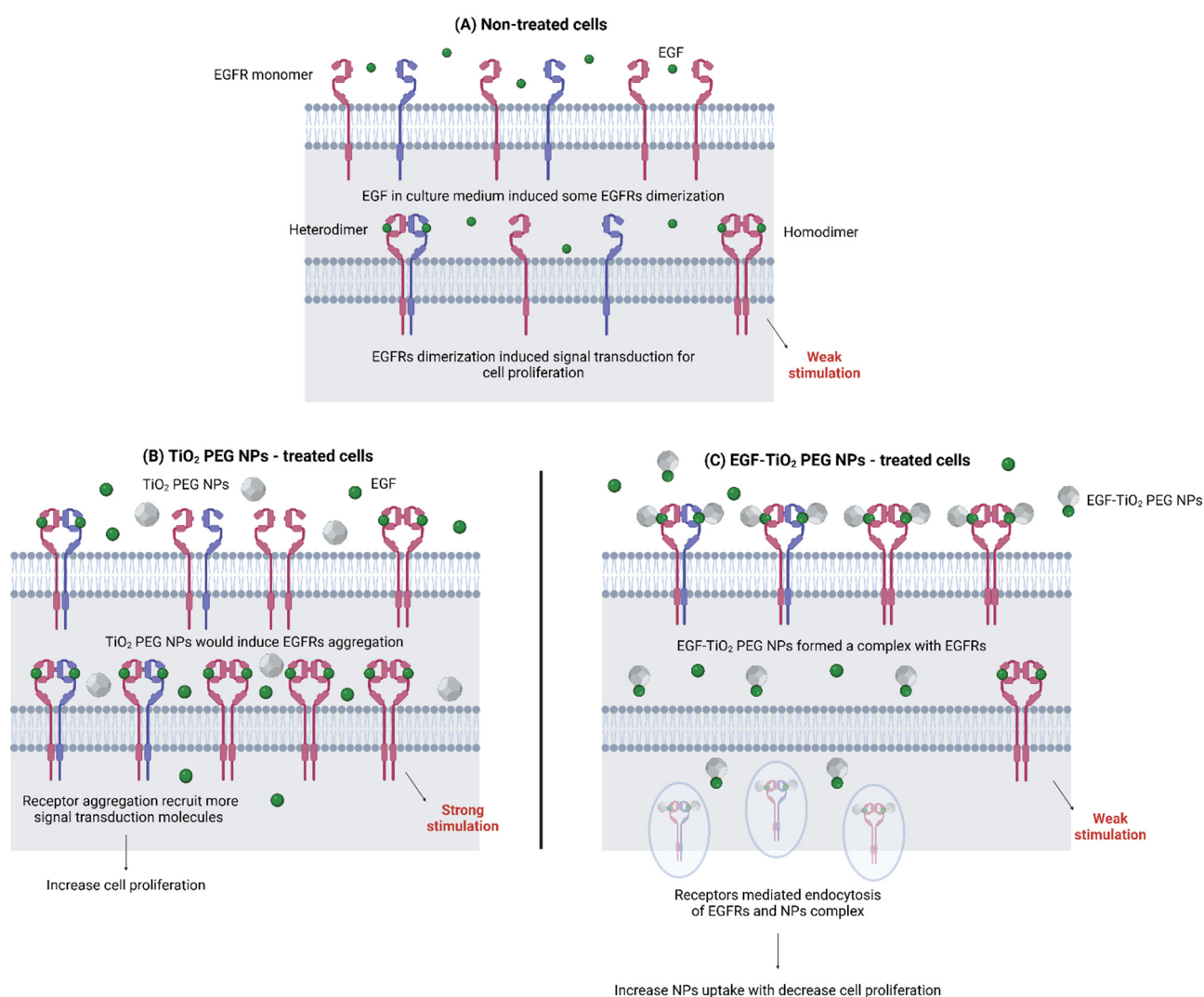

Figure 4. Molecular mechanism for the effect of EGF conjugation on TiO_2 PEG NPs uptake levels and the cell proliferation effect via interaction with EGFRs proposed in [101]. (**A**) Non-treated A431 cells; (**B**) TiO_2 PEG NPs-treated A431 cells; (**C**) EGF-TiO_2 PEG NPs-treated cells. Created with BioRender.com.

Another example of EGF-functionalized AuNPs for photothermal therapy (PTT) consisted of multifunctional hybrid nanocarriers combined with near-infrared (NIR) laser irradiation for the treatment of melanoma [102]. AuNPs were coated with hyaluronic

(HA) and oleic acid (OA) and functionalized with EGF to improve the in vivo efficiency in hairless immunocompromised mice. These cells overexpress multiple receptors, including CD44 and EGFR, which were targeted by HA and EGF, respectively. In vivo experiments with EGF-conjugated HAOA-coated GNPs and NIR laser using different exposure times showed a significant reduction in the volume of melanoma tumor 24 h post-treatment (up to 81% reduction), whereas the control group did not show any significant tumor volume change. Moreover, the nanocarriers did not affect the normal function of organs and did not induce any inflammatory systemic response in the 24 h period post-administration.

Susnik et al. studied the effect of EGF conjugation on cell signaling, modulation of endocytic activity, and the uptake of different SiO_2 NPs (59 and 422 nm) and PEGylated AuNPs in A549 lung epithelial carcinoma cells [103]. Cell stimulation with EGF facilitated the uptake of 59 nm fluorescently labelled SiO_2-BDP FL NPs, in particular under simultaneous and sequential co-exposure scenario. In contrast, reduced uptake of larger NPs was observed, probably due to the differences in F-actin dynamics during endocytosis depending on the NP sizes. In addition, the cellular uptake of EGF-conjugated PEGylated AuNPs carrying antisense oligonucleotides (ASO), complementary to the *c-MYC* transcript (Au@PEG@c-myc), was enhanced in A549 cells and the *c-MYC* silencing efficiency was demonstrated.

Other relevant studies disclosed the conjugation of EGF to AuNPs [104–106], liposomes [107], polymeric NPs [108–111], and lipid-polymer hybrid NPs [112] for anticancer therapy.

3.2. GE11 Peptide

Peptides have increasingly been investigated as targeting agents for cancer active targeting. They are characterized by low immunogenic potential and high penetration capacity into solid tumors. Furthermore, peptides can be easily synthesized, in particular through microwave-assisted solid-phase automated synthesis [113], and conjugated to nanocarriers through multiple functionalization techniques [114]. Multiple EGFR-binding peptides were selected from phage display peptide libraries, such as the dodecapeptide GE11 (YHWYGYTPQNVI). Even if characterized by a lower affinity for EGFR compared with EGF by an order of magnitude (Kd of 22 nM vs. Kd of 2 nM, respectively), higher surface densities of peptide can be achieved, leading to enhanced targeting efficiency [115]. Furthermore, GE11 is exempt from mitogen activity and presents a significantly reduced size compared with EGF or mAbs. Previous studies showed a high potential of GE11 to facilitate NP endocytosis, probably due to an alternative EGFR-dependent actin-driven pathway [115].

Guo et al. developed an EGFR-targeted multifunctional micellar nanoplatform by encapsulating celecoxib and doxorubicin (DOX) into polymeric micelles based on the conjugate of GE11-PEG-b-poly(trimethylene carbonate) to suppress metastatic breast cancer proliferation and metastasis [116]. GE11 conjugation resulted in enhanced tumor-targeted accumulation and cellular uptake. Compared with negative controls (micelles without GE11 or delivering only DOX), systemic administration of the targeted platform into mice bearing subcutaneous 4T1 tumor models led to higher tumor growth suppression and decreased lung metastasis.

Alternatively, ^{64}Cu-labeled GE11-decorated polymeric micellar NPs (PMNPs) were formed through self-assembly of poly(ethylene oxide) (PEO)-*block*-poly(ester)s, based on PEO-*b*-poly(α-benzyl carboxylate-ε-caprolactone) (PEO-b-PBCL) [117]. In comparison with non-targeted PMNPs, GE11-conjugated nanocarriers showed a significantly higher internalization into EGFR-overexpressing colorectal cancer cells HCT116 (Figure 5) and

higher tumor uptake 24 h post-injection. In vivo PET data revealed a 28% increase in tumor accumulation and retention of the radiolabeled GE11-decorated NPs.
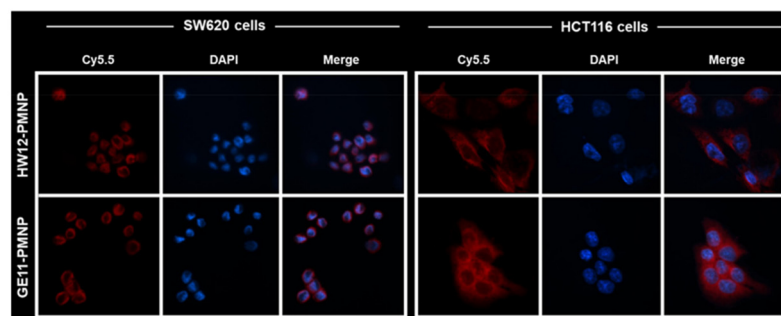

Figure 5. Confocal microscopy images of bare PMNPs and GE11-PMNPs in red (Cy5.5), nucleus in blue (DAPI), and their combination (merged) in SW620 and HCT116 cells. Adapted with permission from [117]. Copyright 2020, American Chemical Society.

A later report focused on GE11-conjugated PMNPs carrying A83B4C63, a novel inhibitor of polynucleotide kinase/phosphatase (PNKP) in colorectal cancer (CRC) [118]. GE11 improved the activity of A83B4C63 in EGFR+ CRC cells in vitro. In vivo, the nanoplatform showed a trend toward increased primary tumor homing in an orthotopic CRC xenograft, even though statistical significance for the accumulation of GE11-modified micelles compared with plain ones was not reached.

Du et al. synthesized salinomycin-loaded GE11-conjugated polymer-lipid hybrid NPs (GE11-NPs-SAL) to target osteosarcoma [119]. The constructs inhibited the migration and proliferation of EGFR-overexpressing U2OS osteosarcoma cells and induced enhanced tumor growth reduction in vivo, compared with non-targeted micelles. GE11-targeted delivery of SAL to breast cancer cells was also achieved with poly-lactic-co-glycolic acid (PLGA)/tocopheryl polyethylene glycol succinate (TPGS) NPs [120]. In vitro flow cytometry assays showed that GE11-SAL NPs were internalized to a higher extent in MCF-7 cells compared with non-targeted SAL NPs. In vivo, GE11-SAL NPs displayed a marked reduction in tumor volume up to 30 days in BALB/C nude mice bearing MCF-7 breast cancer xenografts.

Other studies explored the functionalization of organic nanocarriers, particularly liposomes, with GE11. Tang et al. developed GE11-decorated PEGylated liposomes (GE11-TLs) that exhibited higher retention and uptake in EGFR-overexpressing stromal cells in SMMC-7721 xenograft models [121]. Furthermore, the functionalized nanoplatform reduced the intravasation of liposomes back into blood vessels, enhancing tumor-specific delivery. Zhou et al. developed GE11-installed chimeric polymersomes (GE11-CPs) for EGFR-targeted protein therapy in SMMC-7721 tumor models [122]. Saporin-loaded GE11-CPs (with 10% GE11) showed over 3-fold enhanced uptake in SMMC-7721 cells and significantly increased anticancer potency compared with non-targeted controls. In vivo, biodistribution studies revealed 3-fold higher tumor accumulation of the functionalized nanoplatform.

Additional studies focused on the combination of GE11 targeting and NIR irradiation for targeted therapeutic applications. For example, Huang et al. developed GE11-decorated liposomes encapsulating curcumin and indocyanine green for synergistic cancer therapy (GE11-CUR/ICG-LPs) [123]. In EGFR-overexpressing A549 cells, NIR irradiation triggered hyperthermia for tumor ablation while releasing curcumin to eliminate residual cancer cells. In addition, the system could induce apoptosis by enhancing ROS production and disrupting the cytoskeleton. Lan et al. employed an inorganic carrier, made of galangin (Gal)-loaded mesoporous copper sulfide (CuS) NPs, in contrast to the study described above [124]. The GE11-CuS@Gal nanoplatform showed excellent tumor-targeting ability in

HSC-3 tumor cells. High accumulation increased ROS levels and inhibited the Nrf/OH-1-mediated antioxidant pathway, leading to the inhibition of growth and migration of oral squamous cell carcinoma (OSCC).

Beyond small molecular drugs and proteins, nucleic acid-based therapeutics were also efficiently delivered by GE11-targeted nanocarriers. Supramolecular polymeric NPs assembled through host–guest interactions (cyclodextrin/adamantane) were post-functionalized with GE11 and the pH-sensitive fusogenic peptide GALA for tumor-targeted gene therapy using VEGF shRNA cargos [125]. The systemic delivery of GE11-GALA-conjugated NPs decreased intra-tumoral neovascularization and inhibited A549 tumor growth. Another study highlighted the delivery of mIRNA for gene silencing in T24 cells, based on core–shell mesoporous silica NPs (MSNPs) loaded with miR200c and surface modified with GE11-grafted amino-acid block copolymer to favor endosomal escape [126]. GE11 enhanced the EGFR-mediated uptake and large loaded MSNs (160 nm) exhibited a remarkable gene knockdown efficacy and antitumoral effect. Virus-like particles (VLPs) designed from *Macrobrachium rosenbergii* nodavirus (MrNV), which is a shrimp infectious and non-enveloped virus, were also conjugated to GE11 for the encapsulation of EGFP DNA plasmid [127]. The presence of the targeting peptide allowed for enhanced binding and internalization in EGFR-overexpressing colorectal cancer cells (SW480), through a receptor-specific internalization pathway.

The targeting peptide GE11 was associated with NP-based targeted anticancer therapies in a variety of tumors, including triple-negative breast cancer [128–130], breast cancer [131,132], prostate carcinoma [133], hepatic carcinoma [134,135], pancreatic ductal adenocarcinoma [136,137], lung adenocarcinoma [138–140], colon adenocarcinoma [141,142], epidermoid carcinoma [143], oral squamous cell carcinoma [144] and cervical cancer [135].

3.3. Anti-EGFR Whole Antibodies

Back to the pioneering studies of Hericourt and Richet in 1895 and of Ehrlich in 1913, Abs were already described as "magic bullets" to target cytotoxic compounds to specific regions of the body. Abs, also called immunoglobulins, consist of two heavy and two light chains, which join to form a Y-shaped protein. The two identical heavy and light chains are connected by disulfide bonds [145]. The light chains are made of one variable domain V_L and one constant domain C_L, whereas heavy chains are formed by one variable domain V_H and three to four constant domain C_H. Abs are large proteins of about 10–15 nm in size [146] and a molecular weight of ~150 kDa [147]. Structurally, they are formed by two antigen-binding fragments (Fabs), responsible for the recognition and binding to the target, and a fragment crystallizable region (Fc), in charge of the activation of the immune system and binding to cell receptors. Abs are produced by immune B cells when they come into contact with an antigen. mAbs are artificially produced through genetic engineering to be specific towards any kind of antigenic site. Their very high specificity and availability have made mAbs one of the most used classes of targeting agents for cancer. Representative anti-EGFR mAbs already on the market include cetuximab, panitumumab, nimotuzumab, matuzumab, necitumumab and amivantamab [148]. Besides their targeting abilities, mAbs are also known for inhibiting tumor cell proliferation or angiogenesis by binding specifically to cell surface receptors that are unique or overexpressed by tumor cells, such as EGFR [149]. For the purpose of this review, we will not describe the mechanisms of mAb-mediated cell death, but we will focus on their use as targeting ligands.

Among biological ligands, mAbs have the longest history with respect to targeting specific receptors. Their characteristic three-dimensional shape provides very high affinity for specific substrates. However, due to their dimension, the immobilization of mAbs to NP-based carriers results in significant increases in size and surface patterning, which may

lead to immune responses. Moreover, their correct orientation must be preserved upon conjugation [150], while both random and oriented immobilization routes were reported [151]. Among the possible spatial orientations at NP surfaces, the "end on" (conjugation to Fc) topology is preferred for targeting applications, in order to ensure optimal exposure and accessibility of the Fab which is responsible for the antigen recognition.

The recombinant human/mouse chimeric mAb cetuximab (C225) was the first FDA-approved anti-EGFR mAb, characterized by a molecular weight of 145.8 kDa and a high binding affinity for EGFR (Kd = 0.201 nM). The use of C225 for active cancer targeting of nanotherapies was abundantly reported.

C225 functionalization has been extensively investigated on both organic and inorganic nanocarriers. In the first category, Fang et al. produced C225-modified lipid NPs for chemo-phototherapy of EGFR-overexpressing CRC [152]. The system, consisting of PLGA-lipid-based NPs, demonstrated enhanced pH/NIR-triggered drug release, photothermal response, cellular uptake and ROS generation compared with the non-targeted counterparts. Under NIR irradiation, the system exhibited IC_{50} values of 22.84 ± 1.11 µM at 24 h and 5.01 ± 1.06 µM at 48 h. Juan et al. developed C225-conjugated polylactide (PLA) NPs via polyethyleneimine (PEI) cross-linking (ACNPs) [153]. In vivo, the targeted system exhibited enhanced targeting of EGFR-expressing head and neck tumors in a xenograft model. Furthermore, alpelisib-loaded ACNPs significantly reduced cell viability and induced apoptosis. Duwa et al. conjugated C225 to temozolomide (TMZ)-loaded poly(lactic-co-glycolic acid) (PLGA) NPs (Cmab-TMZ-PLGA-NPs) [154]. In vitro, EGFR-overexpressing U-87MG cells showed higher TMZ uptake compared with SW480 or SK-Mel 28 cells, with the C225-conjugated system outperforming the non-targeted one. A similar polymeric system based on PLGA was exploited to conjugate C225 to docetaxel (DTX)-loaded NPs for the treatment of NSCLC [155]. The targeted NPs exhibited higher uptake in EGFR-overexpressing lung cancer cells A549 and NCI-H23. Furthermore, the targeted platform improved therapeutic efficiency with lower IC_{50} values, and significantly reduced tumor growth and proliferation in lung cancer mouse models. Hosseini et al. developed C225-functionalized poly amido amines (PAMAM) nanocarriers labelled with Lutetium-177 (^{177}Lu) for theranostic applications [156]. In the EGFR-overexpressing SW480 cells, the targeted system showed enhanced uptake and significant anti-tumor effects. In vivo, the targeted nanoplatform exhibited rapid blood clearance and high tumor targeting, with minimal uptake in non-target organs. Yue et al. developed a C225-polymersome-mertansine nanodrug (C-P-DM1) for targeted therapy of EGFR-positive cancers [157]. The targeted system showed significantly higher cellular uptake in EGFR-overexpressing MD-MB-231, SMMC-7721 and A549 cells, with 10.5-, 35.8- and 18.2-fold increases, respectively. Furthermore, C-P-DM1 exhibited the greatest cytotoxicity in MDA-MB-231 and SMMC-7721 cells, with IC_{50} values of 33.8 and 27.1 nM, respectively, significantly lower than P-DM1. In vivo, C-P-Cy5 rapidly accumulated at the tumor site in MDA-MB-231 TNBC-bearing mice, without causing toxic side effects (Figure 6).

Another type of organic carrier that was investigated for C225 functionalization consists of albumin NPs. Ye et al. developed C225-modified albumin NPs loaded with MC-Val-Cit-PAB-DOX as antibody-drug conjugates (ADCs) for targeted therapy [158]. In vitro, the targeted system showed specific uptake in EGFR-overexpressing RKO cells, with minimal uptake in LS174T cells. Cytotoxicity assays confirmed the greater antitumor effect in RKO cells. In vivo, the targeted platform inhibited tumor growth in RKO-tumor bearing mice without causing significant weight loss, while free doxorubicin (DOX) caused severe toxicity and led to 20% mortality. Similarly, egg serum albumin NPs were functionalized with C225 and crosslinked with glutaraldehyde to target and treat Caco-2 colon cancer cells [159]. Cytotoxicity assays showed that the targeted formulation had the highest

antitumor efficacy after 24 h (IC$_{50}$ of 120 µg/mL), outperforming C225, albumin NPs and pure albumin. The enhanced toxicity and apoptosis were attributed to improved internalization and penetration via the targeted platform.
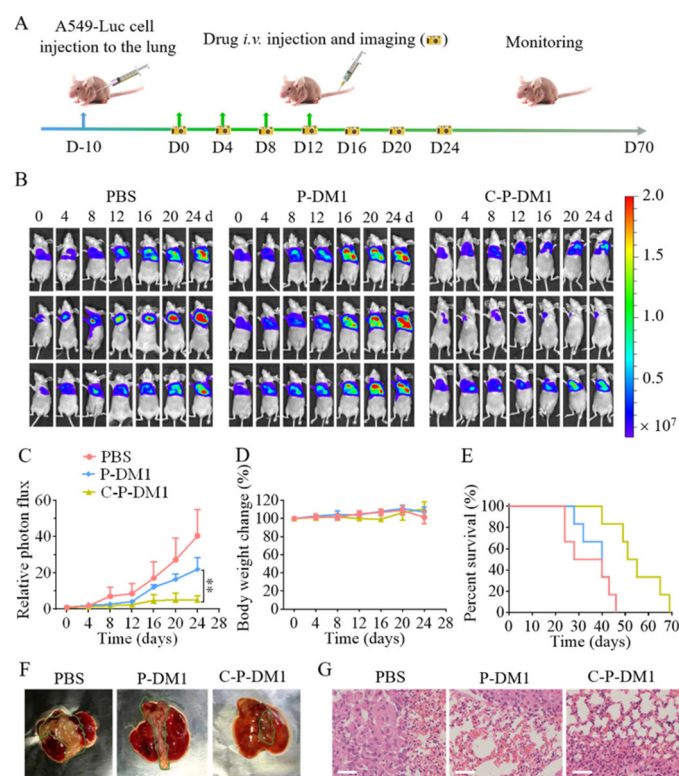

Figure 6. Therapeutic efficacy of C-P-DM1 in orthotopic A549-Luc NSCLC-bearing mice. (**A**) Establishment, therapy and monitoring scheme of the orthotopic A549-Luc NSCLC model. (**B**) Bioluminescence imaging and (**C**) quantitative bioluminescence levels of mice from day 0 to day 24 ($n = 3$). (**D**) Body weight change and (**E**) survival curves of mice ($n = 6$, C-P-DM1 vs. P-DM1 and PBS, ** $p < 0.01$). (**F**) Photographs and (**G**) H&E stained images of lung isolated from different groups on day 24. Scale bars are 50 µm. Adapted with permission from [157]. Copyright 2021, American Chemical Society.

Combining organic and inorganic nanocarriers, Chen et al. integrated MSNPs and PEGylated lipid bilayers (SLBs) to achieve a C225-targeted hybrid nanoplatform (SLB-MSN) for the treatment of CRC [160]. In vitro, the targeted system showed enhanced toxicity against HCT-116 cells compared with free 5-FU, MSN/5-FU and SLB-MSN/5-FU, with higher efficacy linked to elevated EGFR expression. In vivo, biodistribution studies showed significantly higher accumulation in HCT-116 tumors than SW-620 tumors, confirming the tumor-specific targeting ability of the platform. Another example displaying the combination of organic and inorganic carriers is found in the work of Dorjsuren et al., who grafted C225 to the surface of thermo-sensitive liposomes (TSLs) and loaded them with iron oxide NPs and DOX [161]. In EGFR-overexpressing SKBR-3 cells, the targeted system showed higher uptake than non-targeted TSLs, while no significant difference was detected in EGFR-low expressing MCF-7 cells.

Several studies on C225 functionalization have also been reported on inorganic nanocarriers. Ma et al. developed C225-conjugated perfluorohexane (PFH)/AuNPs for low-intensity focused ultrasound (LIFUS) diagnosis ablation of anaplastic thyroid carcinoma (ATC) [162]. In vitro, the targeted platform triggered apoptosis in C625 thyroid carcinoma, while in vivo the system exhibited antitumor properties in human thyroid carcinoma xenografts. C225-functionalized AuNPs were also exploited for the treatment

of metastatic CRC [163]. Among tested sizes, 60 nm C225-AuNPs exhibited the highest cytotoxicity in BRAF-mutant HT-29 cells, inducing 27.86% apoptosis compared with 15.68% for free C225, and 12.22% for free AuNPs. The enhanced efficacy was attributed to increased EGFR endocytosis and downstream signaling suppression. Wang et al. produced a C225-decorated drug delivery system based on NIR-activated NPs loaded with Pt(IV)-prodrug and indocyanine green (ICG) [164]. In EGFR-overexpressing A431 cells, the targeted system exhibited higher uptake and accumulation compared with minimal uptake obtained with free ICG, and NIR irradiation showed to enhance the efficacy even more. Moreover, the C225-decorated nanoplatform resulted in superior therapeutic effects and cell viability compared with free cisplatin, likely due to the sustained release of Pt(IV)-prodrug from the NPs.

Other anti-EGFR mAbs, including nimotuzumab (Nm) and panitumumab (Pm), were investigated for conjugation to nanocarriers.

Nm is an IgG1 mAb against human EGFR, with a lower immunogenicity profile than other mAbs [165]. Due to a lower affinity (Kd of ~20 nM) [166] and bivalent binding to EGFR, Nm usually targets cells with high EGFR density, resulting in reduced binding to normal cells and lower toxicity profiles than C225 [167]. Nm-AuNPs conjugates, assembled through thiol-mediated surface immobilization, achieved 4- to 5-fold enhanced cell growth inhibition compared with free Nm on the EGFR-overexpressing skin cancer cells A431, and EGFR-low expressing lung cancer cells A549 [168]. Nm also enhanced the uptake of AuNPs through specific EGFR-targeted activity.

Pm is an IgG2 isotype mAb, presenting almost 8-fold higher EGFR affinity than C225 (Kd of 0.05 nM) [169], and reduced immunogenic activity. Seminal reports on the use of Pm for targeted anticancer nanotherapies include the EGFR-mediated enhanced uptake of Pm-conjugated PLGA NPs loaded with TMZ, which resulted in increased ROS levels in EGFR-overexpressing U-87 MG cells [170]. Similarly, Pm-functionalized polycaprolactone (PCL) NPs improved the cytotoxicity of bosutinib in HCT-116 cells and induced 88% reduction in tumor size in mice with severe combined immunodeficiency disorders [171].

In the recent literature, full Abs were reported to improve the performance of NP-based carriers [172,173] for the delivery of small molecular chemotherapeutics, such as 5-fluorouracil [174,175], DOX [161,176], irinotecan [152,177], alpelisib [153] and DTX [178].

3.4. Anti-EGFR Antibody Fragments

A growing interest was observed over the past decades for the development of smaller Ab fragments, derived from conventional full Ab structures or produced recombinantly [179]. Despite their high binding affinity toward their target receptor [43], full Abs suffer from multiple limitations, including (i) bulky nature and high molecular weights; (ii) high immunogenicity; (iii) poor stability; and (iv) challenging control over oriented conjugation [180–182]. Ab fragments appeared as valuable substitutes due to their small size, which allows increased tumor penetration, their low immunogenicity due to the lack of Fc region, ease of production, high binding affinity, permeability across all biological barriers, high loading capacities and controlled orientation [183–185]. High tissue penetration is usually paired with faster renal clearance, a limitation that can be overcome with the conjugation of the targeting ligand to nanocarriers [186].

A meta-analysis by Mittelheisser et al. [187] of 161 studies (2009 to 2021) found that targeting efficiency of mAb-NPs or fragment mAb-NPs depends on the nanocarrier type. Fragment mAb-NPs exhibited higher tumor uptake with lipid NPs, while full mAb-NPs performed better with polymeric and organic/inorganic NPs. Smaller platform sizes consistently correlated with higher targeting efficiency. However, the underlying mechanism responsible for this phenomenon remains unidentified.

Fragmentation of full mAbs can be achieved via enzymatic digestion or recombinant expression [188,189]. Pepsin digestion yields bivalent F(ab')2 fragments (110 kDa), while papain digestion produces monovalent Fab fragments (50 kDa). Fab' fragments (55 kDa) result from the reduction of F(ab')2 fragments, leaving a free sulfhydryl group. Smaller fragments, like Fv, retain antigen-binding properties but lack constant regions, while single chain variable fragments (scFv) link variable regions with a short peptide. Novel formulations include domain antibodies (dAb), engineered single variable domains, and diabodies, bivalent dimers with linked V_H and V_L domains [179,190].

Table 1 presents recent examples of studies exploring NPs modified with anti-EGFR Ab fragments for cancer active targeting.

Table 1. Examples of nanocarriers decorated with anti-EGFR Ab fragments.

Ab Fragment	Type of NPs	Applications and Outcomes	References
scFv (husA)	Inorganic (FITC-labelled DOX-loaded MSNPs)	Reduction in viability of EGFR-overexpressing A431, HeLa and MCF-7 cells; higher uptake in EGFR-overexpressing A431 cells than in EGFR-low expressing HEK293 cells; inhibited tumor growth in A431 tumor-bearing mice.	[191]
scFv	Inorganic (Fe_3O_4/AuNPs)	MRI bioprobe for detection and treatment of NSCLC; higher uptake in EGFR-overexpressing SPC-A1 cells than in EGFR-low expressing H69 cells; in vivo tumor accumulation in SPC-A1 tumors and not in H69 tumors.	[192]
scFv	Organic (si-RNA-loaded engineered exosomes)	Inhibition of lung cancer brain metastasis; higher uptake in EGFR-overexpressing lung cancer cells PC9; efficient siRNA delivery across blood–brain barrier (BBB) in tumor-bearing mice.	[193]
scFv	Inorganic-organic (superparamagnetic iron oxide NPs (SPIONs) coated with PEG and chitosan)	siRNA delivery into TNBC cells; higher cellular uptake (1.5x) in EGFR-overexpressing MDA-MB-231 cells; protection of siRNA and 69.4% in vitro transfection efficiency.	[194]

Other recent reports highlighted the use of single Ab fragments [195–198], combinations of Ab fragments [199,200], or combinations of Ab fragments with full Abs [201] for the targeting of NP-based delivery platforms.

3.5. Anti-EGFR Nanobodies

Nanobodies (Nbs) are artificially designed antibody mimetics, representing the smallest intact antigen-binding fragment. Nbs are considered single domain Abs, since they consist of a single amino acid chain that forms only one domain [202,203], and their Kd is in the range of 2–25 nM [204]. These heavy-chain variable domains (V_{HH}) are antigen-binding fragments of camelid and shark heavy-chain Abs (HcAbs) with dimensions in the nanometer range (4 nm long and 2.5 nm wide) [205]. They are characterized by a molecular weight of ~12–15 kDa (10 times smaller than conventional Abs and 2–4 times smaller than Fab fragments or scFv), which provides them with excellent tissue penetration properties. The small sizes are also accompanied by reduced interaction surface with the antigen-binding site, leading to the recognition of unique epitopes which are often hidden to full Abs. Furthermore, they possess good solubility due to their highly hydrophilic nature. Nbs are non-immunogenic since they lack constant domains, which are usually responsible for the activation of the complement system and antibody-dependent cell-mediated cytotoxicity (ADCC) due to the Fc region. Nbs are much more stable than conventional Abs, they can

be stored at high temperatures and can be effectively renatured after thermal denaturation. Furthermore, they maintain their biological activity under strong acid and basic conditions. However, Nbs suffer from short half-lives and rapid clearance from circulation, which could limit their clinical applications. Nevertheless, their half-life can be extended by PEGylation [206] or fusion with antiserum albumin [207,208].

Liu et al. demonstrated the targeting ability of anti-EGFR Ega1 Nbs conjugated to micellar constructs loaded with meta-tetra(hydroxyphenyl)chlorin for selective PDT [209] (Figure 7). EGFR-mediated internalization was observed in A431 cells, resulting in enhanced cellular uptake and photocytotoxicity, as compared to control EGFR-low expressing HeLa cells. In vivo pharmacokinetics highlighted extended circulation of the micellar nanocarriers, as compared to the free drug.
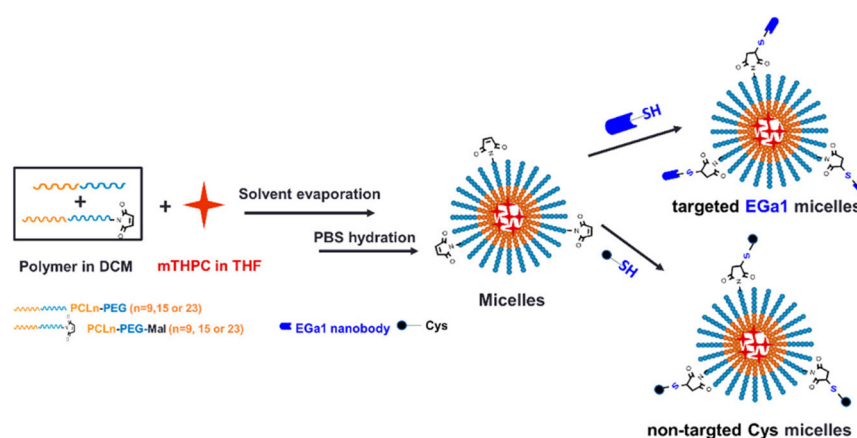

Figure 7. Preparation of polymeric micelles conjugated with EGa1 (targeted) or Cys (non-targeted). Adapted with permission from [209]. Copyright 2020, American Chemical Society.

Hernàndez et al. developed an anti-EGFR Nbs-targeted PDT platform (NiBh) for the selective treatment of oral squamous cell carcinoma (OSCC) in cats [210]. The targeted platform demonstrated high affinity for human and feline EGFR, effectively killing EGFR-overexpressing cells (LD_{50} in the nanomolar range), while leaving the surrounding EGFR-low expressing cells unharmed.

Other relevant studies have been conducted conjugating anti-EGFR Nbs to different types of nanocarriers for cancer active targeting [211–214].

3.6. Anti-EGFR Affibodies

Affibodies (Afbs) are scaffold-based affinity reagents [215], featuring the Z-domain, a designed variant of the IgG-binding protein A derived from *Straphylococcus aureus*. Afbs are composed of a three-helix bundle formed by 58 amino acids [216,217]. Variations in 13 of these amino acids give rise to a very large number of ligand libraries, from which powerful binders with high affinity and specificity can be isolated through a variety of display methods [218]. Phage display libraries provided receptor specific Afbs with affinities (Kd) in the μM to pM range [219], such as the matured anti-EGFR Afb $Z_{EGFR:1907}$ which exhibits 2.8 nM affinity to EGFR [220]. As an alternative, Afbs can also be produced by solid phase peptide synthesis (SPPS), allowing site-specific incorporation of reactive moieties [221], avoiding time-consuming bacterial expression and protein purification. Afbs are made of a single polypeptide unit, which allows rapid folding, and they do not contain cysteine residues in their structure [222]. Born as a novel class of mAbs mimetics, Afbs possess several advantages over full Abs, including their smaller size (6 kDa vs. 150 kDa, respectively), which leads to faster and more effective tumor penetration and more rapid clearance. Moreover, the binding site and affinity are similar to those of Abs.

They are highly soluble and stable in harsh conditions, including alkaline pH and elevated temperatures, that usually denature most proteins [223].

Afbs-functionalized nanocarriers have demonstrated significant versatility and have been investigated for a broad range of applications, including imaging, diagnostics, and therapeutic purposes. As an example of the first category, Wu et al. developed gadolinium (Gd)-encapsulated carbonaceous dots (Gd@C-dots) modified with Ac-Cys-$Z_{EGFR:1907}$ (Gd@C-dots-Cys-$Z_{EGFR:1907}$) as an MRI contrast agent, demonstrating specific EGFR targeting in vitro and in vivo [224]. Larger NP size (~20 nm) allowed the achievement of enhanced tumor affinity and targeting in EGFR-overexpressing xenografts, while maintaining efficient renal clearance. Smaller NP sizes (~3 nm), on the other hand, showed reduced signal enhancement due to poor receptor binding. As a tool for diagnostics, Afbs-functionalized polystyrene microbeads (AffiBeads) were designed and produced for the specific detection of EGFR-overexpressing exosomes as diagnostic markers for NSCLC [225]. The system allowed sensitive detection of as few as 12 exosomes per bead via flow cytometry. Among the several Afbs-based targeted formulations explored for therapeutic applications, anti-EGFR Afbs-modified porous platinum NPs (pPt NPs) were developed [226]. The system showed enhanced EGFR-specific targeting and tumor homing in A431 models, outperforming the unmodified platform. Moreover, the functionalized nanocarrier demonstrated superior radiotherapy sensitization, inhibiting HIF-1α expression and increasing DNA damage after only two treatments. Roy et al. developed an enzyme prodrug therapy based on upconverting NPs and photo-cross-linkable anti-EGFR Afbs (UC-ACD) [227], leading to a 4-fold higher retention in irradiated colorectal cancer cells in vitro (Figure 8). Upon binding, the targeted system converted 5-fluorocytosine to 5-fluorouracil, reducing tumor growth by 2-fold. In vivo, combination of UC-ACD and NIR irradiation increased tumor accumulation by 5-fold compared to controls.
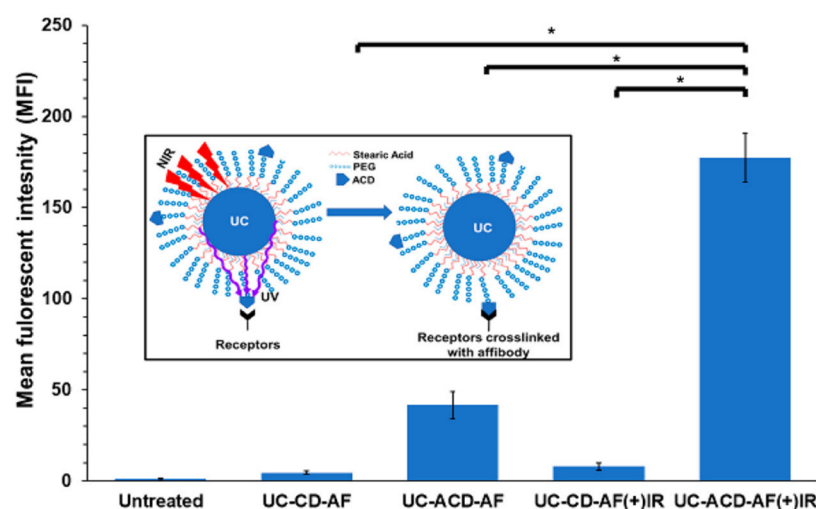

Figure 8. Mean fluorescent intensity from human colorectal Caco-2 cancer cells after incubation with Alexa Fluor 555-modified UC-ACD (targeted) and UC-CD (non-targeted), with and without NIR irradiation. MFI of UCNP-protein complex is 4.38 ± 0.32 times higher in the cells treated with UC-ACD-AF (+) IR than that of the non-irradiated control (UC-ACD-AF, $n = 3$, * $p < 0.05$). Inset: schematic showing the UC-ACD conjugate structure and the NIR activation of the UCNPs, followed by upconversion to UV, resulting in a photoreaction between the affibody-enzyme ACD and EGF receptors. This chemical association allows enzymatic conversion of systematically delivered prodrug 5-FC to active drug 5-FU at the cancer site. Adapted with permission from [227]. Copyright 2022, American Chemical Society.

Karyagina et al. formulated EGFR-targeting modular nanotransporters (MNT) using Z_{1907} Afbs as targeting ligand to deliver the cytotoxic agent ^{111}In directly to tumor cell

nuclei [228]. The use of the nanoplatform allowed the achievement of significantly higher cytotoxicity compared to free ^{111}In, highlighting Afbs-MNT as a promising vehicle for targeted anticancer therapy.

Several other studies have been reported to investigate the effect of anti-EGFR Afbs-functionalized nanocarriers in vitro and in vivo [229–232].

3.7. Anti-EGFR Aptamers

Discovered 30 years ago, aptamers have been investigated as an alternative class of targeting agents in addition to peptides and proteins [233–235]. Aptamers are short single stranded DNA or RNA molecules of ~20–100 bps [236]. RNA aptamers have been shown to assume more diverse and intricate three-dimensional structures than DNA aptamers, allowing a higher number of conformations [237,238]. However, DNA aptamers are more stable than RNA aptamers, with in vivo half-life values in plasma of 30 to 60 min or a few seconds, respectively [239]. The use of native RNA aptamers is partly limited by their low stability; however, conjugation of RNA aptamers to NPs can shield the oligonucleotides from enzymatic degradation, thereby extending their in vivo half-life [240–243]. Additionally, various strategies have been explored to enhance RNA stability and mitigate nuclease degradation. These include chemical modifications, such as substitution of the natural hydroxyl group at the 2′ position of RNA bases with fluorine, protection of the 5′ and 3′ ends of RNA aptamers through capping, or circularization of RNA [244–246]. The ability of aptamers to fold into specific 3D conformations allows them to recognize and bind with very high affinity to their receptors, through electrostatic interactions, van der Waals forces and hydrogen bonds [247]. In the study of Li et al., one of the selected aptamers against hEGFR, E07, bound tightly to the wild-type receptor with a Kd of 2.4 nM [248].

Known as "chemical antibodies", aptamers are chemically synthesized, which allows site-specific modifications of their nucleotide chains. One of the most famous processes of aptamer identification and synthesis is known as systematic evolution of ligands by exponential enrichment (SELEX) [235,249]. It consists of sequential steps, including incubation of random ssDNA or ssRNA libraries with the target molecules, separation of aptamer-target complexes from non-binding sequences, amplification of the target-bound nucleic acid sequences by PCR (for DNA aptamer selection) or RT-PCR and RNA transcription (for RNA aptamer selection), incubation of targets with a new library for the next round of enrichment and repeating for a fixed number of cycles. The repeated selection cycles allow an increase in the high affinity binding of the selected nucleic acids [250]. Advantages of the use of aptamers over Abs include smaller sizes (8–25 kDa), better tissue penetration, thermal stability, higher pH resistance, lower immunogenicity and toxicity in vivo, easier modification and conjugation, and easier synthesis and production with minimal batch-to-batch variations [251,252]. Furthermore, due to the SELEX identification process, aptamers can have an unlimited range of targets. However, there are still some areas in which Abs outperform aptamers. Regardless of their shelf stability, aptamers suffer from shorter half-lives in vivo due to renal filtration and nuclease digestion [253,254].

Ibarra et al. developed polymer NPs (CPNs) conjugated with either anti-EGFR or TNBC-specific RNA aptamers for phototherapy applications [255]. The anti-EGFR aptamer enhanced binding, cell internalization, and phototoxic effects in vitro compared to bare or scrambled aptamer-functionalized nanocarriers. In the development of therapeutic options for TNBC, Agnello et al. conjugated the anti-EGFR aptamer CL4 to (Cis-Pt)-loaded fluorescent polymeric NPs (PNPs-CL4) to achieve rapid and efficient uptake in EGFR-overexpressing MDA-MB-231 and BT-549 cells (10-fold higher uptake than the non-targeted NPs), increased toxicity (12-fold higher than the free drug), and enhanced intra-tumor

accumulation in MDA-MB-231 tumor-bearing nude mice (Figure 9) [256]. Effective drug dosage was reduced by five in comparison with the minimum free Cis-Pt dosage.
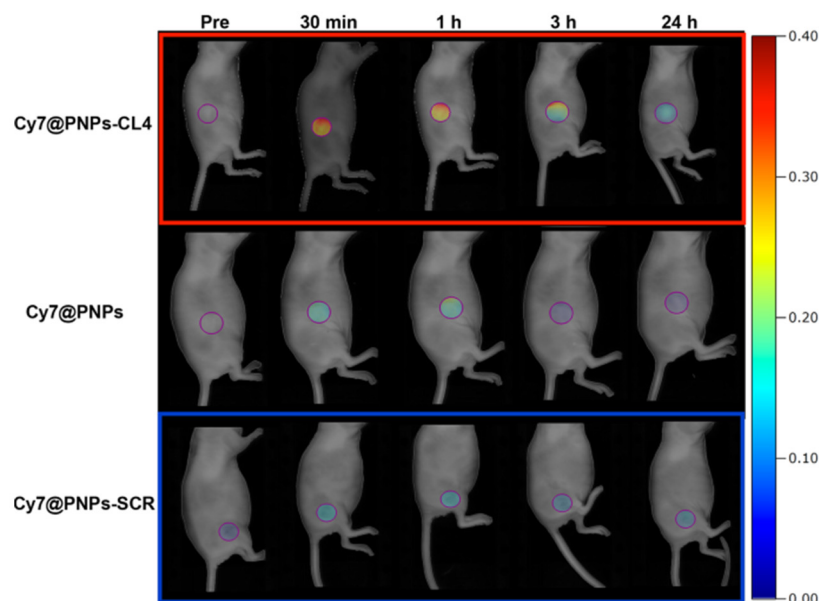

Figure 9. Selective tumor targeting of Cy7@PNPs-CL4 compared to Cy7@PNPs-SCR and Cy7@PNPs. Nude mice bearing subcutaneous MDA-MB-231 xenografts were i.v. injected with Cy7@PNPs-CL4, Cy7@PNPs or Cy7@PNPs-SCR (5 nmol Cy7/100 μL) and analyzed by in vivo FRI imaging at the indicated time points (i.e., Pre: before injection, 30 min, 1, 3 and 24 h acquisitions). Adapted from [256]. Copyright 2021, Springer Nature.

To address the heterogeneity of cancer cells, anti-EGFR/CD44 dual-RNA aptamers were conjugated to solid lipid NPs functionalized with dexamethasone for DOX delivery to MDA-MB-468 cells, overexpressing EGFR and CD44 [257]. While monotargeted NPs induced a significant reduction of cell viability, the presence of dual targeting aptamers enhanced the cell death levels. In a similar strategy, Camorani et al. prepared a multifunctional platform displaying two different surface-conjugated RNA aptamers on iridium(III) (Ir$_{en}$)-embedded Au-core/silica-shell-based NPs for synergistic PDT and PTT [258]. Anti-EGFR CL4 and anti-PDGFRβ RNA aptamers were selected for tumor and stromal cells targeting, respectively. The efficacy and synergistic effect of the dual-aptamer-decorated NPs were established on TNBC cells, luminal/HER2-positive breast cancer cells, epidermoid carcinoma cells, and adipose-derived mesenchymal stem cells. Tested on preclinical 3D stroma-rich breast cancer models, the multifunctional NPs were also effective in spheroids and organoids, highlighting the superiority of dual targeting.

The co-delivery of gefitinib and rapamycin, loaded in aptamer-conjugated chitosan NPs, was assessed to overcome EGFR-TKI resistance in NSCLC by promoting autophagy [259]. While enhanced cytotoxicity was observed in EGFR-overexpressing cells (H1975), non-targeted cell lines were not impacted. Furthermore, the high therapeutic efficacy was validated on tumor xenografts.

The targeting ability of aptamers was also combined with GSH-responsive polymeric NPs for the enhanced delivery of homoharringtonine to EGFR-overexpressing A549 breast cancer cells [260]. In vivo administration to A549 tumor-bearing nude mice confirmed the highest tumor-suppression potential of the targeted NPs.

Yang et al. developed anti-EGFR RNA aptamer-loaded NPs (EGFR$_{apt}$-3WJ-si$KRAS^{G12C}$) for targeted delivery of siRNA to NSCLC cells [261]. The platform showed enhanced cell association and KRAS suppression compared to the non-targeted nanocarriers, with higher

uptake mediated by EGFR expression. In vivo, EGFR-targeted platforms led to higher tumor accumulation and efficient tumor suppression, unlike the non-targeted counterparts.

Other recent studies highlighted RNA aptamers-functionalized NPs for targeted breast cancer therapy [262,263], aptamer-conjugated nanoplatforms for the delivery of poorly water-soluble chemotherapeutic agent paclitaxel [262,264], aptamer-functionalized AuNPs [265,266], and nanocarriers functionalized with a combination of targeting aptamers and Abs [265].

Table 2 presents a summary of the reported anti-EGFR targeting ligands used for functionalization of nanocarriers.

Table 2. Anti-EGFR targeting ligands used for conjugation to nanocarriers.

Targeting Ligand	Advantages	Limitations	Structure and MW	Kd	References
EGF	Small size enabling high tumor penetration; smaller final size of the system obtained; high natural affinity for EGFR; low cytotoxicity; moderate stability in vitro; stability at physiological conditions and neutral pH; ease of conjugation to nanocarriers; availability via recombinant expression	Expensive production; possible antigenicity issues and immune responses in vivo; prone to proteolysis in vivo	Small protein of 53 amino acids, 6 kDa	2 nM	[99–112]
GE11	Very small size facilitating tumor penetration and diffusion; smaller final size of the system obtained; no mitogenic activity; high chemical stability; ease of production and synthesis; cost-effective manufacture	Lower affinity for EGFR but sufficient for targeting purposes	Small peptide of 12 amino acids, 1.54 kDa	22 nM	[116–144]
Antibodies	Large size allowing increased circulation time and long half-life in vivo; larger final size of the system obtained; possible aggregation of the system observed; possible multivalent receptor binding; highest binding affinity; longest history of usage; possible therapeutic effects through EGFR pathway inhibition	Poor tissue penetration due to bulky nature and large size; high immunogenicity, poor stability, challenging control over oriented conjugation	Y-shaped protein consisting of two heavy and two light chains, 150 kDa	0.05–20 nM	[152–164,168,170–178]
Ab fragments	Smaller size than full Abs facilitating higher tumor penetration; smaller final size of the system obtained; reduced immunogenicity due to lack of Fc regions; easier and cheaper production compared to full mAbs; retained high affinity of the binding regions; high loading capacity; controlled orientation	Generally lower binding affinity than full Abs; faster renal clearance and reduced circulation times (that can be overcome with conjugation to NPs)	F(ab′)2: two antigen-binding sites joined at the hinge region through disulfide bonds, 110 kDa Fab′: reduced F(ab′)2 fragment, containing a free sulfhydryl group, 55 kDa Fab: monovalent fragments composed of the V_H, C_{H1}, V_L and C_L regions, 50 kDa	1–10 nM	[191–201]
Nanobodies	Small size enabling high tumor penetration; smaller final size of the system obtained; high stability being resistant to denaturation and proteolysis; low immunogenicity; good solubility; binding to unique epitopes; versatile functionalization; easy and cost-effective production	Short half-life and rapid clearance from circulation (that can be overcome with conjugation to NPs); limited applications and clinical studies compared to full mAbs and Ab fragments	Heavy-chain variable domains (V_{HH}) of camelid and shark Abs, 12–15 kDa	2–25 nM	[209–214]
Affibodies	Small size enabling high tumor penetration; smaller final size of the system obtained; high thermal and chemical stability; low immunogenicity due to Ab mimics and engineered protein scaffold nature; good solubility; large number of libraries available; versatile functionalization; ease of production and synthesis	Short half-life, rapid clearance from circulation (that can be overcome with conjugation to NPs); limited applications and clinical studies compared to full mAbs and Ab fragments	Three-helix bundle formed by 58 amino acids, 6 kDa	2.8 nM	[224–232]

Table 2. *Cont.*

Targeting Ligand	Advantages	Limitations	Structure and MW	Kd	References
Aptamers	Small size and flexibility enabling excellent tumor penetration; smaller final size of the system obtained; lower electrostatic adsorption to nanocarriers compared to protein ligands; high binding affinity, high thermal and chemical stability; versatile binding capability; low immunogenicity and toxicity in vivo; large number of libraries available; versatile functionalization and chemical modification; easy and cost-effective production; minimal batch-to-batch variations	Short half-life, rapid clearance from circulation (that can be overcome with conjugation to NPs); susceptible to nuclease degradation without chemical modifications; limited applications and clinical studies compared to full mAbs and Ab fragments	Short single-stranded DNA or RNA molecules with specific 3D architectures, 6–25 kDa	2.4 nM	[255–266]

4. Bioconjugation Strategies

There are several chemical strategies available to graft anti-EGFR ligands to the surface of nanocarriers, including covalent and non-covalent approaches. In this section, the various methodologies are described and significant examples of functionalization are discussed, highlighting the benefits and limitations of each strategy.

4.1. Covalent Conjugation Strategies

4.1.1. Carbodiimide Chemistry

Amide bond formation stands among the most common conjugation strategies for NP functionalization. An amide bond is a stable linkage formed between a primary or secondary amine and a carboxylic acid. The reaction relies on the pre-activation of the carboxyl groups with the use of coupling agents, such as 1-ethyl-3-(-3-dimethylaminopropyl) carbodiimide (EDC), leading to an O-acylisourea intermediate [267]. N-hydroxysuccinimide (NHS) or its water-soluble version (sulfo-NHS) are often paired with EDC to improve the reaction efficiency, through the stabilization of the O-acylisourea intermediate [268].

Amide bond formation can be efficiently performed without spacing the reactive functionality (amine or carboxylic acid) from the NP surface, therefore maintaining the hydrodynamic sizes of the initial nanocarriers. The reaction is sensitive to pH and is more efficient when performed in acidic medium (pH 4–5) [267]. To prevent competition with extraneous carboxyl or amine groups, the reactions need to be run in buffers which are devoid of these reactive chemical moieties, such as 4-morpholinoethanesulfonic acid (MES) buffer or phosphate buffers.

This strategy is one of the most reported for NP functionalization because it is easy to perform and accessible. Furthermore, the amino and carboxyl chemical handles are naturally found in several biomolecules, such as proteins and peptides, where amino acid residues tend to be the target for conjugation. The common anchoring points include the ε-amino group of lysine side chains, the N-terminal primary amine, the carboxyl group on aspartic acid and glutamic acid, or the C-terminus [54]. While protein- or peptide-based targeting ligands do not require chemical modifications, nucleic acids are generally functionalized through site-specific reactions to introduce the amino or carboxyl moieties, allowing further amide bond coupling to the NP surface.

When applied to protein ligands such as Abs, this strategy does not allow for controlling their orientation due to the wide and random distribution of amino and carboxyl groups on their backbone. Surface immobilization through their antigen binding sites may reduce the specificity of the resulting nanoplatform [182]. However, a number of studies highlighted the use of amide-bond couplings for NP functionalization with anti-EGFR ligands.

Table 3 provides examples of carbodiimide chemistry used as a strategy for the conjugation of anti-EGFR targeting ligands to NPs.

Table 3. Examples of nanocarriers functionalized with anti-EGFR ligands using carbodiimide chemistry.

Targeting Ligand	NP Type	Main Observations	References
C225	Multilayered polyelectrolyte capsules, optically encoded with fluorescent quantum dots	~87% Ab coupling efficiency; random Ab orientation reduced steric hindrance while maintaining selective interaction with targets.	[269]
GE11 peptide	SPIONs	Complete peptide conjugation confirmed via mass spectroscopy analysis of the filtrate; maximum cellular uptake was achieved in 24 h; internalization was proportional to EGFR expression of the cell line tested.	[137]
EGF	Carboplatin-loaded alginate poly(amidoamine) (PAMAM) hybrid NPs	Success of EGF conjugation confirmed in 2D and 3D in vitro setting; final NP size after conjugation was smaller than 400 nm; conjugated EGF at the surface increased with respect to its concentration in the reaction media; EGF-conjugated platforms exerted the highest therapeutic potential in vivo.	[111]
Anti-EGFR aptamers	Ganoderenic acid D-loaded PEGylated graphene oxide-based carrier	Simultaneous conjugation of aptamers and FITC via amino groups; successful anti-tumor effects of targeted platform were confirmed in vitro and in vivo.	[270]
Anti-EGFR Afbs	Gadolinium-encapsulated carbonaceous dots	Higher uptake in EGFR-overexpressing cells and tumor xenografts was confirmed by fluorescence and T1-weighted MRI results; efficient clearance of targeted platform by the renal system was achieved.	[224]
Anti-EGFR ScFv	Human serum albumin-coupled, FITC-labeled and DOX-loaded mesoporous silica NPs	In vitro and in vivo anti-tumor activity and safety of the targeted platform was verified; prolonged circulation, targeted accumulation, and enzyme/pH-responsive drug release properties were confirmed.	[191]

Although this chemical strategy is one of the most-employed, accessible and easy to perform, it is characterized by low site specificity due to the generally high abundance of carboxyl and amino groups in biological ligands, such as Abs. This can therefore lead to a lack of ligand orientation, impacting the overall final targeting efficiency [271].

4.1.2. Schiff Base Reaction

The derivatization of NP surfaces with aldehyde functionalities is used to immobilize targeting ligands containing primary amines through the formation of imines, also known as Schiff bases [272,273]. Similar to amide coupling, this technique does not allow for controlling the orientation of conjugated Abs or peptides. Alternatively, mild oxidation of the carbohydrate units of the Ab-Fc region leads to the introduction of aldehyde or ketone moieties that can be selectively reacted with hydrazine/hydrazide-modified NPs to control the orientation of the immobilized ligands through hydrazone bonds [274].

Following this pathway, Jordan et al. performed a directional conjugation of an anti-EGFR Ab to the surface of barium titanate NPs (BTNPs) [173]. The Ab was first reacted with

sodium periodate to induce oxidation of the Fc region, yielding reactive aldehyde groups, which were covalently conjugated to a *N-ε*-maleimidocaproic acid hydrazide (EMCH) cross-linker via hydrazone bonds (Figure 10). The maleimide groups further reacted with thiol-modified BTNPs and the resulting thioesters ensured that the Ab binding region was facing outward to increase the targeting efficiency.
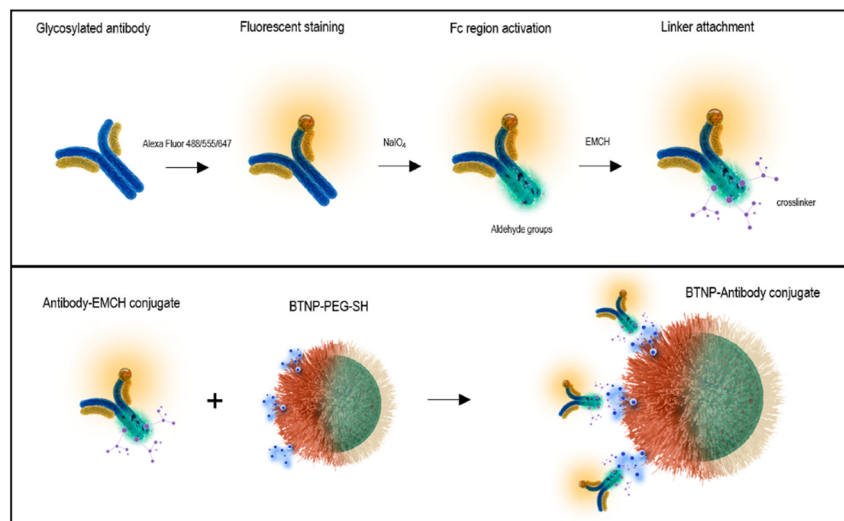

Figure 10. Schematic representation of the directional Ab conjugation chemistry. A glycosylated Ab is first fluorescently labelled, and then aldehyde groups are created on the Fc region. The hydrazide portion of an EMCH cross-linker binds to the aldehyde groups while the maleimide portion attaches to the thiolated BTNP surface. Adapted with permission from [173]. Copyright 2020, American Chemical Society.

Similarly, Kawelah et al. reported a bifunctional PEG linker presenting amino- and DBCO-end functionalities for the stepwise conjugation to oxidized anti-EGFR Abs (imine formation) and azido-modified indocyanine green J-loaded polymersomes (copper-free click reaction) [275].

Another study highlighted the modification of iron oxide NPs with oxidized sodium alginate, allowing post-conjugation to the targeting peptide GE11 through imine formation [276]. The resulting nanocarriers were used for the MRI of nasopharyngeal carcinoma and targeted delivery of cisplatin.

Despite being less common than amide-based conjugations, Schiff base reactions favor proper spatial orientation of Ab ligands, resulting in enhanced targeting capabilities [277].

4.1.3. Thiol-Maleimide Chemistry

Another very common conjugation strategy for NPs functionalization with targeting ligands involves the 1,4-addition of thiols to maleimide groups, which can be performed at neutral pHs and under mild conditions. This strategy requires the presence of free sulfhydryl groups, either on the ligands or on the NPs surface, which can be achieved in two main ways: (i) reduction of native disulfide bonds in the presence of mild reagents, such as tris(carboxylethyl)phospine (TCEP), dithiothreitol (DTT) or 2-mercaptoethanol (BME) [278]; or (ii) conversion of amines into thiols by using 2-iminothiolane (Traut's reagent) and N-succinimidyl S-acetylthioacetate (SATA) [279]. NPs are generally modified with maleimide groups, using heterobifunctional linkers. This strategy is more site-selective than carbodiimide chemistry due to the limited number of sulfhydryl groups in proteins, in comparison with amines, and benefits from faster kinetics at neutral pH [280]. However, thiol-maleimide chemistry does not allow proper control over the orientation of Abs-conjugated NPs.

Aptamers, Afbs and Nbs are subjected to site-specific modification with a free thiol group, allowing for selective thiol-maleimide conjugation. However, the resulting thioether linkages are sensitive to reducing potential and can be cleaved by exogenous glutathione (GSH), a reducing agent found naturally in the circulation and cellular compartments [281]. In addition, when using Ab-based targeting ligands, the reduction step might damage the Ab tertiary structure and decrease its binding activity [282].

Nevertheless, thiol-maleimide conjugation was used for the immobilization of a large variety of targeting ligands to nanocarriers. For example, Guo et al. successfully conjugated a free thiol-bearing GE11 peptide to a dual drug-loaded polymeric micellar system using a Michael-type thiol-ene reaction [116]. The approach ensured effective reaction of the terminal maleimide groups with GE11, leading to functionalized NPs based on amphiphilic polycarbonate, whose systemic administration in vivo resulted in increased tumor growth suppression and reduced metastasis and toxicity compared to the non-targeted platform. Mesquita et al. conjugated anti-EGFR Nbs to zinc phthalocyanine-loaded polymeric micelles via thiol-maleimide chemistry (Figure 11) [211]. The presence of the targeting ligand at the surface of the NPs generally enhanced the association and phototoxicity in cells overexpressing the target receptor.
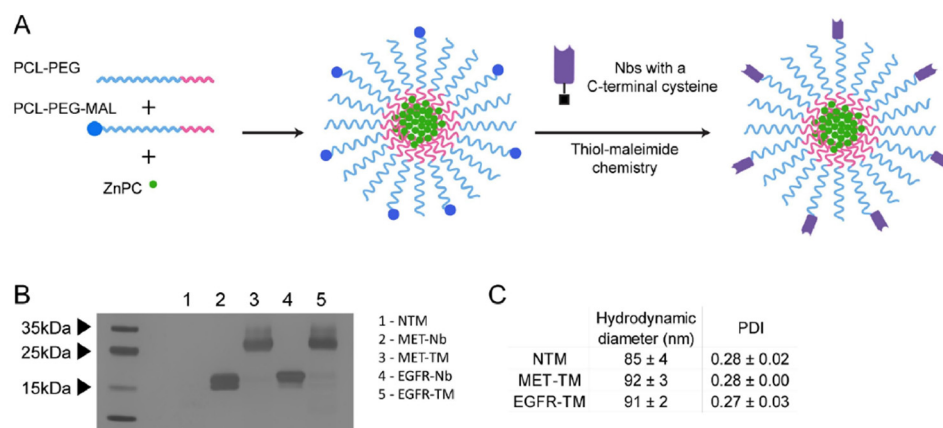

Figure 11. Nbs targeting MET or EGFR were successfully conjugated to zinc phthalocyanine-loaded micelles. (**A**) Schematic of Nb-targeted micelles prepared via thiol-maleimide chemistry. (**B**) SDS-PAGE with silver staining of (1) Non-targeted micelles, (2) MET-Nb, (3) MET-targeted micelles, (4) EGFR-Nb, (5) EGFR-targeted micelles before the centrifugation step. (**C**) Size and polydispersity of non-targeted micelles, MET-targeted micelles and EGFR-targeted micelles (N = 3). Adapted with permission from [211]. Copyright 2024, Elsevier.

Geddie et al. engineered Fabs with strategically placed disulfide bonds to avoid over-reduction during initial processing while preserving their binding ability [283]. When functionalized to immunoliposomes via thiol-maleimide chemistry, the engineered Fabs enhanced uptake in multiple cell lines compared to the non-targeted counterparts. Ye et al. designed ADCs by grafting a previously reduced C225 to DOX using a maleimide-bearing linker, followed by adsorption onto the surface of BSA NPs [158]. Flow cytometry analysis demonstrated higher binding and accumulation in EGFR-overexpressing cells. Furthermore, in vivo studies showed higher tumor inhibition efficacy and lower system toxicity for the targeted system compared to the non-targeted control. In another study, anti-EGFR Afbs were grafted to DOX-loaded PEGylated liposomes using thiol-maleimide chemistry [231]. In vitro studies revealed a higher DOX uptake in EGFR-overexpressing cells compared to EGFR-low expressing cells, highlighting the selective enhanced cytotoxicity. In vivo, the targeted platform exhibited long circulation time and efficient accumulation

in EGFR-overexpressing tumors. Moreover, low-dose treatment could not only produce an ideal antitumor effect but also reduce its systemic toxicity.

4.1.4. Dative Chemistry (Thiol-Metal Bond)

Another strategy for the direct conjugation of biomolecules to NP surfaces involves dative (coordination) bonds, which are less robust than covalent linkages, due to extended lengths, higher energy and sensitivity to pH variation, oxidation or replacement by similar molecules [284,285]. However, dative bonds can be enhanced by increasing the number of interactions. Known examples of dative bonds include chelation of metal ions (coordination by electron-donating amino acids) and gold-thiol chemisorption, which is commonly used for the functionalization of AuNPs with thiolated biomolecules, including proteins, peptides and oligonucleotides.

Table 4 presents examples of nanocarriers decorated with anti-EGFR targeting ligands via gold-thiol chemisorption.

Table 4. Conjugation of anti-EGFR targeting ligands to AuNPs through gold-thiol chemisorption.

Targeting Ligand	Application	Main Observations	References
EGF	Development of a new contrast agent for early stage tumors based on AuNPs and gadopentetic acid	Au@Gd-EGF exhibited significant MRI signal intensity for diagnostic applications, allowing for high specificity and sensitivity; the targeted nanocontrast agent showed good biocompatibility and low cytotoxicity in vitro.	[286]
C225	Systematic comprehensive characterization and stability assessment of a targeted nanocomplex with high potential for biomedical applications	After 24 months manufacturing, decoupling Ab from AuNPs was not observed, suggesting irreversible immobilization; efficient EGFR binding and induced tumor cell death due to apoptosis were confirmed.	[287]
Anti-EGFR aptamer (U2)	Development of a novel brain-targeting complex for glioblastoma multiforme therapy	The U2-AuNPs inhibited the proliferation and invasion of EGFR-overexpressing cells; the targeted platform allowed to cross the blood–brain barrier and prolonged survival time of glioblastoma-bearing mice.	[266]
Anti-EGFR aptamer + Anti-EGFR Ab	Development of multi-functionalized probe for detection of EGFR-positive cancer cells	Dual targeted platform showed higher target specificity to EGFR-positive cancer cells, compared to Apt- or Ab-functionalized probes; main benefits of the platform are its potential to facilitate the detection of binding to cell surface markers with low expression levels.	[265]

4.1.5. Click Chemistry

Click chemistry refers to a group of chemical reactions, described by Sharpless et al. in 2001 and presenting high potential for NP functionalization due to their high selectivity, favorable reaction rates, compatibility with mild aqueous conditions, minimal production of by-products and high yields [288,289]. Click reactions mostly include copper-catalyzed azide-alkyne 1,3 dipolar cycloaddition (CuAAC) [290], strain-promoted azide-alkyne cycloaddition (SPAAC) [291], and inverse electron-demand Diels-Alder reaction (IEDDA) between tetrazine (Tz) and trans-cyclooctene (TCO) [292,293]. Such reactions are considered "biorthogonal", because the reactive groups are highly selective and inert toward

other functionalities present in biological systems, such as carboxyls, amines, hydroxyls, thiols, alkenes, amides, esters, disulfides and phosphodiesters.

Despite this favorable profile, click reactions require the introduction of the non-native reactive handles on the targeting ligand and NP surface. For example, azido groups can be site-specifically introduced on the heavy chain of the Fc of Abs by using an enzymatic modification, leading to further controlled oriented conjugation (Figure 12) [294,295]. As a result, the conjugation of Abs to NPs was 5- to 8-fold more efficient through click reactions than amide reactions [296,297].
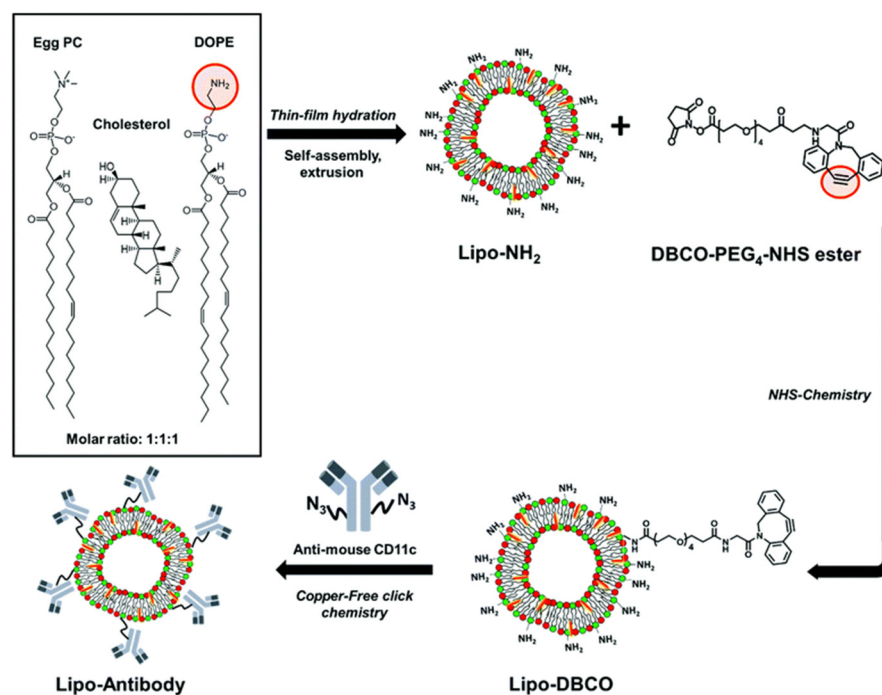
Figure 12. Schematic illustration of step-by-step liposome synthesis, surface functionalization and site-selective Ab attachment. Adapted with permission from [294]. Copyright 2020, Royal Society of Chemistry.

Both inorganic and organic NPs were efficiently functionalized through click reactions. Porous silicon NPs, modified with DBCO-terminated PAMAM dendrimers, were conjugated to azido-containing anti-EGFR Nbs for the co-delivery of siRNA and DOX [298]. Similarly, DBCO-modified UCNPs underwent SPAAC in the presence of photo-cross-linkable anti-EGFR Afbs-enzymes. The introduction of the azido reactive handle on the targeting construct involved a PEG spacer [227]. Alternatively, DBCO-modified anti-EGFR Abs were efficiently immobilized on azido-functionalized MSNPs [299].

The versatility of SPAAC reactions was further demonstrated by Tran et al. in the preparation of customized antisense oligonucleotides (ASOs)-loaded red blood cell-derived extracellular vesicles (RBCEVs) to selectively target mutations in the EGFR gene [300]. Their specificity was enhanced following SPAAC immobilization of azido-modified anti-EGFR Nbs. Other examples include the conjugation of C225 to azido-decorated polymersomes [157]. In these approaches, the introduction of the reactive handles, via bifunctional linkers, made use of conventional carbodiimide chemistry, therefore resulting in random orientation of the immobilized targeting ligands [301].

The demonstration of the oriented conjugation of anti-EGFR targeting ligands mediated by click chemistry was not yet reported. However, examples are found with similar receptors, such as CD11 [294] and HER2 [296].

4.2. Non-Covalent Conjugation Strategies

4.2.1. Interaction by Adapter Molecules

One of the most represented non-covalent approaches exploits the strong binding affinity between biotin and biotin-binding proteins, such as avidin or its analogues, including neutravidin and streptavidin. Avidin is a tetrameric glycoprotein characterized by a molecular weight of ~68 kDa, and composed of four identical subunits of 128 amino acids. Avidin has been extensively reported to bind biotin with high affinity and specificity (Kd ~ 10^{-15} M), making the avidin-biotin interaction one of the most specific and stable non-covalent interactions [302,303]. NP surfaces can be coated with avidin (by electrostatic interactions or covalent conjugation strategies) and targeting ligands can be chemically modified with biotin for subsequent specific immobilization through avidin-biotin interactions. In particular, this technique offers an oriented conjugation of Abs to NP surfaces, since Abs can be engineered with biotin molecules at their Fc region. The main advantages of this strategy rely on its high stability and robustness against temperatures, pH, harsh organic solvents and other denaturing reagents [304]. However, avidin has a high degree of non-specific binding, due to its basic isoelectric point (pI) and high glycosylation degree. Superior variants of avidin include the deglycosylated streptavidin (pI of ~5–6) [305] and neutravidin (pI of ~6.3) [306,307].

Among the applications of this non-covalent approach, one can cite the functionalization of neutravidin-coated gold nanorods with biotinylated anti-EGFR Ab (Figure 13) [308], the production of C225-conjugated vaterite NPs for the release of immunotherapeutic proteins [309], and the decoration of red blood cell-derived extracellular vesicles with anti-EGFR Ab for the delivery of therapeutic RNA via intrapulmonary administration [310].
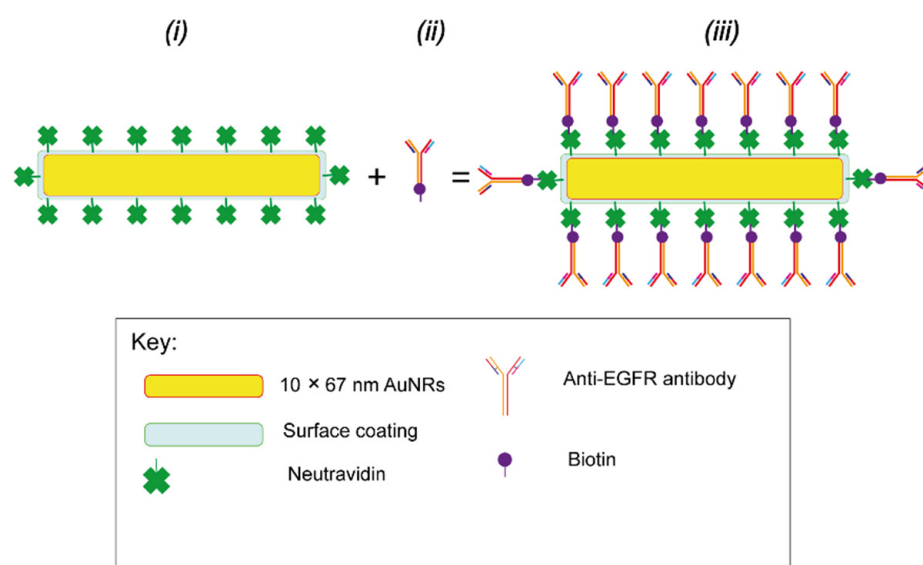

Figure 13. Schematic representation of the functionalization of neutravidin-coated gold nanorods with biotinylated anti-EGFR Abs. (i) Neutravidin-coated 10 nm × 67 nm gold nanorods, (ii) biotinylated 5.2 nm × 5.2 nm anti-EGFR Abs, (iii) Biotinylated anti-EGFR Abs-coated neutravidin gold nanorods. Adapted with permission from [308]. Copyright 2021, MDPI.

4.2.2. Electrostatic Interaction

Non-covalent bioconjugation techniques rely on the adsorption of ligands to the surface of nanocarriers through electrostatic interactions, hydrogen bonding, hydrophobic interactions and van der Waals forces. Despite their cost-effectiveness and ease of implementation, non-covalent interactions are much less robust than covalent bonds and more prone to degradation. Furthermore, these interactions are non-specific and sensitive to

changes in experimental conditions, such as temperature, ionic strength and pH. Since this type of chemistry often requires only stoichiometric mixing of the NPs and biomolecules, it can be referred to as "self-assembly". Electrostatic adsorption approaches rely on the attraction between oppositely charged species: charged nanocarriers will attract oppositely charged targeting ligands [311]. For example, the strong negative charge of phosphate groups in oligonucleotides causes adsorption on the surface of positively charged NPs [312]. Proteins usually present a higher tendency to electrostatically adsorb to NP surfaces, with a trend that depends on their pI values. Research conducted on polystyrene NPs showed that proteins with lower pI (<5.5), such as albumin, mainly adsorb on positively charged NPs, whereas those with higher pI (~7–8), such as IgG, tend to adsorb on negatively charged NPs [313]. In general, neutral NPs are less prone to non-covalent immobilization of proteins [314]. The layer-by-layer adsorption technique relies on the sequential deposition of alternating layers of anionic and cationic polyelectrolytes on a substrate, providing high loading of ligands, since multilayer structures are formed on the surface of the nanocarriers [315–318].

Examples of electrostatic interactions used as a bioconjugation strategy include the synthesis of polyarginine-tailed anti-EGFR Afbs and its incorporation into methotrexate-loaded 11-mercaptoundecanoic acid-modified gold nanoclusters via charge-based self-assembly, forming a shell to seal in the loaded drug [319]. The targeted system exhibited good biocompatibility, efficient drug loading, precise targeting of EGFR-overexpressing cells and dual-responsive drug release. C225 was electrostatically adsorbed onto polydopamine NPs co-loaded with 5-fluorouracil, irinotecan and leucovorin for metastatic colorectal cancer therapy [320]. Cellular uptake studies performed in HTC116 and HT29 human cell lines revealed rapid NP internalization, beginning after 30 min of incubation. In vitro cytotoxicity assays showed a synergistic effect among the nanocarrier, the encapsulated drugs and the adsorbed mAb, resulting in a reduction in the survival rates of HCT116 and HT29 cells by 22% and 30%, respectively, after 72 h incubation. Liu et al. developed a multifunctional nanodrug delivery system based on gefitinib- and EGFR siRNA-loaded imidazolate framework-8 (Apt/(siRNA + GEF)@ZIF-8 NPs) to suppress the drug-resistant gene expression in tumors (Figure 14) [321]. Anti-EGFR aptamers were conjugated at the surface via electrostatic adsorption, allowing for enhanced accumulation at tumor sites.

Salama et al. investigated the decoration of the surface of PEGylated TiO_2 NPs with EGF via physical adsorption processes [101], demonstrating the safety and increased cellular uptake of the platform when used on EGFR-overexpressing cells.

Despite its accessibility and ease of conjugation, the immobilization of targeting ligands through non-covalent interactions suffers from several shortcomings, including limited stability and random orientation of the surface-adsorbed ligands, which impacts their functionality. Anaki et al. investigated the targeting and therapeutic potential of C225, immobilized on AuNPs through covalent (amide bond) and non-covalent (adsorption) interactions [322]. First, the conjugation efficiency was enhanced at low initial Ab mass through adsorption and at high initial Ab mass through amide coupling. Then, despite the random orientation of surface-conjugated C225, the covalent strategy resulted in enhanced anti-cancer activity on human squamous carcinoma A431 cells, as compared to the non-covalent constructs.
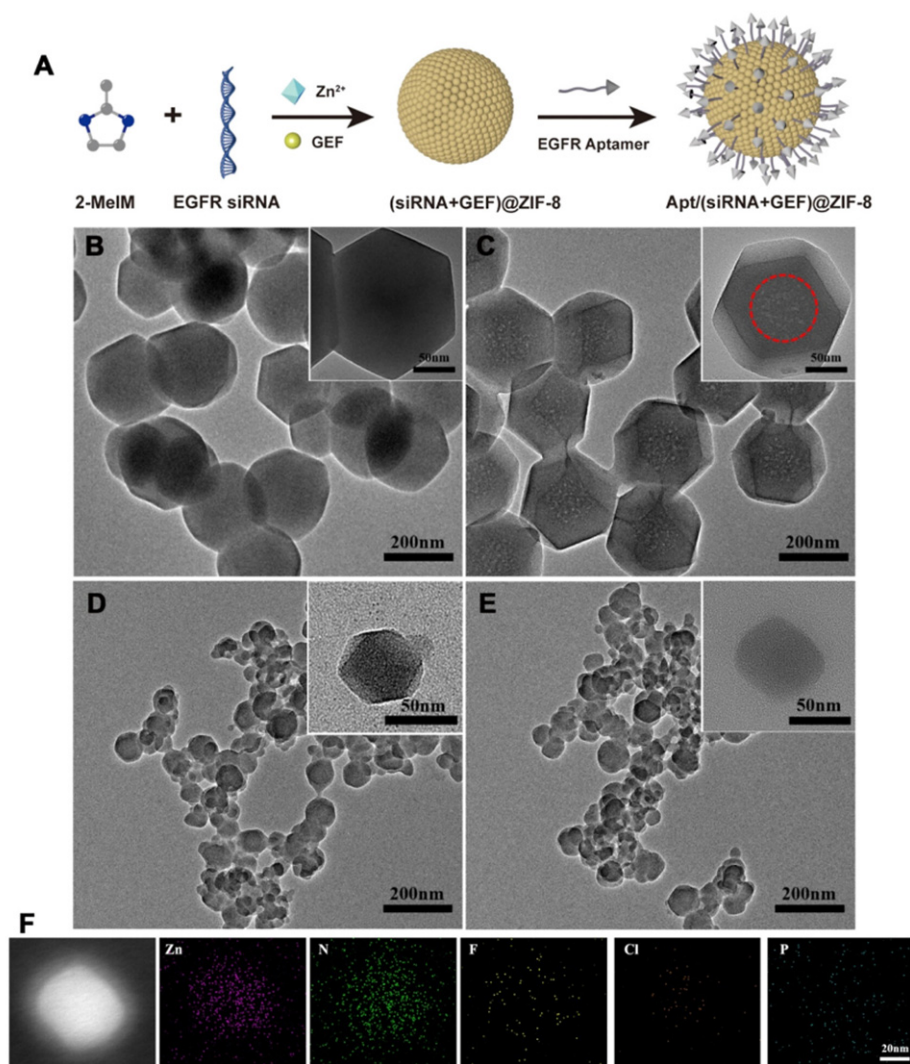
Figure 14. Characterization of multifunctional NPs. (**A**) Schematic illustration of the synthesis procedures for Apt/(siRNA + GEF)@ZIF-8 NPs. (**B**–**E**) TEM analysis of ZIF-8, GEF@ZIF-8, (siRNA + GEF)@ZIF-8 and Apt/(siRNA + GEF)@ZIF-8 NPs, respectively. Red circle highlighting the white dots in (**C**) gives evidence of the successful encapsulation of GEF. (**F**) Dark-field TEM image and elemental mappings of Apt/(siRNA + GEF)@ZIF-8 NPs. Adapted with permission from [321]. Copyright 2022, American Chemical Society.
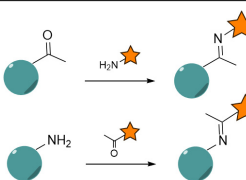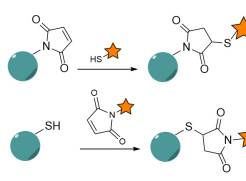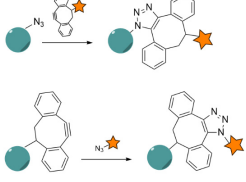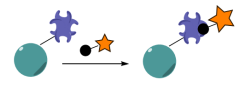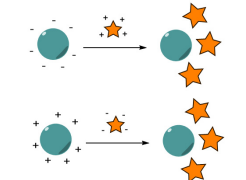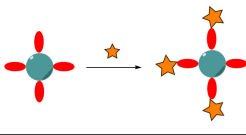
4.2.3. Fc-Binding Receptors Mediated Conjugation

As described above, most of the non-covalent conjugation strategies do not provide a controlled and oriented ligand conjugation, leading to reduced targeting efficiency. Alternatively, the use of Fc-binding protein spacers (i.e., protein A, protein G, protein A/G and Fc receptors) was developed to ensure oriented conjugation.

Hirata et al. reported the use of genetically modified staphylococcal protein A, containing a lysine cluster, for the sequential electrostatic immobilization on anionic liposomes and subsequent binding to the Fc region of anti-EGFR Abs [323]. The Anchored Secondary scFv Enabling Targeting (ASSET) technology [324], which relies on a membrane anchored protein, was applied to the oriented and uniform functionalization of LNPs with anti-EGFR Abs for cell-specific siRNA delivery, resulting in 100% bioconjugation efficiency [325].

Table 5 presents an overview of the available bioconjugation strategies of anti-EGFR ligands to nanocarriers, highlighting their advantages and limitations.

Table 5. Bioconjugation strategies for grafting anti-EGFR ligands to nanocarriers.

Bioconjugation Chemistry	Mechanism	Advantages	Limitations	References
Carbodiimide chemistry		Easy to perform and accessible, generally no need for chemical modification, high stability, high conjugation efficiency	Sensitivity to pH, inability to control orientation, possible competition by extraneous carboxyl or amine groups	[111,137,191,224,269–271]
Schiff base reaction		Mild reaction conditions, possibility of oriented conjugation	Specific functional groups and modifications required, sensitivity to pH	[173,275–277]
Thiol-maleimide chemistry		Fast and efficient reactions, mild reaction conditions, higher selectivity compared to carbodiimide chemistry, possibility of reversible linkages	Inability to control orientation, introduction of linkers or modifications required, possibility to hinder biological activity of ligands after reduction, sensitivity of thioether linkages to endogenous reducing potentials	[116,158,211,231,283]
Dative chemistry		Direct conjugation, no modification or introduction of functional moieties required	Sensitivity to pH, oxidation or replacement by similar molecules, weaker bonds than covalent linkages	[265,266,286,287]
Click chemistry		High selectivity, mild reaction conditions, high yields, favorable reaction rates, irreversible chemical linkages, no complex purification required, biorthogonal reactions, possibility of oriented conjugation	Toxicity of Cu(I) catalyst in CuAAC	[157,227,294,296,298–301]
Interaction by adapter molecules		Strongest non-covalent interaction, oriented conjugation, modifications required, high stability	Non-specific binding mediated by avidin, possible aggregation and big sizes due to the presence of the bulky protein	[308–310]
Electrostatic interaction		No modification required, cost-effective synthesis and post-functionalization	Less robust and more prone to degradation than covalent linkages, sensitive to experimental conditions, non-oriented conjugation	[101,319–322]
Fc-binding receptors mediated conjugation		Oriented conjugation, no modifications required, mild reaction conditions	Weaker nature compared to covalent bonds, potential immune activation due to the presence of Fc regions	[323,325]

5. Characterization Techniques

The last section of this review highlights the main characterization methods (qualitative and/or quantitative) which are currently available to monitor the conjugation of anti-EGFR targeting ligands at the surface of nanocarriers.

5.1. Dynamic Light Scattering

Dynamic light scattering (DLS) is a common technique to evaluate the hydrodynamic size and surface charge (zeta potential) of nanocarriers, based on the intensity of light scattered by the particles during their movement in a medium (Brownian motion) [326]. DLS provides valuable insight into the surface and colloidal properties at different steps of

functionalization. While NP size values have direct impact on their circulation time in the bloodstream and their ability for cell and tissue penetration [327], zeta potential values are linked to their stability in the studied medium. Ab conjugation to the surface of nanocarriers tends to increase their hydrodynamic size (up to 50 nm size increase), as a result of both the steric hindrance of the immobilized ligand [328] and potential NP aggregation [329]. The variation of zeta potential upon functionalization is less significant and depends on several parameters, including the initial NP surface charge (nature and density of reactive moieties), the pI value of the ligand and the pH of the medium (Figure 15) [256,258]. The conjugation of smaller targeting ligands, such as aptamers, leads to smaller variations of the NP hydrodynamic size. For example, Li et al. observed a 3 nm increase of the size of branched RNA four-way junction NPs upon functionalization with EGFR-specific aptamers [330]. In such cases, the assessment of surface conjugation by means of DLS measurement is less reliable.
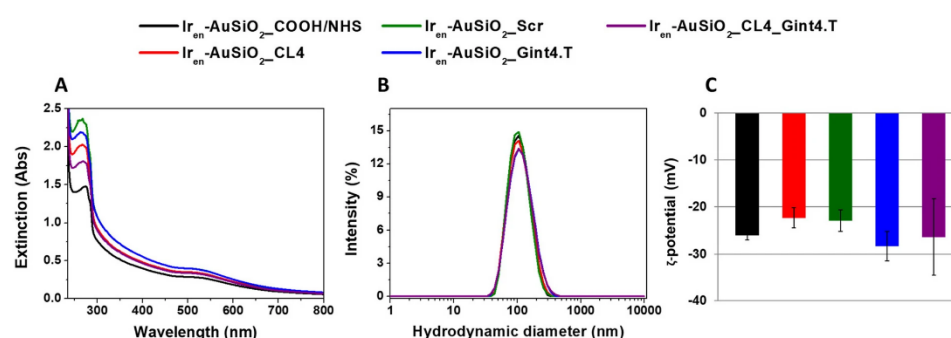

Figure 15. Characterization of aptamer-functionalized NPs at different steps of functionalization. (**A**) UV-Vis spectra. (**B**) Hydrodynamic diameters. (**C**) Zeta potential values of the systems dispersed in water. Adapted with permission from [258]. Copyright 2024, Springer Nature.

Noticeably, the hydrodynamic size of nanocarriers might also be reduced upon surface functionalization. Cruz de Sousa et al. reported that cabazitaxel-loaded liposomes evolved from 136.7 ± 2.2 to 95.0 ± 3.9 nm upon thiol-maleimide mediated conjugation of C225 [331]. The authors validated the Ab immobilization by gel electrophoresis and ELISA test, which confirmed the preserved structure and conformation for receptor binding.

DLS measurements provide valuable indications on the evolution of the hydrodynamic sizes and surface charge of nanocarriers along functionalization pathways. However, additional characterizations are needed to give evidence for the conjugation to targeting ligands.

5.2. Fluorescence Experiments

A more reliable and quantitative characterization method consists in the fluorescence detection of targeting agents, mainly Abs, at the NPs surface, using either the direct fluorescence emission of labelled targeting Abs or the indirect fluorescence emission of a labelled secondary Ab. Recording the fluorescence emission levels of Alexa Fluor 555-labelled anti-EGFR Abs conjugated to BTNPs allowed to quantify the Ab concentration in studied samples, with values of 4.59 ± 1.67 µg/mL [173]. For the indirect characterization of anti-EGFR Ab conjugation to PLGA-based NPs, secondary complementary Abs labelled with Dylight 488 [332] or fluorescein (Figure 16) [333] were reported.
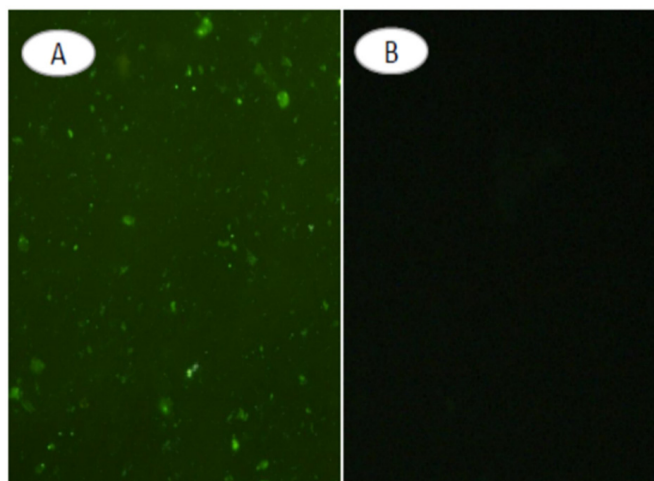
Figure 16. Microscopy images of the secondary Ab labeled with fluorescein bound to mAb-functionalized PLGA NPs. (**A**) mAb-functionalized PLGA NPs were incubated with fluorescein-conjugated secondary Ab. (**B**) mAb-functionalized PLGA NPs without fluorophore. Adapted with permission from [333]. Copyright 2020, Elsevier.

5.3. Electrophoretic Techniques

Surface bound proteins and oligonucleotides can be evidenced by electrophoretic techniques. In particular, proteins are separated by molecular mass using sodium dodecyl sulfate (SDS)-polyacrylamide (PAGE) gel electrophoresis [334,335], while agarose gel electrophoresis is applied to charged molecules like DNA/RNA [336]. Successful functionalization is indicated by a fluorescent band of ligand-functionalized NPs at the baseline, with no visible band for free ligands (Figure 17).
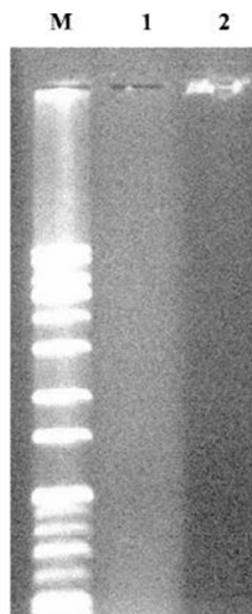

Figure 17. Characterization of aptamer-decorated erlotinib-loaded chitosan NPs. Agarose gel electrophoresis of (1) erlotinib-loaded chitosan NPs and (2) aptamer-decorated erlotinib-loaded chitosan NPs. Adapted with permission from [337]. Copyright 2020, Elsevier.

Table 6 presents examples of nanocarriers functionalized with anti-EGFR targeting ligands and characterized through electrophoretic techniques.

Table 6. Examples of nanocarriers functionalized with anti-EGFR ligands and characterized via electrophoretic techniques.

Targeting Ligand	NP Type	Electrophoretic Method	References
Anti-EGFR Abs	AuNPs	SDS-PAGE	[168]
Anti-EGFR Abs	PLGA NPs	SDS-PAGE	[338]
Anti-EGFR aptamers	Chitosan NPs	Agarose gel electrophoresis	[337]
Anti-EGFR aptamers	Liposomes	Agarose gel electrophoresis	[339]

Similar to light scattering methods, electrophoretic techniques do not provide a precise quantification of the grafted agents, but can be used as qualitative assessment of the presence of the ligands.

5.4. Protein-Based Assays

When protein-based targeting ligands are used, two commonly employed colorimetric quantification methods are the Bradford assay [340] and the bicinchoninic (BCA) assay [341].

The first one is based on the absorption shift—from 465 to 595 nm—that is observed in the spectrum of the Coomassie brilliant blue dye when bound to a protein [342]. This simple method allows for quantification of surface-conjugated proteins and is compatible with most solvents, reducing agents and salts. However, it cannot be performed in the presence of surfactants, even at low concentrations, and suffers from high protein-to-protein variation and linearity over a narrow window of concentrations.

More sensitive and reliable than the Bradford assay is the BCA assay. The BCA assay relies on the formation of Cu^{2+}-protein complex under alkaline conditions and subsequent reduction to Cu^+ ions, which are quantified upon formation of a Cu^{+1}-$(BCA)_2$ complex characterized by a deep blue color and absorption maximum at 562 nm [343]. This assay is characterized by a detection range of 20–2000 μg/mL (5–250 μg/mL for enhanced BCA assay) and is less prone to interference from non-protein sources, including lipids and detergents, that can impact other protein-based assays. In addition, it provides a high protein-to-protein uniformity, not being affected by differences in protein compositions. However, BCA assay is longer to perform, with incubation times ranging from 30 min to 2 h. Furthermore, the presence of reducing agents or copper chelating agents could impact the reliability of the results.

Table 7 shows examples of nanocarriers functionalized with peptides or proteins anti-EGFR targeting ligands and characterized through protein-based techniques.

Table 7. Examples of nanocarriers functionalized with anti-EGFR ligands and characterized via protein-based techniques.

Targeting Ligand	NP Type	Result of Quantification	References
C225	Chitosan/hyaluronic acid NPs	Bradford assay revealed a degree of conjugation of 81.5%.	[344]
C225	Sialic acid-coated chitosan NPs	Bradford assay revealed a degree of conjugation of 72.9% ± 3.5% for chitosan NPs, and of 63.2% ± 2.1% for sialic acid-coated chitosan NPs. The second is lower probably due to the presence of sialic acid residues along with C225.	[345]
C225	Silica-coated AuNPs	BCA assay performed on the supernatant revealed 91% ± 6% of Abs conjugated to the NP surface.	[346]
GE11	DOX-loaded extracellular vesicles	BCA assay was performed to measure the total protein content of EVs and used to add equivalent EVs to EGFR-overexpressing cell lines (uptake value to be compared with the uptake by EGFR-negative cell lines).	[347]

In conclusion, the presence and density of protein ligands conjugated to nanocarriers can be efficiently assessed by the BCA and Bradford assays.

5.5. Spectroscopy Techniques

Spectroscopy methods, such as Fourier Transform IR spectroscopy (FTIR), nuclear magnetic resonance (NMR) and X-ray photoelectron spectroscopy (XPS), can be used for qualitative investigation of NP surface-conjugated targeting ligands. FTIR allows for the identification of surface functionalities according to their vibrational signatures (Figure 18) [348,349], and for their quantification in case a standard curve of known concentrations of the sample is available. NMR is a non-destructive physicochemical analytical technique capable of elucidating structural and dynamic properties of complex nanocarriers [350]. While detailed characterization at the atomic level is not possible for high molecular mass systems beyond 50 kDa, solid- and liquid-state NMR provide insights into the chemical structure and location of surface bound ligands and the nature of their interactions with the nanocarrier. Quantitative or semi-quantitative evaluation of the density of surface functionalities can also be achieved by NMR [351]. XPS is extensively used for surface characterization, providing semi-quantitative analysis of the chemical elements composing the material surface, except hydrogen and helium [352]. Applied to functionalized NPs, XPS allows to assess surface elemental composition, presence of contaminants, density of surface immobilized molecules, and thickness of layers and coatings [353].
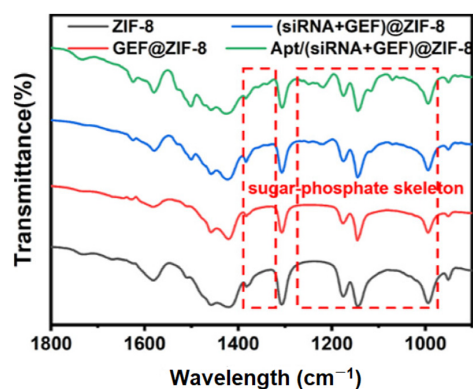

Figure 18. FTIR spectra of the aptamer-functionalized NPs at different steps of functionalization. Adapted with permission from [321]. Copyright 2023, American Chemical Society.

The examples listed in Table 8 illustrate the versatility of spectroscopy techniques to investigate functionalized nanocarriers and characterize their payloads and surface-conjugated targeting ligands.

Table 8. Examples of nanocarriers functionalized with anti-EGFR ligands and characterized via spectroscopic techniques.

Targeting Ligand	NP Type	Characterization Technique	Analyzed Components	References
Anti-EGFR Ab (Nm)	AuNPs	FTIR	Appearance of a small peak at 3300 cm^{-1}, related to the region of amide A formed by the crosslinking between the Abs and the NHS linker causing a N-H stretch, was detected. The band at 1600–1700 cm^{-1} revealed the presence of amide-I band related to the amide C=O stretching vibrations. The band at 2500–2600 cm^{-1} indicated the presence of S-H in the conjugates coming from the thiol-gold bond.	[168]

Table 8. *Cont.*

Targeting Ligand	NP Type	Characterization Technique	Analyzed Components	References
Anti-EGFR aptamer	ZIF-8 NPs	FTIR	Special adsorption of the sugar-phosphate skeleton of siRNA and aptamers related with the peaks from 1300 to 900 and 1320 to 1380 cm^{-1} was observed.	[321]
GE11	DOX-loaded polymeric conjugates	^{1}H NMR	Additional peaks corresponding to the GE11 peptide appeared at 6.98–6.63 ppm, revealing successful conjugation of the peptide to the NP surface.	[116]
C225	Chitosan NPs	XPS	Percentages of N 1s, O 1s and C 1s in the targeted system were 9.74%, 22.54% and 67.74%, respectively, whereas for the non-targeted counterpart, these were of 1.04%, 15.19% and 83.77%. The higher percentage nitrogen in the targeted platform indicated the presence of a large number of nitrogen atoms (N = 1732) in the Ab molecules.	[354]
C225	Chitosan/hyaluronic acid NPs	XPS	Atomic percentage of N exhibited a significant increase from 3.53% in the non-targeted system to 7.74% in the targeted system, together with the apparition of a sulfur peak (0.13%). The phosphorous peak due to the crosslinker used during the ionic gelation of NPs was significantly decreased in the case of the targeted system, further indication of NP functionalization.	[344]

5.6. Thermogravimetric Analysis

Thermogravimetric analysis (TGA), which evaluates the change in mass of a sample as a function of temperature and time under controlled conditions, can be applied to the detection of organic ligands conjugated to inorganic NPs [355]. While it does not require any special sample preparation beyond drying, TGA is a destructive characterization method, consuming several milligrams of material [356].

Wang et al. developed neutron-activated ^{153}Sm-filled multi-walled carbon nanotubes, which were further conjugated to C225 and evaluated for their therapeutic efficiency in a lung metastatic melanoma model [357]. TGA analysis of the constructs at 650 °C allowed for the quantification of immobilized Ab (220 mg/g material, Figure 19), in line with the value obtained via the BCA assay (173 mg/g).
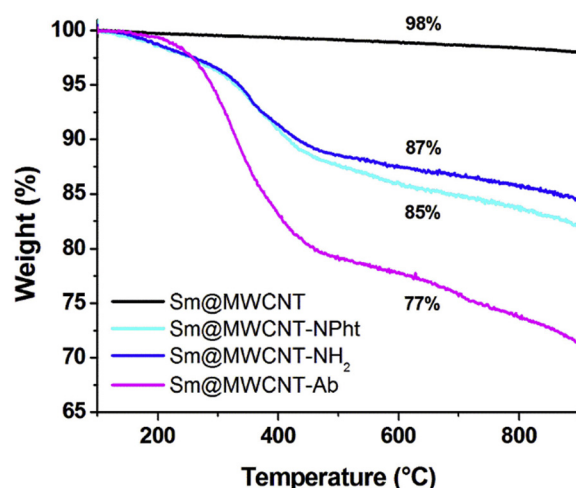

Figure 19. TGA curves of Ab-functionalized NPs at different steps of functionalization. The analyses were performed under N$_2$ using a ramp of 10 °C/min. The level of functionalization was calculated from the weight loss values at 650 °C. Adapted with permission from [357]. Copyright 2020, Elsevier.

However, another study focusing on EGF-functionalized nanoceria pointed toward a diminution of the weight loss after ligand conjugation, which was probably resulting from partial detachment of the coating layer upon EGF immobilization [358].

TGA is therefore a valuable technique to assess and quantify immobilized ligands at the surface of nanocarriers but is limited to the study of functionalized inorganic NPs.

Table 9 provides a summary of the available characterization methods to monitor the correct grafting of anti-EGFR targeting agents to nanocarriers.

Table 9. Characterization methods to evaluate the conjugation of anti-EGFR targeting ligands at the NP surface.

Characterization Technique	Type of Information	Purpose	Advantages	Limitations	References
Dynamic light scattering	Qualitative	Measurement of hydrodynamic size, polydispersity and surface charge	Quick and easy to perform, any types of NPs	Often not reliable or informative enough, no quantification possible	[256,258,328–331]
Fluorescence experiments	Quantitative	Measurements of the density of ligands via indirect or direct fluorescence reading	Generally high sensitivity; precise quantification via comparison with calibration standards	Modification of ligand with fluorophore or use of fluorophore-tagged secondary ligand is required, thorough purification to remove excess of fluorophore-tagged ligand is needed	[173,332,333]
Electrophoretic techniques	Qualitative	Separation and visualization of protein or DNA-based ligands depending on their migration rates	Visual method	Mainly used for protein and oligonucleotide ligands, quantification is generally difficult to perform	[168,337–339]
Protein-based assays	Quantitative	Measurements of the density of protein ligands by absorbance readings	Sensitive methods, precise quantification possible, fast procedures	Only protein-based ligands can be investigated, sensitivity to reducing agents or detergents is observed	[344–347]
Spectroscopy techniques	Qualitative	Determine the nature of surface functional groups, identify the elemental composition and investigate molecular structure of ligands	different types of NPs can be investigated	Quantification not possible (except in some techniques by using calibration standards), high densities and thorough purification are required in some techniques	[116,168,321,344,354]
Thermogravimetric analysis	Qualitative /quantitative	Measure mass change depending on temperature to determine the surface coverage	Quantification is possible, simple procedure	Usable only to investigate surface of inorganic NPs, high amount of material is generally required for analysis	[357,358]

6. Conclusions

Active targeting has been shown to offer several advantages over passive targeting in improving the efficacy and specificity of cancer therapeutics. This type of approach relies on the presence of ligands that recognize specific receptors, including EGFR, which are overexpressed on the surface of cancer cells. Nanodelivery systems functionalized with EGFR-targeting ligands at their surface have been increasingly investigated as promising tools to achieve enhanced specificity via receptor-mediated endocytosis.

Several anti-EGFR targeting agents, such as peptides, proteins, Abs, Ab fragments and oligonucleotides, have been identified and are currently used. The selection of the most appropriate ligand for NP functionalization depends on the specific application, since they all have different binding affinities for EGFR and each class of ligands has its own benefits and drawbacks. Various bioconjugation strategies are available for grafting anti-EGFR agents to nanocarriers' surfaces, among which are non-covalent and covalent linkages. The choice of the

conjugation chemistry plays a vital role in the determination of the final stability and efficacy of the functionalized nanocarrier. In general, opting for a chemical approach that allows for achieving oriented conjugation of the ligands leads to improved interaction between the targeting agents and the receptors, resulting in enhanced targeting efficiency. In addition, reliable characterization techniques are essential to investigate the surface functionalization pattern, including the chemical composition, integrity and density of immobilized ligands, the nature of the conjugation interactions and the stability of the nanoconstructs.

In conclusion, nanocarriers modified with anti-EGFR targeting ligands represent a promising approach for targeted cancer therapy, offering enhanced specificity and efficacy for cancer treatment. The integration of the design of functionalized nanocarriers, appropriate conjugation strategies and reliable characterization methods is critical to improve cancer therapy and patient outcomes.

Author Contributions: Conceptualization, analysis, writing—original draft preparation, writing—review and editing, A.S.; writing—review and editing, project administration, funding acquisition, S.G.-L. All authors have read and agreed to the published version of the manuscript.

Data Availability Statement: We do not present original data in the manuscript as it is a review article.

Conflicts of Interest: The authors declare no conflicts of interest. The funders had no role in the writing of the manuscript or in the decision to publish this review.

References

1. Gavas, S.; Quazi, S.; Karpiński, T.M. Nanoparticles for Cancer Therapy: Current Progress and Challenges. *Nanoscale Res. Lett.* **2021**, *16*, 173. [CrossRef]
2. Chehelgerdi, M.; Chehelgerdi, M.; Allela, O.Q.B.; Pecho, R.D.C.; Jayasankar, N.; Rao, D.P.; Thamaraikani, T.; Vasanthan, M.; Viktor, P.; Lakshmaiya, N.; et al. Progressing Nanotechnology to Improve Targeted Cancer Treatment: Overcoming Hurdles in Its Clinical Implementation. *Mol. Cancer* **2023**, *22*, 169. [CrossRef] [PubMed]
3. Fonseca, M.; Jarak, I.; Victor, F.; Domingues, C.; Veiga, F.; Figueiras, A. Polymersomes as the Next Attractive Generation of Drug Delivery Systems: Definition, Synthesis and Applications. *Materials* **2024**, *17*, 319. [CrossRef] [PubMed]
4. Wang, J.; Li, B.; Qiu, L.; Qiao, X.; Yang, H. Dendrimer-Based Drug Delivery Systems: History, Challenges, and Latest Developments. *J. Biol. Eng.* **2022**, *16*, 18. [CrossRef] [PubMed]
5. Bose, A.; Roy Burman, D.; Sikdar, B.; Patra, P. Nanomicelles: Types, Properties and Applications in Drug Delivery. *IET Nanobiotechnol.* **2021**, *15*, 19–27. [CrossRef] [PubMed]
6. Vallet-Regí, M.; Schüth, F.; Lozano, D.; Colilla, M.; Manzano, M. Engineering Mesoporous Silica Nanoparticles for Drug Delivery: Where Are We after Two Decades? *Chem. Soc. Rev.* **2022**, *51*, 5365–5451. [CrossRef]
7. Montiel Schneider, M.G.; Martín, M.J.; Otarola, J.; Vakarelska, E.; Simeonov, V.; Lassalle, V.; Nedyalkova, M. Biomedical Applications of Iron Oxide Nanoparticles: Current Insights Progress and Perspectives. *Pharmaceutics* **2022**, *14*, 204. [CrossRef] [PubMed]
8. Yafout, M.; Ousaid, A.; Khayati, Y.; El Otmani, I.S. Gold Nanoparticles as a Drug Delivery System for Standard Chemotherapeutics: A New Lead for Targeted Pharmacological Cancer Treatments. *Sci. Afr.* **2021**, *11*, e00685. [CrossRef]
9. Hamidu, A.; Pitt, W.G.; Husseini, G.A. Recent Breakthroughs in Using Quantum Dots for Cancer Imaging and Drug Delivery Purposes. *Nanomaterials* **2023**, *13*, 2566. [CrossRef] [PubMed]
10. Nsairat, H.; Khater, D.; Sayed, U.; Odeh, F.; Al Bawab, A.; Alshaer, W. Liposomes: Structure, Composition, Types, and Clinical Applications. *Heliyon* **2022**, *8*, e09394. [CrossRef] [PubMed]
11. Mehta, M.; Bui, T.A.; Yang, X.; Aksoy, Y.; Goldys, E.M.; Deng, W. Lipid-Based Nanoparticles for Drug/Gene Delivery: An Overview of the Production Techniques and Difficulties Encountered in Their Industrial Development. *ACS Mater. Au* **2023**, *3*, 600–619. [CrossRef] [PubMed]
12. Zielińska, A.; Carreiró, F.; Oliveira, A.M.; Neves, A.; Pires, B.; Venkatesh, D.N.; Durazzo, A.; Lucarini, M.; Eder, P.; Silva, A.M.; et al. Polymeric Nanoparticles: Production, Characterization, Toxicology and Ecotoxicology. *Molecules* **2020**, *25*, 3731. [CrossRef] [PubMed]

13. Tonga, G.Y.; Moyano, D.F.; Kim, C.S.; Rotello, V.M. Inorganic Nanoparticles for Therapeutic Delivery: Trials, Tribulations and Promise. *Curr. Opin. Colloid Interface Sci.* **2014**, *19*, 49–55. [CrossRef]

14. Khalid, K.; Tan, X.; Mohd Zaid, H.F.; Tao, Y.; Lye Chew, C.; Chu, D.-T.; Lam, M.K.; Ho, Y.-C.; Lim, J.W.; Chin Wei, L. Advanced in Developmental Organic and Inorganic Nanomaterial: A Review. *Bioengineered* **2020**, *11*, 328–355. [CrossRef] [PubMed]

15. Bhatti, R.; Shakeel, H.; Malik, K.; Qasim, M.; Khan, M.A.; Ahmed, N.; Jabeen, S. Inorganic Nanoparticles: Toxic Effects, Mechanisms of Cytotoxicity and Phytochemical Interactions. *Adv. Pharm. Bull.* **2022**, *12*, 757–762. [CrossRef] [PubMed]

16. Dhiman, N.; Awasthi, R.; Sharma, B.; Kharkwal, H.; Kulkarni, G.T. Lipid Nanoparticles as Carriers for Bioactive Delivery. *Front. Chem.* **2021**, *9*, 580118. [CrossRef]

17. Ghasemiyeh, P.; Mohammadi-Samani, S. Solid Lipid Nanoparticles and Nanostructured Lipid Carriers as Novel Drug Delivery Systems: Applications, Advantages and Disadvantages. *Res. Pharm. Sci.* **2018**, *13*, 288–303. [CrossRef] [PubMed]

18. Sun, L.; Liu, H.; Ye, Y.; Lei, Y.; Islam, R.; Tan, S.; Tong, R.; Miao, Y.-B.; Cai, L. Smart Nanoparticles for Cancer Therapy. *Signal Transduct. Target. Ther.* **2023**, *8*, 418. [CrossRef] [PubMed]

19. Abbasi, R.; Shineh, G.; Mobaraki, M.; Doughty, S.; Tayebi, L. Structural Parameters of Nanoparticles Affecting Their Toxicity for Biomedical Applications: A Review. *J. Nanopart. Res.* **2023**, *25*, 43. [CrossRef] [PubMed]

20. Elumalai, K.; Srinivasan, S.; Shanmugam, A. Review of the Efficacy of Nanoparticle-Based Drug Delivery Systems for Cancer Treatment. *Biomed. Technol.* **2024**, *5*, 109–122. [CrossRef]

21. Yoo, H.; Kim, Y.; Kim, J.; Cho, H.; Kim, K. Overcoming Cancer Drug Resistance with Nanoparticle Strategies for Key Protein Inhibition. *Molecules* **2024**, *29*, 3994. [CrossRef] [PubMed]

22. Yang, L.; Zhang, Y.; Lai, Y.; Xu, W.; Lei, S.; Chen, G.; Wang, Z. A Computer-Aided, Heterodimer-Based "Triadic" Carrier-Free Drug Delivery Platform to Mitigate Multidrug Resistance in Lung Cancer and Enhance Efficiency. *J. Colloid Interface Sci.* **2025**, *677*, 523–540. [CrossRef] [PubMed]

23. Yusuf, A.; Almotairy, A.R.Z.; Henidi, H.; Alshehri, O.Y.; Aldughaim, M.S. Nanoparticles as Drug Delivery Systems: A Review of the Implication of Nanoparticles' Physicochemical Properties on Responses in Biological Systems. *Polymers* **2023**, *15*, 1596. [CrossRef] [PubMed]

24. Mahmoudi, M.; Landry, M.P.; Moore, A.; Coreas, R. The Protein Corona from Nanomedicine to Environmental Science. *Nat. Rev. Mater.* **2023**, *8*, 422–438. [CrossRef] [PubMed]

25. Zhang, M.; Gao, S.; Yang, D.; Fang, Y.; Lin, X.; Jin, X.; Liu, Y.; Liu, X.; Su, K.; Shi, K. Influencing Factors and Strategies of Enhancing Nanoparticles into Tumors in Vivo. *Acta Pharm. Sin. B* **2021**, *11*, 2265–2285. [CrossRef] [PubMed]

26. Hoshyar, N.; Gray, S.; Han, H.; Bao, G. The Effect of Nanoparticle Size on in Vivo Pharmacokinetics and Cellular Interaction. *Nanomedicine* **2016**, *11*, 673–692. [CrossRef]

27. Grandhi, S.; Al-Tabakha, M.; Avula, P.R. Enhancement of Liver Targetability through Statistical Optimization and Surface Modification of Biodegradable Nanocapsules Loaded with Lamivudine. *Adv. Pharmacol. Pharm. Sci.* **2023**, *2023*, 8902963. [CrossRef]

28. Blanco, E.; Shen, H.; Ferrari, M. Principles of Nanoparticle Design for Overcoming Biological Barriers to Drug Delivery. *Nat. Biotechnol.* **2015**, *33*, 941–951. [CrossRef] [PubMed]

29. Suk, J.S.; Xu, Q.; Kim, N.; Hanes, J.; Ensign, L.M. PEGylation as a Strategy for Improving Nanoparticle-Based Drug and Gene Delivery. *Adv. Drug Deliv. Rev.* **2016**, *99*, 28–51. [CrossRef] [PubMed]

30. Wang, Y.; Zhan, J.; Huang, J.; Wang, X.; Chen, Z.; Yang, Z.; Li, J. Dynamic Responsiveness of Self-Assembling Peptide-Based Nano-Drug Systems. *Interdiscip. Med.* **2023**, *1*, e20220005. [CrossRef]

31. Chen, Z.; Kankala, R.K.; Long, L.; Xie, S.; Chen, A.; Zou, L. Current Understanding of Passive and Active Targeting Nanomedicines to Enhance Tumor Accumulation. *Coord. Chem. Rev.* **2023**, *481*, 215051. [CrossRef]

32. Wu, J. The Enhanced Permeability and Retention (EPR) Effect: The Significance of the Concept and Methods to Enhance Its Application. *J. Pers. Med.* **2021**, *11*, 771. [CrossRef] [PubMed]

33. Subhan, M.A.; Parveen, F.; Filipczak, N.; Yalamarty, S.S.K.; Torchilin, V.P. Approaches to Improve EPR-Based Drug Delivery for Cancer Therapy and Diagnosis. *J. Pers. Med.* **2023**, *13*, 389. [CrossRef] [PubMed]

34. Matsumura, Y.; Maeda, H. A New Concept for Macromolecular Therapeutics in Cancer Chemotherapy: Mechanism of Tumoritropic Accumulation of Proteins and the Antitumor Agent Smancs. *Cancer Res.* **1986**, *46*, 6387–6392. [PubMed]

35. Hori, K.; Suzuki, M.; Tanda, S.; Saito, S.; Shinozaki, M.; Zhang, Q.-H. Fluctuations in Tumor Blood Flow under Normotension and the Effect of Angiotensin II-Induced Hypertension. *Jpn. J. Cancer Res.* **1991**, *82*, 1309–1316. [CrossRef]

36. Shi, J.; Kantoff, P.W.; Wooster, R.; Farokhzad, O.C. Cancer Nanomedicine: Progress, Challenges and Opportunities. *Nat. Rev. Cancer* **2017**, *17*, 20–37. [CrossRef] [PubMed]

37. Carita, A.C.; Eloy, J.O.; Chorilli, M.; Lee, R.J.; Leonardi, G.R. Recent Advances and Perspectives in Liposomes for Cutaneous Drug Delivery. *Curr. Med. Chem.* **2018**, *25*, 606–635. [CrossRef] [PubMed]

38. Chen, H.; Zhang, W.; Zhu, G.; Xie, J.; Chen, X. Rethinking Cancer Nanotheranostics. *Nat. Rev. Mater.* **2017**, *2*, 17024. [CrossRef] [PubMed]

39. Liu, X.; Jiang, J.; Meng, H. Transcytosis—An Effective Targeting Strategy That Is Complementary to "EPR Effect" for Pancreatic Cancer Nano Drug Delivery. *Theranostics* **2019**, *9*, 8018. [CrossRef] [PubMed]

40. Zhang, Y.; Cao, J.; Yuan, Z. Strategies and Challenges to Improve the Performance of Tumor-Associated Active Targeting. *J. Mater. Chem. B* **2020**, *8*, 3959–3971. [CrossRef] [PubMed]

41. Salahpour Anarjan, F. Active Targeting Drug Delivery Nanocarriers: Ligands. *Nano-Struct. Nano-Objects* **2019**, *19*, 100370. [CrossRef]

42. Morales-Cruz, M.; Delgado, Y.; Castillo, B.; Figueroa, C.M.; Molina, A.M.; Torres, A.; Milián, M.; Griebenow, K. Smart Targeting to Improve Cancer Therapeutics. *Drug Des. Dev. Ther.* **2019**, *13*, 3753–3772. [CrossRef] [PubMed]

43. Yan, S.; Na, J.; Liu, X.; Wu, P. Different Targeting Ligands-Mediated Drug Delivery Systems for Tumor Therapy. *Pharmaceutics* **2024**, *16*, 248. [CrossRef] [PubMed]

44. Akhtar, M.J.; Ahamed, M.; Alhadlaq, H.A.; Alrokayan, S.A.; Kumar, S. Targeted Anticancer Therapy: Overexpressed Receptors and Nanotechnology. *Clin. Chim. Acta* **2014**, *436*, 78–92. [CrossRef] [PubMed]

45. Thomas, R.; Weihua, Z. Rethink of EGFR in Cancer with Its Kinase Independent Function on Board. *Front. Oncol.* **2019**, *9*, 800. [CrossRef] [PubMed]

46. Salomon, D.S.; Brandt, R.; Ciardiello, F.; Normanno, N. Epidermal Growth Factor-Related Peptides and Their Receptors in Human Malignancies. *Crit. Rev. Oncol. Hematol.* **1995**, *19*, 183–232. [CrossRef] [PubMed]

47. Mitsudomi, T.; Yatabe, Y. Epidermal Growth Factor Receptor in Relation to Tumor Development: EGFR Gene and Cancer. *FEBS J.* **2010**, *277*, 301–308. [CrossRef] [PubMed]

48. Tian, X.; Zhang, H.; Han, Y.; Gu, B.; Zhang, Z. Current Status and Future Prospects of Combined Immunotherapy and Epidermal Growth Factor Receptor Inhibitors in Head and Neck Squamous Cell Carcinoma. *Cancer Treat. Rev.* **2025**, *132*, 102864. [CrossRef] [PubMed]

49. Saba, N.F.; Chen, Z.G.; Haigentz, M.; Bossi, P.; Rinaldo, A.; Rodrigo, J.P.; Mäkitie, A.A.; Takes, R.P.; Strojan, P.; Vermorken, J.B.; et al. Targeting the EGFR and Immune Pathways in Squamous Cell Carcinoma of the Head and Neck (SCCHN): Forging a New Alliance. *Mol. Cancer Ther.* **2019**, *18*, 1909–1915. [CrossRef]

50. Li, L.; Deng, L.; Meng, X.; Gu, C.; Meng, L.; Li, K.; Zhang, X.; Meng, Y.; Xu, W.; Zhao, L.; et al. Tumor-Targeting Anti-EGFR x Anti-PD1 Bispecific Antibody Inhibits EGFR-Overexpressing Tumor Growth by Combining EGFR Blockade and Immune Activation with Direct Tumor Cell Killing. *Transl. Oncol.* **2021**, *14*, 100916. [CrossRef] [PubMed]

51. Rubio-Pérez, L.; Lázaro-Gorines, R.; Harwood, S.L.; Compte, M.; Navarro, R.; Tapia-Galisteo, A.; Bonet, J.; Blanco, B.; Lykkemark, S.; Ramírez-Fernández, Á.; et al. A PD-L1/EGFR Bispecific Antibody Combines Immune Checkpoint Blockade and Direct Anti-Cancer Action for an Enhanced Anti-Tumor Response. *OncoImmunology* **2023**, *12*, 2205336. [CrossRef]

52. Li, Y.; Du, Y.; Liang, X.; Sun, T.; Xue, H.; Tian, J.; Jin, Z. EGFR-Targeted Liposomal Nanohybrid Cerasomes: Theranostic Function and Immune Checkpoint Inhibition in a Mouse Model of Colorectal Cancer. *Nanoscale* **2018**, *10*, 16738–16749. [CrossRef]

53. Ardeshiri, K.; Hassannia, H.; Ghalamfarsa, G.; Jafary, H.; Jadidi, F. Simultaneous Blockade of the CD73/EGFR Axis Inhibits Tumor Growth. *IUBMB Life* **2025**, *77*, e2933. [CrossRef] [PubMed]

54. Sapsford, K.E.; Algar, W.R.; Berti, L.; Gemmill, K.B.; Casey, B.J.; Oh, E.; Stewart, M.H.; Medintz, I.L. Functionalizing Nanoparticles with Biological Molecules: Developing Chemistries That Facilitate Nanotechnology. *Chem. Rev.* **2013**, *113*, 1904–2074. [CrossRef] [PubMed]

55. Marques, A.C.; Costa, P.J.; Velho, S.; Amaral, M.H. Functionalizing Nanoparticles with Cancer-Targeting Antibodies: A Comparison of Strategies. *J. Control. Release* **2020**, *320*, 180–200. [CrossRef]

56. Yi, W.; Xiao, P.; Liu, X.; Zhao, Z.; Sun, X.; Wang, J.; Zhou, L.; Wang, G.; Cao, H.; Wang, D.; et al. Recent Advances in Developing Active Targeting and Multi-Functional Drug Delivery Systems via Bioorthogonal Chemistry. *Signal Transduct. Target. Ther.* **2022**, *7*, 386. [CrossRef] [PubMed]

57. Attia, M.F.; Anton, N.; Wallyn, J.; Omran, Z.; Vandamme, T.F. An Overview of Active and Passive Targeting Strategies to Improve the Nanocarriers Efficiency to Tumour Sites. *J. Pharm. Pharmacol.* **2019**, *71*, 1185–1198. [CrossRef]

58. Nguyen, P.V.; Allard-Vannier, E.; Chourpa, I.; Hervé-Aubert, K. Nanomedicines Functionalized with Anti-EGFR Ligands for Active Targeting in Cancer Therapy: Biological Strategy, Design and Quality Control. *Int. J. Pharm.* **2021**, *605*, 120795. [CrossRef] [PubMed]

59. Carpenter, G.; King, L.; Cohen, S. Epidermal Growth Factor Stimulates Phosphorylation in Membrane Preparations in Vitro. *Nature* **1978**, *276*, 409–410. [CrossRef]

60. Purba, E.R.; Saita, E.; Maruyama, I.N. Activation of the EGF Receptor by Ligand Binding and Oncogenic Mutations: The "Rotation Model". *Cells* **2017**, *6*, 13. [CrossRef] [PubMed]

61. Chia, C.M.; Winston, R.M.L.; Handyside, A.H. EGF, TGF-α and EGFR Expression in Human Preimplantation Embryos. *Development* **1995**, *121*, 299–307. [CrossRef]

62. Kaufman, N.E.M.; Dhingra, S.; Jois, S.D.; Vicente, M.d.G.H. Molecular Targeting of Epidermal Growth Factor Receptor (EGFR) and Vascular Endothelial Growth Factor Receptor (VEGFR). *Molecules* **2021**, *26*, 1076. [CrossRef] [PubMed]

63. Hubbard, S.R.; Till, J.H. Protein Tyrosine Kinase Structure and Function. *Annu. Rev. Biochem.* **2000**, *69*, 373–398. [CrossRef] [PubMed]

64. Dawson, J.P.; Berger, M.B.; Lin, C.-C.; Schlessinger, J.; Lemmon, M.A.; Ferguson, K.M. Epidermal Growth Factor Receptor Dimerization and Activation Require Ligand-Induced Conformational Changes in the Dimer Interface. *Mol. Cell. Biol.* **2005**, *25*, 7734–7742. [CrossRef]

65. London, M.; Gallo, E. Epidermal Growth Factor Receptor (EGFR) Involvement in Epithelial-Derived Cancers and Its Current Antibody-Based Immunotherapies. *Cell Biol. Int.* **2020**, *44*, 1267–1282. [CrossRef] [PubMed]

66. Rodriguez, S.M.B.; Kamel, A.; Ciubotaru, G.V.; Onose, G.; Sevastre, A.-S.; Sfredel, V.; Danoiu, S.; Dricu, A.; Tataranu, L.G. An Overview of EGFR Mechanisms and Their Implications in Targeted Therapies for Glioblastoma. *Int. J. Mol. Sci.* **2023**, *24*, 11110. [CrossRef] [PubMed]

67. Sigismund, S.; Avanzato, D.; Lanzetti, L. Emerging Functions of the EGFR in Cancer. *Mol. Oncol.* **2018**, *12*, 3–20. [CrossRef] [PubMed]

68. Wilson, K.J.; Gilmore, J.L.; Foley, J.; Lemmon, M.A.; Riese, D.J. Functional Selectivity of EGF Family Peptide Growth Factors: Implications for Cancer. *Pharmacol. Ther.* **2009**, *122*, 1–8. [CrossRef]

69. Wilson, K.J.; Mill, C.; Lambert, S.; Buchman, J.; Wilson, T.R.; Hernandez-Gordillo, V.; Gallo, R.M.; Ades, L.M.C.; Settleman, J.; Riese, D.J. EGFR Ligands Exhibit Functional Differences in Models of Paracrine and Autocrine Signaling. *Growth Factors* **2012**, *30*, 107–116. [CrossRef]

70. Akbarzadeh Khiavi, M.; Safary, A.; Barar, J.; Ajoolabady, A.; Somi, M.H.; Omidi, Y. Multifunctional Nanomedicines for Targeting Epidermal Growth Factor Receptor in Colorectal Cancer. *Cell. Mol. Life Sci.* **2020**, *77*, 997–1019. [CrossRef]

71. Gullick, W.J.; Marsden, J.J.; Whittle, N.; Ward, B.; Bobrow, L.; Waterfield, M.D. Expression of Epidermal Growth Factor Receptors on Human Cervical, Ovarian, and Vulval Carcinomas. *Cancer Res.* **1986**, *46*, 285–292. [PubMed]

72. Ciardiello, F.; Tortora, G. Epidermal Growth Factor Receptor (EGFR) as a Target in Cancer Therapy: Understanding the Role of Receptor Expression and Other Molecular Determinants That Could Influence the Response to Anti-EGFR Drugs. *Eur. J. Cancer* **2003**, *39*, 1348–1354. [CrossRef] [PubMed]

73. Ali, R.; Wendt, M.K. The Paradoxical Functions of EGFR during Breast Cancer Progression. *Signal Transduct. Target. Ther.* **2017**, *2*, 16042. [CrossRef] [PubMed]

74. Rocha-Lima, C.M.; Soares, H.P.; Raez, L.E.; Singal, R. EGFR Targeting of Solid Tumors. *Cancer Control* **2007**, *14*, 295–304. [CrossRef] [PubMed]

75. Li, D.; Ji, H.; Zaghlul, S.; McNamara, K.; Liang, M.-C.; Shimamura, T.; Kubo, S.; Takahashi, M.; Chirieac, L.R.; Padera, R.F.; et al. Therapeutic Anti-EGFR Antibody 806 Generates Responses in Murine de Novo EGFR Mutant–Dependent Lung Carcinomas. *J. Clin. Investig.* **2007**, *117*, 346. [CrossRef] [PubMed]

76. Wu, L.; Ke, L.; Zhang, Z.; Yu, J.; Meng, X. Development of EGFR TKIs and Options to Manage Resistance of Third-Generation EGFR TKI Osimertinib: Conventional Ways and Immune Checkpoint Inhibitors. *Front. Oncol.* **2020**, *10*, 602762. [CrossRef] [PubMed]

77. Abourehab, M.A.S.; Alqahtani, A.M.; Youssif, B.G.M.; Gouda, A.M. Globally Approved EGFR Inhibitors: Insights into Their Syntheses, Target Kinases, Biological Activities, Receptor Interactions, and Metabolism. *Molecules* **2021**, *26*, 6677. [CrossRef] [PubMed]

78. Hrustanovic, G.; Lee, B.J.; Bivona, T.G. Mechanisms of Resistance to EGFR Targeted Therapies. *Cancer Biol. Ther.* **2013**, *14*, 304–314. [CrossRef] [PubMed]

79. Veeraraghavan, V.P.; Daniel, S.; Dasari, A.K.; Aileni, K.R.; Patil, C.; Patil, S.R. Emerging Targeted Therapies in Oral Oncology: Focus on EGFR Inhibition. *Oral Oncol. Rep.* **2024**, *11*, 100592. [CrossRef]

80. Alsaed, B.; Lin, L.; Son, J.; Li, J.; Smolander, J.; Lopez, T.; Eser, P.Ö.; Ogino, A.; Ambrogio, C.; Eum, Y.; et al. Intratumor Heterogeneity of EGFR Expression Mediates Targeted Therapy Resistance and Formation of Drug Tolerant Microenvironment. *Nat. Commun.* **2025**, *16*, 28. [CrossRef] [PubMed]

81. Ang, K.K.; Berkey, B.A.; Tu, X.; Zhang, H.-Z.; Katz, R.; Hammond, E.H.; Fu, K.K.; Milas, L. Impact of Epidermal Growth Factor Receptor Expression on Survival and Pattern of Relapse in Patients with Advanced Head and Neck Carcinoma1. *Cancer Res.* **2002**, *62*, 7350–7356. [PubMed]

82. Sakai, A.; Tagami, M.; Kakehashi, A.; Katsuyama-Yoshikawa, A.; Misawa, N.; Wanibuchi, H.; Azumi, A.; Honda, S. Expression, Intracellular Localization, and Mutation of EGFR in Conjunctival Squamous Cell Carcinoma and the Association with Prognosis and Treatment. *PLoS ONE* **2020**, *15*, e0238120. [CrossRef] [PubMed]

83. de Melo Maia, B.; Fontes, A.M.; Lavorato-Rocha, A.M.; Rodrigues, I.S.; de Brot, L.; Baiocchi, G.; Stiepcich, M.M.; Soares, F.A.; Rocha, R.M. EGFR Expression in Vulvar Cancer: Clinical Implications and Tumor Heterogeneity. *Hum. Pathol.* **2014**, *45*, 917–925. [CrossRef] [PubMed]

84. Fan, X.; Liu, B.; Xu, H.; Yu, B.; Shi, S.; Zhang, J.; Wang, X.; Wang, J.; Lu, Z.; Ma, H.; et al. Immunostaining with *EGFR* Mutation–Specific Antibodies: A Reliable Screening Method for Lung Adenocarcinomas Harboring *EGFR* Mutation in Biopsy and Resection Samples. *Hum. Pathol.* **2013**, *44*, 1499–1507. [CrossRef]

85. Fakih, M.; Vincent, M. Adverse Events Associated with Anti-EGFR Therapies for the Treatment of Metastatic Colorectal Cancer. *Curr. Oncol.* **2010**, *17*, S18–S30. [CrossRef] [PubMed]

86. Batis, N.; Brooks, J.M.; Payne, K.; Sharma, N.; Nankivell, P.; Mehanna, H. Lack of Predictive Tools for Conventional and Targeted Cancer Therapy: Barriers to Biomarker Development and Clinical Translation. *Adv. Drug Deliv. Rev.* **2021**, *176*, 113854. [CrossRef] [PubMed]

87. Yang, Z.; Tam, K.Y. Combination Strategies Using EGFR-TKi in NSCLC Therapy: Learning from the Gap between Pre-Clinical Results and Clinical Outcomes. *Int. J. Biol. Sci.* **2018**, *14*, 204–216. [CrossRef]

88. Bell, G.I.; Fong, N.M.; Stempien, M.M.; Wormsted, M.A.; Caput, D.; Ku, L.L.; Urdea, M.S.; Rall, L.B.; Sanchez-Pescador, R. Human Epidermal Growth Factor Precursor: cDNA Sequence, Expression in Vitro and Gene Organization. *Nucleic Acids Res.* **1986**, *14*, 8427–8446. [CrossRef] [PubMed]

89. Cohen, S.; Carpenter, G. Human Epidermal Growth Factor: Isolation and Chemical and Biological Properties. *Proc. Natl. Acad. Sci. USA* **1975**, *72*, 1317–1321. [CrossRef] [PubMed]

90. Gregory, H. Isolation and Structure of Urogastrone and Its Relationship to Epidermal Growth Factor. *Nature* **1975**, *257*, 325–327. [CrossRef] [PubMed]

91. Lee, D.-N.; Kuo, T.-Y.; Chen, M.-C.; Tang, T.-Y.; Liu, F.-H.; Weng, C.-F. Expression of Porcine Epidermal Growth Factor in Pichia Pastoris and Its Biology Activity in Early-Weaned Piglets. *Life Sci.* **2006**, *78*, 649–654. [CrossRef] [PubMed]

92. Cohen, S. Epidermal Growth Factor. *Biosci. Rep.* **1986**, *6*, 1017–1028. [CrossRef] [PubMed]

93. Hardwicke, J.; Schmaljohann, D.; Boyce, D.; Thomas, D. Epidermal Growth Factor Therapy and Wound Healing—Past, Present and Future Perspectives. *Surgeon* **2008**, *6*, 172–177. [CrossRef] [PubMed]

94. Milani, S.; Calabrò, A. Role of Growth Factors and Their Receptors in Gastric Ulcer Healing. *Microsc. Res. Tech.* **2001**, *53*, 360–371. [CrossRef]

95. Boonstra, J.; Rijken, P.; Humbel, B.; Cremers, F.; Verkleij, A.; van Bergen en Henegouwen, P. The Epidermal Growth Factor. *Cell Biol. Int.* **1995**, *19*, 413–430. [CrossRef] [PubMed]

96. Kennedy, L.C.; Bickford, L.R.; Lewinski, N.A.; Coughlin, A.J.; Hu, Y.; Day, E.S.; West, J.L.; Drezek, R.A. A New Era for Cancer Treatment: Gold-Nanoparticle-Mediated Thermal Therapies. *Small* **2011**, *7*, 169–183. [CrossRef] [PubMed]

97. Master, A.M.; Gupta, A.S. EGF Receptor-Targeted Nanocarriers for Enhanced Cancer Treatment. *Nanomedicine* **2012**, *7*, 1895–1906. [CrossRef] [PubMed]

98. Matrisian, L.M.; Planck, S.R.; Magun, B.E. Intracellular Processing of Epidermal Growth Factor. I. Acidification of 125I-Epidermal Growth Factor in Intracellular Organelles. *J. Biol. Chem.* **1984**, *259*, 3047–3052. [CrossRef] [PubMed]

99. Zhang, A.; Nakanishi, J. Improved Anti-Cancer Effect of Epidermal Growth Factor-Gold Nanoparticle Conjugates by Protein Orientation through Site-Specific Mutagenesis. *Sci. Technol. Adv. Mater.* **2021**, *22*, 616–626. [CrossRef] [PubMed]

100. Castilho, M.L.; Jesus, V.P.S.; Vieira, P.F.A.; Hewitt, K.C.; Raniero, L. Chlorin E6-EGF Conjugated Gold Nanoparticles as a Nanomedicine Based Therapeutic Agent for Triple Negative Breast Cancer. *Photodiagnosis Photodyn. Ther.* **2021**, *33*, 102186. [CrossRef]

101. Salama, B.; Chang, C.-J.; Kanehira, K.; El-Sherbini, E.-S.; El-Sayed, G.; El-Adl, M.; Taniguchi, A. EGF Conjugation Improves Safety and Uptake Efficacy of Titanium Dioxide Nanoparticles. *Molecules* **2020**, *25*, 4467. [CrossRef]

102. Lopes, J.; Ferreira-Gonçalves, T.; Figueiredo, I.V.; Rodrigues, C.M.P.; Ferreira, H.; Ferreira, D.; Viana, A.S.; Faísca, P.; Gaspar, M.M.; Coelho, J.M.P.; et al. Proof-of-Concept Study of Multifunctional Hybrid Nanoparticle System Combined with NIR Laser Irradiation for the Treatment of Melanoma. *Biomolecules* **2021**, *11*, 511. [CrossRef]

103. Susnik, E.; Bazzoni, A.; Taladriz-Blanco, P.; Balog, S.; Moreno-Echeverri, A.M.; Glaubitz, C.; Brito Oliveira, B.; Ferreira, D.; Viana Baptista, P.; Petri-Fink, A.; et al. Epidermal Growth Factor Alters Silica Nanoparticle Uptake and Improves Gold-Nanoparticle-Mediated Gene Silencing in A549 Cells. *Front. Nanotechnol.* **2023**, *5*, 1220514. [CrossRef] [PubMed]

104. Yamamoto, S.; Nakanism, J. Epidermal Growth Factor-Gold Nanoparticle Conjugates-Induced Cellular Responses: Effect of Interfacial Parameters between Cell and Nanoparticle. *Anal. Sci.* **2021**, *37*, 741–745. [CrossRef]

105. Mal, S.; Saha, T.; Halder, A.; Paidesetty, S.K.; Das, S.; Wui, W.T.; Chatterji, U.; Roy, P. EGF-Conjugated Bio-Safe Luteolin Gold Nanoparticles Induce Cellular Toxicity and Cell Death Mediated by Site-Specific Rapid Uptake in Human Triple Negative Breast Cancer Cells. *J. Drug Deliv. Sci. Technol.* **2023**, *80*, 104148. [CrossRef]

106. Zhang, S.; Ouyang, T.; Reinhard, B.M. Multivalent Ligand-Nanoparticle Conjugates Amplify Reactive Oxygen Species Second Messenger Generation and Enhance Epidermal Growth Factor Receptor Phosphorylation. *Bioconjug. Chem.* **2022**, *33*, 1716–1728. [CrossRef] [PubMed]

107. Skóra, B.; Piechowiak, T.; Szychowski, K.A. Epidermal Growth Factor-Labeled Liposomes as a Way to Target the Toxicity of Silver Nanoparticles into EGFR-Overexpressing Cancer Cells In Vitro. *Toxicol. Appl. Pharmacol.* **2022**, *443*, 116009. [CrossRef] [PubMed]

108. Wu, P.; Zhou, Q.; Zhu, H.; Zhuang, Y.; Bao, J. Enhanced Antitumor Efficacy in Colon Cancer Using EGF Functionalized PLGA Nanoparticles Loaded with 5-Fluorouracil and Perfluorocarbon. *BMC Cancer* **2020**, *20*, 354. [CrossRef] [PubMed]

109. Yasami-Khiabani, S.; Karkhaneh, A.; Ali Shokrgozar, M.; Amanzadeh, A.; Golkar, M. Size Effect of Human Epidermal Growth Factor-Conjugated Polystyrene Particles on Cell Proliferation. *Biomater. Sci.* **2020**, *8*, 4832–4840. [CrossRef] [PubMed]

110. Wang, J.; Zhang, Y.; Zhang, G.; Xiang, L.; Pang, H.; Xiong, K.; Lu, Y.; Li, J.; Dai, J.; Lin, S.; et al. Radiotherapy-Induced Enrichment of EGF-Modified Doxorubicin Nanoparticles Enhances the Therapeutic Outcome of Lung Cancer. *Drug Deliv.* **2022**, *29*, 588–599. [CrossRef] [PubMed]

111. Ilhan-Ayisigi, E.; Saglam-Metiner, P.; Sanci, E.; Bakan, B.; Yildirim, Y.; Buhur, A.; Yavasoglu, A.; Yavasoglu, N.U.K.; Yesil-Celiktas, O. Receptor Mediated Targeting of EGF-Conjugated Alginate-PAMAM Nanoparticles to Lung Adenocarcinoma: 2D/3D in Vitro and in Vivo Evaluation. *Int. J. Biol. Macromol.* **2024**, *261*, 129758. [CrossRef] [PubMed]

112. Li, S.; Xu, Z.; Alrobaian, M.; Afzal, O.; Kazmi, I.; Almalki, W.H.; Altamimi, A.S.A.; Al-Abbasi, F.A.; Alharbi, K.S.; Altowayan, W.M.; et al. EGF-Functionalized Lipid–Polymer Hybrid Nanoparticles of 5-Fluorouracil and Sulforaphane with Enhanced Bioavailability and Anticancer Activity against Colon Carcinoma. *Biotechnol. Appl. Biochem.* **2022**, *69*, 2205–2221. [CrossRef] [PubMed]

113. Colzani, B.; Biagiotti, M.; Speranza, G.; Dorati, R.; Modena, T.; Conti, B.; Tomasi, C.; Genta, I. Smart Biodegradable Nanoparticulate Materials: Poly-Lactide-Co-Glycolide Functionalization with Selected Peptides. *Curr. Nanosci.* **2016**, *12*, 347–356. [CrossRef]

114. Mickler, F.M.; Möckl, L.; Ruthardt, N.; Ogris, M.; Wagner, E.; Bräuchle, C. Tuning Nanoparticle Uptake: Live-Cell Imaging Reveals Two Distinct Endocytosis Mechanisms Mediated by Natural and Artificial EGFR Targeting Ligand. *Nano Lett.* **2012**, *12*, 3417–3423. [CrossRef] [PubMed]

115. Genta, I.; Chiesa, E.; Colzani, B.; Modena, T.; Conti, B.; Dorati, R. GE11 Peptide as an Active Targeting Agent in Antitumor Therapy: A Minireview. *Pharmaceutics* **2018**, *10*, 2. [CrossRef] [PubMed]

116. Guo, Z.; Sui, J.; Li, Y.; Wei, Q.; Wei, C.; Xiu, L.; Zhu, R.; Sun, Y.; Hu, J.; Li, J.-L. GE11 Peptide-Decorated Acidity-Responsive Micelles for Improved Drug Delivery and Enhanced Combination Therapy of Metastatic Breast Cancer. *J. Mater. Chem. B* **2022**, *10*, 9266–9279. [CrossRef] [PubMed]

117. Paiva, I.; Mattingly, S.; Wuest, M.; Leier, S.; Vakili, M.R.; Weinfeld, M.; Lavasanifar, A.; Wuest, F. Synthesis and Analysis of ^{64}Cu-Labeled GE11-Modified Polymeric Micellar Nanoparticles for EGFR-Targeted Molecular Imaging in a Colorectal Cancer Model. *Mol. Pharm.* **2020**, *17*, 1470–1481. [CrossRef] [PubMed]

118. de Paiva, I.M.; Vakili, M.R.; Soleimani, A.H.; Tabatabaei Dakhili, S.A.; Munira, S.; Paladino, M.; Martin, G.; Jirik, F.R.; Hall, D.G.; Weinfeld, M.; et al. Biodistribution and Activity of EGFR Targeted Polymeric Micelles Delivering a New Inhibitor of DNA Repair to Orthotopic Colorectal Cancer Xenografts with Metastasis. *Mol. Pharm.* **2022**, *19*, 1825–1838. [CrossRef] [PubMed]

119. Du, L.; Xu, Y.; Han, B.; Wang, Y.; Zeng, Q.; Shao, M.; Yu, Z. EGFR-Targeting Peptide Conjugated Polymer–Lipid Hybrid Nanoparticles for Delivery of Salinomycin to Osteosarcoma. *J. Cancer Res. Ther.* **2023**, *19*, 1544. [CrossRef]

120. Li, K.; Pang, L.; Pan, X.; Fan, S.; Wang, X.; Wang, Q.; Dai, P.; Gao, W.; Gao, J. GE11 Modified PLGA/TPGS Nanoparticles Targeting Delivery of Salinomycin to Breast Cancer Cells. *Technol. Cancer Res. Treat.* **2021**, *20*, 15330338211004954. [CrossRef]

121. Tang, H.; Rui, M.; Mai, J.; Guo, W.; Xu, Y. Reimaging Biological Barriers Affecting Distribution and Extravasation of PEG/Peptide-Modified Liposomes in Xenograft SMMC7721 Tumor. *Acta Pharm. Sin. B* **2020**, *10*, 546–556. [CrossRef] [PubMed]

122. Zhou, C.; Xia, Y.; Wei, Y.; Cheng, L.; Wei, J.; Guo, B.; Meng, F.; Cao, S.; van Hest, J.C.M.; Zhong, Z. GE11 Peptide-Installed Chimaeric Polymersomes Tailor-Made for High-Efficiency EGFR-Targeted Protein Therapy of Orthotopic Hepatocellular Carcinoma. *Acta Biomater.* **2020**, *113*, 512–521. [CrossRef] [PubMed]

123. Huang, X.; Chen, L.; Zhang, Y.; Zhou, S.; Cai, H.-H.; Li, T.; Jin, H.; Cai, J.; Zhou, H.; Pi, J. GE11 Peptide Conjugated Liposomes for EGFR-Targeted and Chemophotothermal Combined Anticancer Therapy. *Bioinorg. Chem. Appl.* **2021**, *2021*, 5534870. [CrossRef] [PubMed]

124. Lan, Q.; Wang, S.; Chen, Z.; Hua, J.; Hu, J.; Luo, S.; Xu, Y. Near-Infrared-Responsive GE11-CuS@Gal Nanoparticles as an Intelligent Drug Release System for Targeting Therapy against Oral Squamous Cell Carcinoma. *Int. J. Pharm.* **2024**, *649*, 123667. [CrossRef] [PubMed]

125. Lu, S.; Bao, X.; Hai, W.; Shi, S.; Chen, Y.; Yu, Q.; Zhang, M.; Xu, Y.; Peng, J. Multi-Functional Self-Assembled Nanoparticles for pVEGF-shRNA Loading and Anti-Tumor Targeted Therapy. *Int. J. Pharm.* **2020**, *575*, 118898. [CrossRef] [PubMed]

126. Haddick, L.; Zhang, W.; Reinhard, S.; Möller, K.; Engelke, H.; Wagner, E.; Bein, T. Particle-Size-Dependent Delivery of Antitumoral miRNA Using Targeted Mesoporous Silica Nanoparticles. *Pharmaceutics* **2020**, *12*, 505. [CrossRef] [PubMed]

127. Grataitong, K.; Huault, S.; Chotwiwatthanakun, C.; Jariyapong, P.; Thongsum, O.; Chawiwithaya, C.; Chakrabandhu, K.; Hueber, A.-O.; Weerachatyanukul, W. Chimeric Virus-like Particles (VLPs) Designed from Shrimp Nodavirus (MrNV) Capsid Protein Specifically Target EGFR-Positive Human Colorectal Cancer Cells. *Sci. Rep.* **2021**, *11*, 16579. [CrossRef] [PubMed]

128. Abdulmalek, S.A.; Saleh, A.M.; Shahin, Y.R.; El Azab, E.F. Functionalized siRNA-Chitosan Nanoformulations Promote Triple-Negative Breast Cancer Cell Death via Blocking the miRNA-21/AKT/ERK Signaling Axis: In-Silico and in Vitro Studies. *Naunyn. Schmiedebergs Arch. Pharmacol.* **2024**, *397*, 6941–6962. [CrossRef] [PubMed]

129. Li, D.; Ma, S.; Xu, D.; Meng, X.; Lei, N.; Liu, C.; Zhao, Y.; Qi, Y.; Cheng, Z.; Wang, F. Peptide-Functionalized Therapeutic Nanoplatform for Treatment Orthotopic Triple Negative Breast Cancer and Bone Metastasis. *Nanomed. Nanotechnol. Biol. Med.* **2023**, *50*, 102669. [CrossRef] [PubMed]

130. Gu, H.; Shi, R.; Xu, C.; Lv, W.; Hu, X.; Xu, C.; Pan, Y.; He, X.; Wu, A.; Li, J. EGFR-Targeted Liposomes Combined with Ginsenoside Rh2 Inhibit Triple-Negative Breast Cancer Growth and Metastasis. *Bioconjug. Chem.* **2023**, *34*, 1157–1165. [CrossRef]

131. Song, P.; Wang, B.; Pan, Q.; Jiang, T.; Chen, X.; Zhang, M.; Tao, J.; Zhao, X. GE11-Modified Carboxymethyl Chitosan Micelles to Deliver DOX·PD-L1 siRNA Complex for Combination of ICD and Immune Escape Inhibition against Tumor. *Carbohydr. Polym.* **2023**, *312*, 120837. [CrossRef] [PubMed]

132. Soleimani, A.; Mirzavi, F.; Nikoofal-Sahlabadi, S.; Nikpoor, A.R.; Taghizadeh, B.; Barati, M.; Soukhtanloo, M.; Jaafari, M.R. CD73 Downregulation by EGFR-Targeted Liposomal CD73 siRNA Potentiates Antitumor Effect of Liposomal Doxorubicin in 4T1 Tumor-Bearing Mice. *Sci. Rep.* **2022**, *12*, 10423. [CrossRef] [PubMed]

133. Dong, Z.; Wang, Y.; Guo, J.; Tian, C.; Pan, W.; Wang, H.; Yan, J. Prostate Cancer Therapy Using Docetaxel and Formononetin Combination: Hyaluronic Acid and Epidermal Growth Factor Receptor Targeted Peptide Dual Ligands Modified Binary Nanoparticles to Facilitate the in Vivo Anti-Tumor Activity. *Drug Des. Dev. Ther.* **2022**, *16*, 2683–2693. [CrossRef]

134. Liu, Z.-Y.; Yan, G.-H.; Li, X.-Y.; Zhang, Z.; Guo, Y.-Z.; Xu, K.-X.; Quan, J.-S.; Jin, G.-Y. GE11 Peptide Modified CSO-SPION Micelles for MRI Diagnosis of Targeted Hepatic Carcinoma. *Biotechnol. Biotechnol. Equip.* **2021**, *35*, 1574–1586. [CrossRef]

135. Wang, Y.; Luo, J.; Truebenbach, I.; Reinhard, S.; Klein, P.M.; Höhn, M.; Kern, S.; Morys, S.; Loy, D.M.; Wagner, E.; et al. Double Click-Functionalized siRNA Polyplexes for Gene Silencing in Epidermal Growth Factor Receptor-Positive Tumor Cells. *ACS Biomater. Sci. Eng.* **2020**, *6*, 1074–1089. [CrossRef] [PubMed]

136. Nisar, S.; Handley, S.; Clement, S. Developing a Novel Biodegradable Nanodrug Platform for Overcoming the Challenges in Treating Pancreatic Ductal Adenocarcinoma (PDAC). In Proceedings of the Colloidal Nanoparticles for Biomedical Applications XVI, Online, 6–11 March 2021; SPIE: St. Bellingham, WA, USA, 2021; Volume 11659, pp. 12–31.

137. Verimli, N.; Goralı, S.İ.; Abisoglu, B.; Altan, C.L.; Sucu, B.O.; Karatas, E.; Tulek, A.; Bayraktaroglu, C.; Beker, M.C.; Erdem, S.S. Development of Light and pH-Dual Responsive Self-Quenching Theranostic SPION to Make EGFR Overexpressing Micro Tumors Glow and Destroy. *J. Photochem. Photobiol. B* **2023**, *248*, 112797. [CrossRef] [PubMed]

138. Tang, H.; Li, L.; Wang, B.; Guangxi Scientific Research Center of Traditional Chinese Medicine. Observation of Antitumor Mechanism of GE11-Modified Paclitaxel and Curcumin Liposomes Based on Cellular Morphology Changes. *AAPS Open* **2024**, *10*, 1. [CrossRef]

139. Patel, U.; Rathnayake, K.; Singh, N.; Hunt, E.C. Dual Targeted Delivery of Liposomal Hybrid Gold Nano-Assembly for Enhanced Photothermal Therapy against Lung Carcinomas. *ACS Appl. Bio Mater.* **2023**, *6*, 1915–1933. [CrossRef] [PubMed]

140. Rathnayake, K.; Patel, U.; Hunt, E.C.; Singh, N. Fabrication of a Dual-Targeted Liposome-Coated Mesoporous Silica Core–Shell Nanoassembly for Targeted Cancer Therapy. *ACS Omega* **2023**, *8*, 34481–34498. [CrossRef]

141. Liu, N.; Cui, M.; Hu, N.; Yang, F.; Mu, Y.; Guo, C.; Guan, X.; Xie, Z. An Engineered Three-in-One Hybrid Nanosystem from Elastin-like Polypeptides for Enhanced Cancer Suppression. *Colloids Surf. B Biointerfaces* **2022**, *220*, 112976. [CrossRef]

142. Pethő, L.; Kasza, G.; Lajkó, E.; Láng, O.; Kőhidai, L.; Iván, B.; Mező, G. Amphiphilic Drug–Peptide–Polymer Conjugates Based on Poly(Ethylene Glycol) and Hyperbranched Polyglycerol for Epidermal Growth Factor Receptor Targeting: The Effect of Conjugate Aggregation on in Vitro Activity. *Soft Matter* **2020**, *16*, 5759–5769. [CrossRef] [PubMed]

143. Bao, B.; Yuan, Q.; Feng, Q.; Li, L.; Li, M.; Tang, Y. Regulating Signal Pathway Triggers Circular Reactive Oxygen Species Production to Augment Oxidative Stress with Enzyme-Activated Nanoparticles. *CCS Chem.* **2023**, *6*, 693–708. [CrossRef]

144. Tao, Y.; Liu, Y.; Dong, Z.; Chen, X.; Wang, Y.; Li, T.; Li, J.; Zang, S.; He, X.; Chen, D.; et al. Cellular Hypoxia Mitigation by Dandelion-like Nanoparticles for Synergistic Photodynamic Therapy of Oral Squamous Cell Carcinoma. *ACS Appl. Mater. Interfaces* **2022**, *14*, 44039–44053. [CrossRef] [PubMed]

145. Woof, J.M.; Burton, D.R. Human Antibody–Fc Receptor Interactions Illuminated by Crystal Structures. *Nat. Rev. Immunol.* **2004**, *4*, 89–99. [CrossRef] [PubMed]

146. Reth, M. Matching Cellular Dimensions with Molecular Sizes. *Nat. Immunol.* **2013**, *14*, 765–767. [CrossRef] [PubMed]

147. Sandin, S.; Öfverstedt, L.-G.; Wikström, A.-C.; Wrange, Ö.; Skoglund, U. Structure and Flexibility of Individual Immunoglobulin G Molecules in Solution. *Structure* **2004**, *12*, 409–415. [CrossRef] [PubMed]

148. Cai, W.-Q.; Zeng, L.-S.; Wang, L.-F.; Wang, Y.-Y.; Cheng, J.-T.; Zhang, Y.; Han, Z.-W.; Zhou, Y.; Huang, S.-L.; Wang, X.-W.; et al. The Latest Battles Between EGFR Monoclonal Antibodies and Resistant Tumor Cells. *Front. Oncol.* **2020**, *10*, 1249. [CrossRef] [PubMed]

149. Zahavi, D.; Weiner, L. Monoclonal Antibodies in Cancer Therapy. *Antibodies* **2020**, *9*, 34. [CrossRef] [PubMed]

150. Susini, V.; Ferraro, G.; Fierabracci, V.; Ursino, S.; Sanguinetti, C.; Caponi, L.; Romiti, N.; Rossi, V.L.; Sanesi, A.; Paolicchi, A.; et al. Orientation of Capture Antibodies on Gold Nanoparticles to Improve the Sensitivity of ELISA-Based Medical Devices. *Talanta* **2023**, *260*, 124650. [CrossRef]

151. Brückner, M.; Simon, J.; Landfester, K.; Mailänder, V. The Conjugation Strategy Affects Antibody Orientation and Targeting Properties of Nanocarriers. *Nanoscale* **2021**, *13*, 9816–9824. [CrossRef] [PubMed]

152. Fang, F.; Zhang, X.; Tang, J.; Wang, Y.; Xu, J.; Sun, Y. EGFR-Targeted Hybrid Lipid Nanoparticles for Chemo-Photothermal Therapy against Colorectal Cancer Cells. *Chem. Phys. Lipids* **2023**, *251*, 105280. [CrossRef] [PubMed]

153. Juan, A.; Segrelles, C.; del Campo-Balguerías, A.; Bravo, I.; Silva, I.; Peral, J.; Ocaña, A.; Clemente-Casares, P.; Alonso-Moreno, C.; Lorz, C. Anti-EGFR Conjugated Nanoparticles to Deliver Alpelisib as Targeted Therapy for Head and Neck Cancer. *Cancer Nanotechnol.* **2023**, *14*, 29. [CrossRef]

154. Duwa, R.; Banstola, A.; Emami, F.; Jeong, J.-H.; Lee, S.; Yook, S. Cetuximab Conjugated Temozolomide-Loaded Poly (Lactic-Co-Glycolic Acid) Nanoparticles for Targeted Nanomedicine in EGFR Overexpressing Cancer Cells. *J. Drug Deliv. Sci. Technol.* **2020**, *60*, 101928. [CrossRef]

155. Kumari, L.; Ehsan, I.; Mondal, A.; Al Hoque, A.; Mukherjee, B.; Choudhury, P.; Sengupta, A.; Sen, R.; Ghosh, P. Cetuximab-Conjugated PLGA Nanoparticles as a Prospective Targeting Therapeutics for Non-Small Cell Lung Cancer. *J. Drug Target.* **2023**, *31*, 521–536. [CrossRef]

156. Hosseini, S.M.; Mohammadnejad, J.; Yousefnia, H.; Alirezapour, B.; Rezayan, A.H. Development of ^{177}Lu-Cetuximab-PAMAM Dendrimeric Nanosystem: A Novel Theranostic Radioimmunoconjugate. *J. Cancer Res. Clin. Oncol.* **2023**, *149*, 7779–7791. [CrossRef] [PubMed]

157. Yue, S.; Zhang, Y.; Wei, Y.; Haag, R.; Sun, H.; Zhong, Z. Cetuximab–Polymersome–Mertansine Nanodrug for Potent and Targeted Therapy of EGFR-Positive Cancers. *Biomacromolecules* **2022**, *23*, 100–111. [CrossRef]

158. Ye, Z.; Zhang, Y.; Liu, Y.; Liu, Y.; Tu, J.; Shen, Y. EGFR Targeted Cetuximab-Valine-Citrulline (vc)-Doxorubicin Immunoconjugates—Loaded Bovine Serum Albumin (BSA) Nanoparticles for Colorectal Tumor Therapy. *Int. J. Nanomed.* **2021**, *16*, 2443–2459. [CrossRef]

159. Salim, E.I.; Mosbah, A.M.; Elhussiny, F.A.; Hanafy, N.A.N.; Abdou, Y. Preparation and Characterization of Cetuximab-Loaded Egg Serum Albumin Nanoparticles and Their Uses as a Drug Delivery System against Caco-2 Colon Cancer Cells. *Cancer Nanotechnol.* **2023**, *14*, 4. [CrossRef]

160. Chen, R.; Huang, Y.; Wang, L.; Zhou, J.; Tan, Y.; Peng, C.; Yang, P.; Peng, W.; Li, J.; Gu, Q.; et al. Cetuximab Functionalization Strategy for Combining Active Targeting and Antimigration Capacities of a Hybrid Composite Nanoplatform Applied to Deliver 5-Fluorouracil: Toward Colorectal Cancer Treatment. *Biomater. Sci.* **2021**, *9*, 2279–2294. [CrossRef] [PubMed]

161. Dorjsuren, B.; Chaurasiya, B.; Ye, Z.; Liu, Y.; Li, W.; Wang, C.; Shi, D.; Evans, C.E.; Webster, T.J.; Shen, Y. Cetuximab-Coated Thermo-Sensitive Liposomes Loaded with Magnetic Nanoparticles and Doxorubicin for Targeted EGFR-Expressing Breast Cancer Combined Therapy. *Int. J. Nanomed.* **2020**, *15*, 8201–8215. [CrossRef] [PubMed]

162. Ma, Y.; Peng, X.; Wang, L.; Li, H.; Cheng, W.; Zheng, X.; Liu, Y. Cetuximab-Conjugated Perfluorohexane/Gold Nanoparticles for Low Intensity Focused Ultrasound Diagnosis Ablation of Thyroid Cancer Treatment. *Sci. Technol. Adv. Mater.* **2020**, *21*, 856–866. [CrossRef] [PubMed]

163. El Hallal, R.; Lyu, N.; Wang, Y. Effect of Cetuximab-Conjugated Gold Nanoparticles on the Cytotoxicity and Phenotypic Evolution of Colorectal Cancer Cells. *Molecules* **2021**, *26*, 567. [CrossRef] [PubMed]

164. Wang, Y.; Zhang, X.-M.; Sun, Y.; Chen, H.-L.; Zhou, L.-Y. Cetuximab-Decorated and NIR-Activated Nanoparticles Based on Platinum(IV)-Prodrug: Preparation, Characterization and In-Vitro Anticancer Activity in Epidermoid Carcinoma Cells. *Iran. J. Pharm. Res. IJPR* **2021**, *20*, 371–383. [CrossRef] [PubMed]

165. Quatrale, A.E.; Petriella, D.; Porcelli, L.; Tommasi, S.; Silvestris, N.; Colucci, G.; Angelo, A.; Azzariti, A. Anti-EGFR Monoclonal Antibody in Cancer Treatment: In Vitro and in Vivo Evidence. *Front. Biosci. Landmark Ed.* **2011**, *16*, 1973–1985. [CrossRef] [PubMed]

166. Talavera, A.; Friemann, R.; Gómez-Puerta, S.; Martinez-Fleites, C.; Garrido, G.; Rabasa, A.; López-Requena, A.; Pupo, A.; Johansen, R.F.; Sánchez, O.; et al. Nimotuzumab, an Antitumor Antibody That Targets the Epidermal Growth Factor Receptor, Blocks Ligand Binding While Permitting the Active Receptor Conformation. *Cancer Res.* **2009**, *69*, 5851–5859. [CrossRef] [PubMed]

167. Mazorra, Z.; Chao, L.; Lavastida, A.; Sanchez, B.; Ramos, M.; Iznaga, N.; Crombet, T. Nimotuzumab: Beyond the EGFR Signaling Cascade Inhibition. *Semin. Oncol.* **2018**, *45*, 18–26. [CrossRef] [PubMed]

168. Anisuzzman, M.; Komalla, V.; Tarkistani, M.A.M.; Kayser, V. Anti-Tumor Activity of Novel Nimotuzumab-Functionalized Gold Nanoparticles as a Potential Immunotherapeutic Agent against Skin and Lung Cancers. *J. Funct. Biomater.* **2023**, *14*, 407. [CrossRef] [PubMed]

169. García-Foncillas, J.; Sunakawa, Y.; Aderka, D.; Wainberg, Z.; Ronga, P.; Witzler, P.; Stintzing, S. Distinguishing Features of Cetuximab and Panitumumab in Colorectal Cancer and Other Solid Tumors. *Front. Oncol.* **2019**, *9*, 849. [CrossRef] [PubMed]

170. Banstola, A.; Duwa, R.; Emami, F.; Jeong, J.-H.; Yook, S. Enhanced Caspase-Mediated Abrogation of Autophagy by Temozolomide-Loaded and Panitumumab-Conjugated Poly(Lactic-Co-Glycolic Acid) Nanoparticles in Epidermal Growth Factor Receptor Overexpressing Glioblastoma Cells. *Mol. Pharm.* **2020**, *17*, 4386–4400. [CrossRef] [PubMed]

171. Bhattacharya, S.; Parihar, V.K.; Singh, N.; Hatware, K.; Page, A.; Sharma, M.; Prajapati, M.K.; Kanugo, A.; Pawde, D.; Maru, S.; et al. Targeted Delivery of Panitumumab-Scaffold Bosutinib-Encapsulated Polycaprolactone Nanoparticles for EGFR-Overexpressed Colorectal Cancer. *Nanomedicine* **2023**, *18*, 713–741. [CrossRef]

172. Shukla, V.N.; Vikas; Mehata, A.K.; Setia, A.; Kumari, P.; Mahto, S.K.; Muthu, M.S.; Mishra, S.K. Rational Design of Surface Engineered Albumin Nanoparticles of Asiatic Acid for EGFR Targeted Delivery to Lung Cancer: Formulation Development and Pharmacokinetics. *Colloids Surf. Physicochem. Eng. Asp.* **2023**, *676*, 132188. [CrossRef]

173. Jordan, T.; O'Brien, M.A.; Spatarelu, C.-P.; Luke, G.P. Antibody-Conjugated Barium Titanate Nanoparticles for Cell-Specific Targeting. *ACS Appl. Nano Mater.* **2020**, *3*, 2636–2646. [CrossRef] [PubMed]

174. Bhattacharya, S. Anti-EGFR-mAb and 5-Fluorouracil Conjugated Polymeric Nanoparticles for Colorectal Cancer. *Recent Patents Anticancer Drug Discov.* **2021**, *16*, 84–100. [CrossRef] [PubMed]

175. Liszbinski, R.B.; Romagnoli, G.G.; Gorgulho, C.M.; Basso, C.R.; Pedrosa, V.A.; Kaneno, R. Anti-EGFR-Coated Gold Nanoparticles In Vitro Carry 5-Fluorouracil to Colorectal Cancer Cells. *Materials* **2020**, *13*, 375. [CrossRef]

176. Marshall, S.K.; Saelim, B.; Taweesap, M.; Pachana, V.; Panrak, Y.; Makchuchit, N.; Jaroenpakdee, P. Anti-EGFR Targeted Multifunctional I-131 Radio-Nanotherapeutic for Treating Osteosarcoma: In Vitro 3D Tumor Spheroid Model. *Nanomaterials* **2022**, *12*, 3517. [CrossRef] [PubMed]

177. Fang, F.; Chen, Y.Y.; Zhang, X.-M.; Tang, J.; Liu, Y.-H.; Peng, C.-S.; Sun, Y. EGFR-Targeted and NIR-Triggered Lipid-Polymer Hybrid Nanoparticles for Chemo-Photothermal Colorectal Tumor Therapy. *Int. J. Nanomed.* **2024**, *19*, 9689–9705. [CrossRef] [PubMed]

178. Viswanadh, M.K.; Agrawal, N.; Azad, S.; Jha, A.; Poddar, S.; Mahto, S.K.; Muthu, M.S. Novel Redox-Sensitive Thiolated TPGS Based Nanoparticles for EGFR Targeted Lung Cancer Therapy. *Int. J. Pharm.* **2021**, *602*, 120652. [CrossRef] [PubMed]

179. Bates, A.; Power, C.A. David vs. Goliath: The Structure, Function, and Clinical Prospects of Antibody Fragments. *Antibodies* **2019**, *8*, 28. [CrossRef] [PubMed]

180. Chames, P.; Regenmortel, M.V.; Weiss, E.; Baty, D. Therapeutic Antibodies: Successes, Limitations and Hopes for the Future. *Br. J. Pharmacol.* **2009**, *157*, 220. [CrossRef]

181. Archontakis, E.; Woythe, L.; Hoof, B.v.; Albertazzi, L. Mapping the Relationship between Total and Functional Antibodies Conjugated to Nanoparticles with Spectrally-Resolved Direct Stochastic Optical Reconstruction Microscopy (SR-dSTORM). *Nanoscale Adv.* **2022**, *4*, 4402–4409. [CrossRef] [PubMed]

182. Lin, X.; O'Reilly Beringhs, A.; Lu, X. Applications of Nanoparticle-Antibody Conjugates in Immunoassays and Tumor Imaging. *AAPS J.* **2021**, *23*, 43. [CrossRef] [PubMed]

183. Xenaki, K.T.; Oliveira, S.; van Bergen en Henegouwen, P.M.P. Antibody or Antibody Fragments: Implications for Molecular Imaging and Targeted Therapy of Solid Tumors. *Front. Immunol.* **2017**, *8*, 1287. [CrossRef]

184. Kumar, G.; Nandakumar, K.; Mutalik, S.; Rao, C.M. Biologicals to Direct Nanotherapeutics towards HER2-Positive Breast Cancers. *Nanomed. Nanotechnol. Biol. Med.* **2020**, *27*, 102197. [CrossRef] [PubMed]

185. Nelson, A.L. Antibody Fragments. *mAbs* **2010**, *2*, 77–83. [CrossRef] [PubMed]

186. Khatib, S.E.; Salla, M. The Mosaic Puzzle of the Therapeutic Monoclonal Antibodies and Antibody Fragments—A Modular Transition from Full-Length Immunoglobulins to Antibody Mimetics. *Leuk. Res. Rep.* **2022**, *18*, 100335. [CrossRef] [PubMed]

187. Mittelheisser, V.; Coliat, P.; Moeglin, E.; Goepp, L.; Goetz, J.G.; Charbonnière, L.J.; Pivot, X.; Detappe, A. Optimal Physicochemical Properties of Antibody–Nanoparticle Conjugates for Improved Tumor Targeting. *Adv. Mater.* **2022**, *34*, 2110305. [CrossRef] [PubMed]

188. Vlasak, J.; Ionescu, R. Fragmentation of Monoclonal Antibodies. *mAbs* **2011**, *3*, 253–263. [CrossRef] [PubMed]

189. Wang, A.C.; Wang, I.Y. Cleavage Sites of Human IgGl Immunoglobulin by Papain. *Immunochemistry* **1977**, *14*, 197–200. [CrossRef]

190. Richards, D.A.; Maruani, A.; Chudasama, V. Antibody Fragments as Nanoparticle Targeting Ligands: A Step in the Right Direction. *Chem. Sci.* **2016**, *8*, 63–77. [CrossRef]

191. Wu, H.; Ding, X.; Chen, Y.; Cai, Y.; Yang, Z.; Jin, J. EGFR-Targeted Humanized Single Chain Antibody Fragment Functionalized Silica Nanoparticles for Precision Therapy of Cancer. *Int. J. Biol. Macromol.* **2023**, *253*, 127538. [CrossRef]

192. Lu, Y.; Huang, J.; Li, F.; Wang, Y.; Ding, M.; Zhang, J.; Yin, H.; Zhang, R.; Ren, X. EGFR-Specific Single-Chain Variable Fragment Antibody-Conjugated Fe_3O_4/Au Nanoparticles as an Active MRI Contrast Agent for NSCLC. *Magn. Reson. Mater. Phys. Biol. Med.* **2021**, *34*, 581–591. [CrossRef] [PubMed]

193. Jiang, J.; Lu, Y.; Chu, J.; Zhang, X.; Xu, C.; Liu, S.; Wan, Z.; Wang, J.; Zhang, L.; Liu, K.; et al. Anti-EGFR ScFv Functionalized Exosomes Delivering LPCAT1 Specific siRNAs for Inhibition of Lung Cancer Brain Metastases. *J. Nanobiotechnol.* **2024**, *22*, 159. [CrossRef] [PubMed]

194. Nguyen, P.V.; Hervé-Aubert, K.; David, S.; Lautram, N.; Passirani, C.; Chourpa, I.; Aubrey, N.; Allard-Vannier, E. Targeted Nanomedicine with Anti-EGFR scFv for siRNA Delivery into Triple Negative Breast Cancer Cells. *Eur. J. Pharm. Biopharm.* **2020**, *157*, 74–84. [CrossRef]

195. Tateo, S.; Shinchi, H.; Matsumoto, H.; Nagata, N.; Hashimoto, M.; Wakao, M.; Suda, Y. Optimized Immobilization of Single Chain Variable Fragment Antibody onto Non-Toxic Fluorescent Nanoparticles for Efficient Preparation of a Bioprobe. *Colloids Surf. B Biointerfaces* **2023**, *224*, 113192. [CrossRef] [PubMed]

196. Logan, A.; Howard, C.B.; Huda, P.; Kimpton, K.; Ma, Z.; Thurecht, K.J.; McCarroll, J.A.; Moles, E.; Kavallaris, M. Targeted Delivery of Polo-like Kinase 1 siRNA Nanoparticles Using an EGFR-PEG Bispecific Antibody Inhibits Proliferation of High-Risk Neuroblastoma. *J. Control. Release* **2024**, *367*, 806–820. [CrossRef] [PubMed]

197. Wang, Y.-P.; Liu, I.-J.; Chung, M.-J.; Wu, H.-C. Novel Anti-EGFR scFv Human Antibody-Conjugated Immunoliposomes Enhance Chemotherapeutic Efficacy in Squamous Cell Carcinoma of Head and Neck. *Oral Oncol.* **2020**, *106*, 104689. [CrossRef] [PubMed]

198. Jiang, X.; Zhang, X.; Guo, C.; Ma, B.; Liu, Z.; Du, Y.; Wang, B.; Li, N.; Huang, X.; Ou, L. Genetically Engineered Cell Membrane-Coated Magnetic Nanoparticles for High-Performance Isolation of Circulating Tumor Cells. *Adv. Funct. Mater.* **2024**, *34*, 2304426. [CrossRef]

199. Moles, E.; Chang, D.W.; Mansfeld, F.M.; Duly, A.; Kimpton, K.; Logan, A.; Howard, C.B.; Thurecht, K.J.; Kavallaris, M. EGFR Targeting of Liposomal Doxorubicin Improves Recognition and Suppression of Non-Small Cell Lung Cancer. *Int. J. Nanomed.* **2024**, *19*, 3623–3639. [CrossRef] [PubMed]

200. Wei, P.-S.; Chen, Y.-J.; Lin, S.-Y.; Chuang, K.-H.; Sheu, M.-T.; Ho, H.-O. In Situ Subcutaneously Injectable Thermosensitive PEG-PLGA Diblock and PLGA-PEG-PLGA Triblock Copolymer Composite as Sustained Delivery of Bispecific Anti-CD3 scFv T-Cell/Anti-EGFR Fab Engager (BiTEE). *Biomaterials* **2021**, *278*, 121166. [CrossRef] [PubMed]

201. Lü, J.-M.; Liang, Z.; Liu, D.; Zhan, B.; Yao, Q.; Chen, C. Two Antibody-Guided Lactic-Co-Glycolic Acid-Polyethylenimine (LGA-PEI) Nanoparticle Delivery Systems for Therapeutic Nucleic Acids. *Pharmaceuticals* **2021**, *14*, 841. [CrossRef] [PubMed]

202. Rashidian, M.; Ploegh, H. Nanobodies as Non-Invasive Imaging Tools. *Immuno-Oncol. Technol.* **2020**, *7*, 2–14. [CrossRef] [PubMed]

203. Wagner, T.R.; Rothbauer, U. Nanobodies—Little Helpers Unravelling Intracellular Signaling. *Free Radic. Biol. Med.* **2021**, *176*, 46–61. [CrossRef] [PubMed]

204. Roovers, R.C.; Vosjan, M.J.W.D.; Laeremans, T.; el Khoulati, R.; de Bruin, R.C.G.; Ferguson, K.M.; Verkleij, A.J.; van Dongen, G.A.M.S.; van Bergen en Henegouwen, P.M.P. A Biparatopic Anti-EGFR Nanobody Efficiently Inhibits Solid Tumour Growth. *Int. J. Cancer* **2011**, *129*, 2013–2024. [CrossRef] [PubMed]

205. Muyldermans, S. Nanobodies: Natural Single-Domain Antibodies. *Annu. Rev. Biochem.* **2013**, *82*, 775–797. [CrossRef]

206. Chapman, A.P.; Antoniw, P.; Spitali, M.; West, S.; Stephens, S.; King, D.J. Therapeutic Antibody Fragments with Prolonged in Vivo Half-Lives. *Nat. Biotechnol.* **1999**, *17*, 780–783. [CrossRef]

207. Song, W.; Wei, W.; Lan, X.; Cai, W. Albumin Binding Improves Nanobody Pharmacokinetics for Dual-Modality PET/NIRF Imaging of CEACAM5 in Colorectal Cancer Models. *Eur. J. Nucl. Med. Mol. Imaging* **2023**, *50*, 2591–2594. [CrossRef] [PubMed]

208. Li, Q.; Kong, Y.; Zhong, Y.; Huang, A.; Ying, T.; Wu, Y. Half-Life Extension of Single-Domain Antibody–Drug Conjugates by Albumin Binding Moiety Enhances Antitumor Efficacy. *MedComm* **2024**, *5*, e557. [CrossRef]

209. Liu, Y.; Scrivano, L.; Peterson, J.D.; Fens, M.H.A.M.; Hernández, I.B.; Mesquita, B.; Toraño, J.S.; Hennink, W.E.; van Nostrum, C.F.; Oliveira, S. EGFR-Targeted Nanobody Functionalized Polymeric Micelles Loaded with mTHPC for Selective Photodynamic Therapy. *Mol. Pharm.* **2020**, *17*, 1276–1292. [CrossRef] [PubMed]

210. Hernández, I.B.; Grinwis, G.C.M.; Maggio, A.D.; van Bergen en Henegouwen, P.M.P.; Hennink, W.E.; Teske, E.; Hesselink, J.W.; van Nimwegen, S.A.; Mol, J.A.; Oliveira, S. Nanobody-Targeted Photodynamic Therapy for the Treatment of Feline Oral Carcinoma: A Step towards Translation to the Veterinary Clinic. *Nanophotonics* **2021**, *10*, 3075–3087. [CrossRef] [PubMed]

211. Mesquita, B.; Singh, A.; Prats Masdeu, C.; Lokhorst, N.; Hebels, E.R.; van Steenbergen, M.; Mastrobattista, E.; Heger, M.; van Nostrum, C.F.; Oliveira, S. Nanobody-Mediated Targeting of Zinc Phthalocyanine with Polymer Micelles as Nanocarriers. *Int. J. Pharm.* **2024**, *655*, 124004. [CrossRef] [PubMed]

212. Bitsch, P.; Baum, E.S.; Beltrán Hernández, I.; Bitsch, S.; Harwood, J.; Oliveira, S.; Kolmar, H. Penetration of Nanobody-Dextran Polymer Conjugates through Tumor Spheroids. *Pharmaceutics* **2023**, *15*, 2374. [CrossRef] [PubMed]

213. Pham, T.C.; Jayasinghe, M.K.; Pham, T.T.; Yang, Y.; Wei, L.; Usman, W.M.; Chen, H.; Pirisinu, M.; Gong, J.; Kim, S.; et al. Covalent Conjugation of Extracellular Vesicles with Peptides and Nanobodies for Targeted Therapeutic Delivery. *J. Extracell. Vesicles* **2021**, *10*, e12057. [CrossRef] [PubMed]

214. Jin, D.; Liu, M.; Zhang, Y.; Yu, W.; Yu, J.; Luo, Y.; Cheng, J.; Liu, Y. Active Regulation of Protein Coronas for Enhancing the in Vivo Biodistribution and Metabolism of Nanoparticles. *Inorg. Chem. Front.* **2024**, *11*, 5741–5752. [CrossRef]

215. Hu, X.; Liu, H.; Cheng, Z. Engineered Affibodies in Translational Medicine. In *Engineering in Translational Medicine*; Cai, W., Ed.; Springer: London, UK, 2014; pp. 317–342, ISBN 978-1-4471-4372-7.

216. Nord, K.; Nilsson, J.; Nilsson, B.; Uhlén, M.; Nygren, P.A. A Combinatorial Library of an Alpha-Helical Bacterial Receptor Domain. *Protein Eng.* **1995**, *8*, 601–608. [CrossRef] [PubMed]

217. Nord, K.; Gunneriusson, E.; Ringdahl, J.; Ståhl, S.; Uhlén, M.; Nygren, P.A. Binding Proteins Selected from Combinatorial Libraries of an Alpha-Helical Bacterial Receptor Domain. *Nat. Biotechnol.* **1997**, *15*, 772–777. [CrossRef]

218. Kronqvist, N.; Malm, M.; Gostring, L.; Gunneriusson, E.; Nilsson, M.; Hoiden Guthenberg, I.; Gedda, L.; Frejd, F.Y.; Stahl, S.; Lofblom, J. Combining Phage and Staphylococcal Surface Display for Generation of ErbB3-Specific Affibody Molecules. *Protein Eng. Des. Sel.* **2011**, *24*, 385–396. [CrossRef]

219. Nygren, P.-Å. Alternative Binding Proteins: Affibody Binding Proteins Developed from a Small Three-Helix Bundle Scaffold. *FEBS J.* **2008**, *275*, 2668–2676. [CrossRef]

220. Friedman, M.; Orlova, A.; Johansson, E.; Eriksson, T.L.J.; Höidén-Guthenberg, I.; Tolmachev, V.; Nilsson, F.Y.; Ståhl, S. Directed Evolution to Low Nanomolar Affinity of a Tumor-Targeting Epidermal Growth Factor Receptor-Binding Affibody Molecule. *J. Mol. Biol.* **2008**, *376*, 1388–1402. [CrossRef] [PubMed]

221. Engfeldt, T.; Renberg, B.; Brumer, H.; Nygren, P.Å.; Eriksson Karlström, A. Chemical Synthesis of Triple-Labelled Three-Helix Bundle Binding Proteins for Specific Fluorescent Detection of Unlabelled Protein. *ChemBioChem* **2005**, *6*, 1043–1050. [CrossRef] [PubMed]

222. Tolmachev, V.; Tran, T.A.; Rosik, D.; Sjöberg, A.; Abrahmsén, L.; Orlova, A. Tumor Targeting Using Affibody Molecules: Interplay of Affinity, Target Expression Level, and Binding Site Composition. *J. Nucl. Med. Off. Publ. Soc. Nucl. Med.* **2012**, *53*, 953–960. [CrossRef] [PubMed]

223. Nord, K.; Gunneriusson, E.; Uhlén, M.; Nygren, P.A. Ligands Selected from Combinatorial Libraries of Protein A for Use in Affinity Capture of Apolipoprotein A-1M and Taq DNA Polymerase. *J. Biotechnol.* **2000**, *80*, 45–54. [CrossRef] [PubMed]

224. Wu, Y.; Li, H.; Yan, Y.; Wang, K.; Cheng, Y.; Li, Y.; Zhu, X.; Xie, J.; Sun, X. Affibody-Modified Gd@C-Dots with Efficient Renal Clearance for Enhanced MRI of EGFR Expression in Non-Small-Cell Lung Cancer. *Int. J. Nanomed.* **2020**, *15*, 4691–4703. [CrossRef] [PubMed]

225. Sayyadi, N.; Zhand, S.; Razavi Bazaz, S.; Warkiani, M.E. Affibody Functionalized Beads for the Highly Sensitive Detection of Cancer Cell-Derived Exosomes. *Int. J. Mol. Sci.* **2021**, *22*, 12014. [CrossRef] [PubMed]

226. Wang, H.; Zhao, X.; Zhang, H.; Zou, X.; Jia, D.; Liu, W.; Tian, B.; Yuan, D.; Li, Y.; Zhu, Y.; et al. EGFR-Antagonistic Affibody-Functionalized Pt-Based Nanozyme for Enhanced Tumor Radiotherapy. *Mater. Today Adv.* **2023**, *18*, 100375. [CrossRef]

227. Roy, S.; Curry, S.D.; Corbella Bagot, C.; Mueller, E.N.; Mansouri, A.M.; Park, W.; Cha, J.N.; Goodwin, A.P. Enzyme Prodrug Therapy with Photo-Cross-Linkable Anti-EGFR Affibodies Conjugated to Upconverting Nanoparticles. *ACS Nano* **2022**, *16*, 15873–15883. [CrossRef] [PubMed]

228. Karyagina, T.S.; Ulasov, A.V.; Slastnikova, T.A.; Rosenkranz, A.A.; Lupanova, T.N.; Khramtsov, Y.V.; Georgiev, G.P.; Sobolev, A.S. Targeted Delivery of ^{111}In into the Nuclei of EGFR Overexpressing Cells via Modular Nanotransporters with Anti-EGFR Affibody. *Front. Pharmacol.* **2020**, *11*, 176. [CrossRef] [PubMed]

229. Jia, D.; Wang, F.; Yang, Y.; Hu, P.; Song, H.; Lu, Y.; Wang, R.; Li, G.; Liu, R.; Li, J.; et al. Coupling EGFR-Antagonistic Affibody Enhanced Therapeutic Effects of Cisplatin Liposomes in EGFR-Expressing Tumor Models. *J. Pharm. Sci.* **2022**, *111*, 450–457. [CrossRef] [PubMed]

230. Gao, W.; Xia, X.; Yang, X.; Li, Q.; Xia, X.; Huang, W.; Yan, D. Amphiphilic Affibody-PROTAC Conjugate Self-Assembled Nanoagents for Targeted Cancer Therapy. *Chem. Eng. J.* **2024**, *495*, 153437. [CrossRef]

231. Jia, D.; Yang, Y.; Yuan, F.; Fan, Q.; Wang, F.; Huang, Y.; Song, H.; Hu, P.; Wang, R.; Li, G.; et al. Increasing the Antitumor Efficacy of Doxorubicin Liposomes with Coupling an Anti-EGFR Affibody in EGFR-Expressing Tumor Models. *Int. J. Pharm.* **2020**, *586*, 119541. [CrossRef]

232. Jun, H.; Jang, E.; Kim, H.; Yeo, M.; Park, S.G.; Lee, J.; Shin, K.J.; Chae, Y.C.; Kang, S.; Kim, E. TRAIL & EGFR Affibody Dual-Display on a Protein Nanoparticle Synergistically Suppresses Tumor Growth. *J. Control. Release* **2022**, *349*, 367–378. [CrossRef]

233. Robertson, D.L.; Joyce, G.F. Selection in Vitro of an RNA Enzyme That Specifically Cleaves Single-Stranded DNA. *Nature* **1990**, *344*, 467–468. [CrossRef]

234. Oliphant, A.R.; Brandl, C.J.; Struhl, K. Defining the Sequence Specificity of DNA-Binding Proteins by Selecting Binding Sites from Random-Sequence Oligonucleotides: Analysis of Yeast GCN4 Protein. *Mol. Cell. Biol.* **1989**, *9*, 2944–2949. [CrossRef] [PubMed]

235. Ellington, A.D.; Szostak, J.W. In Vitro Selection of RNA Molecules That Bind Specific Ligands. *Nature* **1990**, *346*, 818–822. [CrossRef] [PubMed]

236. Mahmoudian, F.; Ahmari, A.; Shabani, S.; Sadeghi, B.; Fahimirad, S.; Fattahi, F. Aptamers as an Approach to Targeted Cancer Therapy. *Cancer Cell Int.* **2024**, *24*, 108. [CrossRef] [PubMed]

237. Zhu, Q.; Liu, G.; Kai, M. DNA Aptamers in the Diagnosis and Treatment of Human Diseases. *Molecules* **2015**, *20*, 20979–20997. [CrossRef] [PubMed]

238. Orava, E.W.; Cicmil, N.; Gariépy, J. Delivering Cargoes into Cancer Cells Using DNA Aptamers Targeting Internalized Surface Portals. *Biochim. Biophys. Acta* **2010**, *1798*, 2190–2200. [CrossRef] [PubMed]

239. Shaw, J.P.; Kent, K.; Bird, J.; Fishback, J.; Froehler, B. Modified Deoxyoligonucleotides Stable to Exonuclease Degradation in Serum. *Nucleic Acids Res.* **1991**, *19*, 747–750. [CrossRef] [PubMed]

240. Fu, Z.; Xiang, J. Aptamer-Functionalized Nanoparticles in Targeted Delivery and Cancer Therapy. *Int. J. Mol. Sci.* **2020**, *21*, 9123. [CrossRef] [PubMed]

241. Sun, H.; Zhu, X.; Lu, P.Y.; Rosato, R.R.; Tan, W.; Zu, Y. Oligonucleotide Aptamers: New Tools for Targeted Cancer Therapy. *Mol. Ther.-Nucleic Acids* **2014**, *3*, e182. [CrossRef] [PubMed]

242. Rabiee, N.; Chen, S.; Ahmadi, S.; Veedu, R.N. Aptamer-Engineered (Nano)Materials for Theranostic Applications. *Theranostics* **2023**, *13*, 5183–5206. [CrossRef] [PubMed]

243. Shanaa, O.A.; Rumyantsev, A.; Sambuk, E.; Padkina, M. In Vivo Production of RNA Aptamers and Nanoparticles: Problems and Prospects. *Molecules* **2021**, *26*, 1422. [CrossRef] [PubMed]

244. Kratschmer, C.; Levy, M. Effect of Chemical Modifications on Aptamer Stability in Serum. *Nucleic Acid Ther.* **2017**, *27*, 335–344. [CrossRef] [PubMed]

245. Fallah, A.; Imani Fooladi, A.A.; Havaei, S.A.; Mahboobi, M.; Sedighian, H. Recent Advances in Aptamer Discovery, Modification and Improving Performance. *Biochem. Biophys. Rep.* **2024**, *40*, 101852. [CrossRef] [PubMed]

246. Chen, Z.; Luo, H.; Gubu, A.; Yu, S.; Zhang, H.; Dai, H.; Zhang, Y.; Zhang, B.; Ma, Y.; Lu, A.; et al. Chemically Modified Aptamers for Improving Binding Affinity to the Target Proteins via Enhanced Non-Covalent Bonding. *Front. Cell Dev. Biol.* **2023**, *11*, 1091809. [CrossRef] [PubMed]

247. Mehta, J.; Van Dorst, B.; Rouah-Martin, E.; Herrebout, W.; Scippo, M.-L.; Blust, R.; Robbens, J. In Vitro Selection and Characterization of DNA Aptamers Recognizing Chloramphenicol. *J. Biotechnol.* **2011**, *155*, 361–369. [CrossRef] [PubMed]

248. Li, N.; Nguyen, H.H.; Byrom, M.; Ellington, A.D. Inhibition of Cell Proliferation by an Anti-EGFR Aptamer. *PLoS ONE* **2011**, *6*, e20299. [CrossRef] [PubMed]

249. Tuerk, C.; Gold, L. Systematic Evolution of Ligands by Exponential Enrichment: RNA Ligands to Bacteriophage T4 DNA Polymerase. *Science* **1990**, *249*, 505–510. [CrossRef] [PubMed]

250. Blind, M.; Blank, M. Aptamer Selection Technology and Recent Advances. *Mol. Ther.-Nucleic Acids* **2015**, *4*, e223. [CrossRef] [PubMed]

251. Bayat, P.; Nosrati, R.; Alibolandi, M.; Rafatpanah, H.; Abnous, K.; Khedri, M.; Ramezani, M. SELEX Methods on the Road to Protein Targeting with Nucleic Acid Aptamers. *Biochimie* **2018**, *154*, 132–155. [CrossRef] [PubMed]

252. Sun, H.; Zu, Y. A Highlight of Recent Advances in Aptamer Technology and Its Application. *Molecules* **2015**, *20*, 11959–11980. [CrossRef]

253. Dass, C.R.; Saravolac, E.G.; Li, Y.; Sun, L.-Q. Cellular Uptake, Distribution, and Stability of 10-23 Deoxyribozymes. *Antisense Nucleic Acid Drug Dev.* **2002**, *12*, 289–299. [CrossRef] [PubMed]

254. Dougan, H.; Lyster, D.M.; Vo, C.V.; Stafford, A.; Weitz, J.I.; Hobbs, J.B. Extending the Lifetime of Anticoagulant Oligodeoxynucleotide Aptamers in Blood. *Nucl. Med. Biol.* **2000**, *27*, 289–297. [CrossRef]

255. Ibarra, L.E.; Camorani, S.; Agnello, L.; Pedone, E.; Pirone, L.; Chesta, C.A.; Palacios, R.E.; Fedele, M.; Cerchia, L. Selective Photo-Assisted Eradication of Triple-Negative Breast Cancer Cells through Aptamer Decoration of Doped Conjugated Polymer Nanoparticles. *Pharmaceutics* **2022**, *14*, 626. [CrossRef] [PubMed]

256. Agnello, L.; Tortorella, S.; d'Argenio, A.; Carbone, C.; Camorani, S.; Locatelli, E.; Auletta, L.; Sorrentino, D.; Fedele, M.; Zannetti, A.; et al. Optimizing Cisplatin Delivery to Triple-Negative Breast Cancer through Novel EGFR Aptamer-Conjugated Polymeric Nanovectors. *J. Exp. Clin. Cancer Res.* **2021**, *40*, 239. [CrossRef] [PubMed]

257. Darabi, F.; Saidijam, M.; Nouri, F.; Mahjub, R.; Soleimani, M. Anti-CD44 and EGFR Dual-Targeted Solid Lipid Nanoparticles for Delivery of Doxorubicin to Triple-Negative Breast Cancer Cell Line: Preparation, Statistical Optimization, and In Vitro Characterization. *BioMed Res. Int.* **2022**, *2022*, e6253978. [CrossRef] [PubMed]

258. Camorani, S.; Caliendo, A.; Morrone, E.; Agnello, L.; Martini, M.; Cantile, M.; Cerrone, M.; Zannetti, A.; La Deda, M.; Fedele, M.; et al. Bispecific Aptamer-Decorated and Light-Triggered Nanoparticles Targeting Tumor and Stromal Cells in Breast Cancer Derived Organoids: Implications for Precision Phototherapies. *J. Exp. Clin. Cancer Res.* **2024**, *43*, 92. [CrossRef]

259. Liu, Y.; Dai, X.; Jiang, S.; Qahar, M.; Feng, C.; Guo, D.; Wang, L.; Ma, S.; Huang, L. Targeted Co-Delivery of Gefitinib and Rapamycin by Aptamer-Modified Nanoparticles Overcomes EGFR-TKI Resistance in NSCLC via Promoting Autophagy. *Int. J. Mol. Sci.* **2022**, *23*, 8025. [CrossRef] [PubMed]

260. Zhang, Z.; Cheng, W.; Pan, Y.; Jia, L. An Anticancer Agent-Loaded PLGA Nanomedicine with Glutathione-Response and Targeted Delivery for the Treatment of Lung Cancer. *J. Mater. Chem. B* **2020**, *8*, 655–665. [CrossRef]

261. Yang, L.; Li, Z.; Binzel, D.W.; Guo, P.; Williams, T.M. Targeting Oncogenic KRAS in Non-Small Cell Lung Cancer with EGFR Aptamer-Conjugated Multifunctional RNA Nanoparticles. *Mol. Ther.-Nucleic Acids* **2023**, *33*, 559–571. [CrossRef] [PubMed]

262. Guo, S.; Vieweger, M.; Zhang, K.; Yin, H.; Wang, H.; Li, X.; Li, S.; Hu, S.; Sparreboom, A.; Evers, B.M.; et al. Ultra-Thermostable RNA Nanoparticles for Solubilizing and High-Yield Loading of Paclitaxel for Breast Cancer Therapy. *Nat. Commun.* **2020**, *11*, 972. [CrossRef]

263. Zhang, L.; Mu, C.; Zhang, T.; Yang, D.; Wang, C.; Chen, Q.; Tang, L.; Fan, L.; Liu, C.; Shen, J.; et al. Development of Targeted Therapy Therapeutics to Sensitize Triple-Negative Breast Cancer Chemosensitivity Utilizing Bacteriophage Phi29 Derived Packaging RNA. *J. Nanobiotechnol.* **2021**, *19*, 13. [CrossRef]

264. Xiao, D.; Huang, Y.; Huang, S.; Zhuang, J.; Chen, P.; Wang, Y.; Zhang, L. Targeted Delivery of Cancer Drug Paclitaxel to Chordomas Tumor Cells via an RNA Nanoparticle Harboring an EGFR Aptamer. *Colloids Surf. B Biointerfaces* **2022**, *212*, 112366. [CrossRef] [PubMed]

265. Li, J.; Wang, S.; Kang, W.; Li, N.; Guo, F.; Chang, H.; Wei, W. Multifunctional Gold Nanoparticle Based Selective Detection of Esophageal Squamous Cell Carcinoma Cells Using Resonance Rayleigh Scattering Assay. *Microchem. J.* **2021**, *163*, 105905. [CrossRef]

266. Peng, L.; Liang, Y.; Zhong, X.; Liang, Z.; Tian, Y.; Li, S.; Liang, J.; Wang, R.; Zhong, Y.; Shi, Y.; et al. Aptamer-Conjugated Gold Nanoparticles Targeting Epidermal Growth Factor Receptor Variant III for the Treatment of Glioblastoma. *Int. J. Nanomed.* **2020**, *15*, 1363. [CrossRef]

267. Nakajima, N.; Ikada, Y. Mechanism of Amide Formation by Carbodiimide for Bioconjugation in Aqueous Media. *Bioconjug. Chem.* **1995**, *6*, 123–130. [CrossRef] [PubMed]

268. Karakoti, A.S.; Shukla, R.; Shanker, R.; Singh, S. Surface Functionalization of Quantum Dots for Biological Applications. *Adv. Colloid Interface Sci.* **2015**, *215*, 28–45. [CrossRef]

269. Nifontova, G.; Kalenichenko, D.; Kriukova, I.; Terryn, C.; Audonnet, S.; Karaulov, A.; Nabiev, I.; Sukhanova, A. Impact of Macrophages on the Interaction of Cetuximab-Functionalized Polyelectrolyte Capsules with EGFR-Expressing Cancer Cells. *ACS Appl. Mater. Interfaces* **2023**, *15*, 52137–52149. [CrossRef] [PubMed]

270. Lu, J.; Zhang, A.; Zhang, F.; Linhardt, R.J.; Zhu, Z.; Yang, Y.; Zhang, T.; Lin, Z.; Zhang, S.; Zhao, H.; et al. Ganoderenic Acid D-Loaded Functionalized Graphene Oxide-Based Carrier for Active Targeting Therapy of Cervical Carcinoma. *Biomed. Pharmacother.* **2023**, *164*, 114947. [CrossRef] [PubMed]

271. Lu, L.; Duong, V.T.; Shalash, A.O.; Skwarczynski, M.; Toth, I. Chemical Conjugation Strategies for the Development of Protein-Based Subunit Nanovaccines. *Vaccines* **2021**, *9*, 563. [CrossRef] [PubMed]

272. Nobs, L.; Buchegger, F.; Gurny, R.; Allémann, E. Current Methods for Attaching Targeting Ligands to Liposomes and Nanoparticles. *J. Pharm. Sci.* **2004**, *93*, 1980–1992. [CrossRef] [PubMed]

273. Friedman, A.D.; Claypool, S.E.; Liu, R. The Smart Targeting of Nanoparticles. *Curr. Pharm. Des.* **2013**, *19*, 6315–6329. [CrossRef] [PubMed]

274. Abraham, R.; Moller, D.; Gabel, D.; Senter, P.; Hellström, I.; Hellström, K.E. The Influence of Periodate Oxidation on Monoclonal Antibody Avidity and Immunoreactivity. *J. Immunol. Methods* **1991**, *144*, 77–86. [CrossRef]

275. Kawelah, M.R.; Han, S.; Atila Dincer, C.; Jeon, J.; Brisola, J.; Hussain, A.F.; Jeevarathinam, A.S.; Bouchard, R.; Marras, A.E.; Truskett, T.M.; et al. Antibody-Conjugated Polymersomes with Encapsulated Indocyanine Green J-Aggregates and High Near-Infrared Absorption for Molecular Photoacoustic Cancer Imaging. *ACS Appl. Mater. Interfaces* **2024**, *16*, 5598–5612. [CrossRef]

276. Lu, J.; Yu, C.; Du, K.; Chen, S.; Huang, S. Targeted Delivery of Cisplatin Magnetic Nanoparticles for Diagnosis and Treatment of Nasopharyngeal Carcinoma. *Colloids Surf. B Biointerfaces* **2025**, *245*, 114252. [CrossRef]

277. Zhou, S.; Hu, J.; Chen, X.; Duan, H.; Shao, Y.; Lin, T.; Li, X.; Huang, X.; Xiong, Y. Hydrazide-Assisted Directional Antibody Conjugation of Gold Nanoparticles to Enhance Immunochromatographic Assay. *Anal. Chim. Acta* **2021**, *1168*, 338623. [CrossRef] [PubMed]

278. Agarwal, P.; Bertozzi, C.R. Site-Specific Antibody-Drug Conjugates: The Nexus of Bioorthogonal Chemistry, Protein Engineering, and Drug Development. *Bioconjug. Chem.* **2015**, *26*, 176–192. [CrossRef] [PubMed]

279. Singh, R.; Kats, L.; Blättler, W.A.; Lambert, J.M. Formation of N-Substituted 2-Iminothiolanes When Amino Groups in Proteins and Peptides Are Modified by 2-Iminothiolane. *Anal. Biochem.* **1996**, *236*, 114–125. [CrossRef] [PubMed]

280. Juan, A.; Cimas, F.J.; Bravo, I.; Pandiella, A.; Ocaña, A.; Alonso-Moreno, C. An Overview of Antibody Conjugated Polymeric Nanoparticles for Breast Cancer Therapy. *Pharmaceutics* **2020**, *12*, 802. [CrossRef] [PubMed]

281. Saito, G.; Swanson, J.A.; Lee, K.-D. Drug Delivery Strategy Utilizing Conjugation via Reversible Disulfide Linkages: Role and Site of Cellular Reducing Activities. *Adv. Drug Deliv. Rev.* **2003**, *55*, 199–215. [CrossRef] [PubMed]

282. Mustafaoglu, N.; Kiziltepe, T.; Bilgicer, B. Site-Specific Conjugation of an Antibody on a Gold Nanoparticle Surface for One-Step Diagnosis of Prostate Specific Antigen with Dynamic Light Scattering. *Nanoscale* **2017**, *9*, 8684–8694. [CrossRef] [PubMed]

283. Geddie, M.L.; Kirpotin, D.B.; Kohli, N.; Kornaga, T.; Boll, B.; Razlog, M.; Drummond, D.C.; Lugovskoy, A.A. Development of Disulfide-Stabilized Fabs for Targeting of Antibody-Directed Nanotherapeutics. *mAbs* **2022**, *14*, 2083466. [CrossRef] [PubMed]

284. Daniel, M.-C.; Astruc, D. Gold Nanoparticles: Assembly, Supramolecular Chemistry, Quantum-Size-Related Properties, and Applications toward Biology, Catalysis, and Nanotechnology. *Chem. Rev.* **2004**, *104*, 293–346. [CrossRef] [PubMed]

285. Vilímová, I.; Hervé-Aubert, K.; Chourpa, I. Formation of miRNA Nanoprobes—Conjugation Approaches Leading to the Functionalization. *Molecules* **2022**, *27*, 8428. [CrossRef] [PubMed]

286. Queiroz, S.M.; Veriato, T.S.; Raniero, L.; Castilho, M.L. Gold Nanoparticles Conjugated with Epidermal Growth Factor and Gadolinium for Precision Delivery of Contrast Agents in Magnetic Resonance Imaging. *Radiol. Phys. Technol.* **2024**, *17*, 153–164. [CrossRef] [PubMed]

287. Andrade, L.M.; Martins, E.M.N.; Versiani, A.F.; Reis, D.S.; da Fonseca, F.G.; Souza, I.P.d.; Paniago, R.M.; Pereira-Maia, E.; Ladeira, L.O. The Physicochemical and Biological Characterization of a 24-Month-Stored Nanocomplex Based on Gold Nanoparticles Conjugated with Cetuximab Demonstrated Long-Term Stability, EGFR Affinity and Cancer Cell Death Due to Apoptosis. *Mater. Sci. Eng. C* **2020**, *107*, 110203. [CrossRef] [PubMed]

288. Kolb, H.C.; Finn, M.G.; Sharpless, K.B. Click Chemistry: Diverse Chemical Function from a Few Good Reactions. *Angew. Chem. Int. Ed.* **2001**, *40*, 2004–2021. [CrossRef]

289. Wang, Q.; Chan, T.R.; Hilgraf, R.; Fokin, V.V.; Sharpless, K.B.; Finn, M.G. Bioconjugation by Copper(I)-Catalyzed Azide-Alkyne [3 + 2] Cycloaddition. *J. Am. Chem. Soc.* **2003**, *125*, 3192–3193. [CrossRef]

290. Meldal, M.; Tornøe, C.W. Cu-Catalyzed Azide–Alkyne Cycloaddition. *Chem. Rev.* **2008**, *108*, 2952–3015. [CrossRef] [PubMed]

291. Jewett, J.C.; Bertozzi, C.R. Cu-Free Click Cycloaddition Reactions in Chemical Biology. *Chem. Soc. Rev.* **2010**, *39*, 1272–1279. [CrossRef] [PubMed]

292. Yi, G.; Son, J.; Yoo, J.; Park, C.; Koo, H. Application of Click Chemistry in Nanoparticle Modification and Its Targeted Delivery. *Biomater. Res.* **2018**, *22*, 13. [CrossRef] [PubMed]

293. Devaraj, N.K.; Weissleder, R. Biomedical Applications of Tetrazine Cycloadditions. *Acc. Chem. Res.* **2011**, *44*, 816–827. [CrossRef] [PubMed]

294. Gai, M.; Simon, J.; Lieberwirth, I.; Mailänder, V.; Morsbach, S.; Landfester, K. A Bio-Orthogonal Functionalization Strategy for Site-Specific Coupling of Antibodies on Vesicle Surfaces after Self-Assembly. *Polym. Chem.* **2020**, *11*, 527–540. [CrossRef]

295. Zhang, X.; Ou, C.; Liu, H.; Wang, L.-X. Synthesis and Evaluation of Three Azide-Modified Disaccharide Oxazolines as Enzyme Substrates for Single-Step Fc Glycan-Mediated Antibody-Drug Conjugation. *Bioconjug. Chem.* **2022**, *33*, 1179–1191. [CrossRef]

296. Jeong, S.; Park, J.Y.; Cha, M.G.; Chang, H.; Kim, Y.; Kim, H.-M.; Jun, B.-H.; Lee, D.S.; Lee, Y.-S.; Jeong, J.M.; et al. Highly Robust and Optimized Conjugation of Antibodies to Nanoparticles Using Quantitatively Validated Protocols. *Nanoscale* **2017**, *9*, 2548–2555. [CrossRef] [PubMed]

297. Thorek, D.L.J.; Elias, D.R.; Tsourkas, A. Comparative Analysis of Nanoparticle-Antibody Conjugations: Carbodiimide versus Click Chemistry. *Mol. Imaging* **2009**, *8*, 221–229. [CrossRef] [PubMed]

298. Tieu, T.; Wojnilowicz, M.; Huda, P.; Thurecht, K.J.; Thissen, H.; Voelcker, N.H.; Cifuentes-Rius, A. Nanobody-Displaying Porous Silicon Nanoparticles for the Co-Delivery of siRNA and Doxorubicin. *Biomater. Sci.* **2021**, *9*, 133–147. [CrossRef] [PubMed]

299. Van Zundert, I.; Bravo, M.; Deschaume, O.; Cybulski, P.; Bartic, C.; Hofkens, J.; Uji-i, H.; Fortuni, B.; Rocha, S. Versatile and Robust Method for Antibody Conjugation to Nanoparticles with High Targeting Efficiency. *Pharmaceutics* **2021**, *13*, 2153. [CrossRef] [PubMed]

300. Tran, T.T.T.; Phung, C.D.; Yeo, B.Z.J.; Prajogo, R.C.; Jayasinghe, M.K.; Yuan, J.; Tan, D.S.W.; Yeo, E.Y.M.; Goh, B.C.; Tam, W.L.; et al. Customised Design of Antisense Oligonucleotides Targeting EGFR Driver Mutants for Personalised Treatment of Non-Small Cell Lung Cancer. *eBioMedicine* **2024**, *108*, 105356. [CrossRef] [PubMed]

301. Weller, S.; Li, X.; Petersen, L.R.; Kempen, P.; Clergeaud, G.; Andresen, T.L. Influence of Different Conjugation Methods for Activating Antibodies on Polymeric Nanoparticles: Effects for Polyclonal Expansion of Human CD8+ T Cells. *Int. Immunopharmacol.* **2024**, *129*, 111643. [CrossRef] [PubMed]

302. Jain, A.; Cheng, K. The Principles and Applications of Avidin-Based Nanoparticles in Drug Delivery and Diagnosis. *J. Control. Release Off. J. Control. Release Soc.* **2017**, *245*, 27–40. [CrossRef] [PubMed]

303. Diamandis, E.P.; Christopoulos, T.K. The Biotin-(Strept)Avidin System: Principles and Applications in Biotechnology. *Clin. Chem.* **1991**, *37*, 625–636. [CrossRef] [PubMed]

304. González, M.; Argaraña, C.E.; Fidelio, G.D. Extremely High Thermal Stability of Streptavidin and Avidin upon Biotin Binding. *Biomol. Eng.* **1999**, *16*, 67–72. [CrossRef]

305. Tausig, F.; Wolf, F.J. Streptavidin—A Substance with Avidin-like Properties Produced by Microorganisms. *Biochem. Biophys. Res. Commun.* **1964**, *14*, 205–209. [CrossRef] [PubMed]

306. De Cuyper, M.; Hodenius, M.; Lacava, Z.G.M.; Azevedo, R.B.; da Silva, M.d.F.; Morais, P.C.; Santana, M.H.A. Attachment of Water-Soluble Proteins to the Surface of (Magnetizable) Phospholipid Colloids via NeutrAvidin-Derivatized Phospholipids. *J. Colloid Interface Sci.* **2002**, *245*, 274–280. [CrossRef] [PubMed]

307. Vermette, P.; Gengenbach, T.; Divisekera, U.; Kambouris, P.A.; Griesser, H.J.; Meagher, L. Immobilization and Surface Characterization of NeutrAvidin Biotin-Binding Protein on Different Hydrogel Interlayers. *J. Colloid Interface Sci.* **2003**, *259*, 13–26. [CrossRef] [PubMed]

308. Egnuni, T.; Ingram, N.; Mirza, I.; Coletta, P.L.; McLaughlan, J.R. Evaluation of the Targeting and Therapeutic Efficiency of Anti-EGFR Functionalised Nanoparticles in Head and Neck Cancer Cells for Use in NIR-II Optical Window. *Pharmaceutics* **2021**, *13*, 1651. [CrossRef] [PubMed]

309. Nelemans, L.C.; Choukrani, G.; Ustyanovska-Avtenyuk, N.; Wiersma, V.R.; Dähne, L.; Bremer, E. Design of Vaterite Nanoparticles for Controlled Delivery of Active Immunotherapeutic Proteins. *Part. Part. Syst. Charact.* **2024**, *41*, 2300153. [CrossRef]

310. Peng, B.; Nguyen, T.M.; Jayasinghe, M.K.; Gao, C.; Pham, T.T.; Vu, L.T.; Yeo, E.Y.M.; Yap, G.; Wang, L.; Goh, B.C.; et al. Robust Delivery of RIG-I Agonists Using Extracellular Vesicles for Anti-Cancer Immunotherapy. *J. Extracell. Vesicles* **2022**, *11*, e12187. [CrossRef] [PubMed]

311. Bian, T.; Gardin, A.; Gemen, J.; Houben, L.; Perego, C.; Lee, B.; Elad, N.; Chu, Z.; Pavan, G.M.; Klajn, R. Electrostatic Co-Assembly of Nanoparticles with Oppositely Charged Small Molecules into Static and Dynamic Superstructures. *Nat. Chem.* **2021**, *13*, 940–949. [CrossRef] [PubMed]

312. Götting, N.; Fritz, H.; Maier, M.; von Stamm, J.; Schoofs, T.; Bayer, E. Effects of Oligonucleotide Adsorption on the Physicochemical Characteristics of a Nanoparticle-Based Model Delivery System for Antisense Drugs. *Colloid Polym. Sci.* **1999**, *277*, 145–152. [CrossRef]

313. Gessner, A.; Lieske, A.; Paulke, B.-R.; Müller, R.H. Functional Groups on Polystyrene Model Nanoparticles: Influence on Protein Adsorption. *J. Biomed. Mater. Res. A* **2003**, *65A*, 319–326. [CrossRef] [PubMed]

314. Gessner, A.; Lieske, A.; Paulke, B.R.; Müller, R.H. Influence of Surface Charge Density on Protein Adsorption on Polymeric Nanoparticles: Analysis by Two-Dimensional Electrophoresis. *Eur. J. Pharm. Biopharm.* **2002**, *54*, 165–170. [CrossRef] [PubMed]

315. Cho, J.; Caruso, F. Investigation of the Interactions between Ligand-Stabilized Gold Nanoparticles and Polyelectrolyte Multilayer Films. *Chem. Mater.* **2005**, *17*, 4547–4553. [CrossRef]

316. Huang, B.; Abraham, W.D.; Zheng, Y.; Bustamante López, S.C.; Luo, S.S.; Irvine, D.J. Active Targeting of Chemotherapy to Disseminated Tumors Using Nanoparticle-Carrying T Cells. *Sci. Transl. Med.* **2015**, *7*, 291ra94. [CrossRef] [PubMed]

317. Cavalcante, M.F.; Kazuma, S.M.; Bender, E.A.; Adorne, M.D.; Ullian, M.; Veras, M.M.; Saldiva, P.H.N.; Maranhão, A.Q.; Guterres, S.S.; Pohlmann, A.R.; et al. A Nanoformulation Containing a scFv Reactive to Electronegative LDL Inhibits Atherosclerosis in LDL Receptor Knockout Mice. *Eur. J. Pharm. Biopharm.* **2016**, *107*, 120–129. [CrossRef] [PubMed]

318. Antonow, M.B.; Franco, C.; Prado, W.; Beckenkamp, A.; Silveira, G.P.; Buffon, A.; Guterres, S.S.; Pohlmann, A.R. Arginylglycy-laspartic Acid-Surface-Functionalized Doxorubicin-Loaded Lipid-Core Nanocapsules as a Strategy to Target Alpha(V) Beta(3) Integrin Expressed on Tumor Cells. *Nanomaterials* **2018**, *8*, 2. [CrossRef] [PubMed]

319. Zhao, N.; Ding, B.; Zhang, Y.; Klockow, J.L.; Lau, K.; Chin, F.T.; Cheng, Z.; Liu, H. Reactive Oxygen Species and Enzyme Dual-Responsive Biocompatible Drug Delivery System for Targeted Tumor Therapy. *J. Control. Release* **2020**, *324*, 330–340. [CrossRef] [PubMed]

320. Djermane, R.; Nieto, C.; Vega, M.A.; del Valle, E.M.M. EGFR-Targeting Polydopamine Nanoparticles Co-Loaded with 5-Fluorouracil, Irinotecan, and Leucovorin to Potentially Enhance Metastatic Colorectal Cancer Therapy. *Sci. Rep.* **2024**, *14*, 29265. [CrossRef]

321. Liu, M.; Sun, C.; Jiang, J.; Wan, L.; Hu, C.; Wen, C.; Huang, G.; Ruan, Q.; Wu, S.; Qiao, D.; et al. Aptamer-Functionalized ZIF-8 Nanomedicine for Targeted Delivery of Gefitinib and siRNA to Treat Tyrosine-Kinase-Inhibitor-Resistant Nonsmall-Cell Lung Cancer. *ACS Appl. Nano Mater.* **2023**, *6*, 21587–21602. [CrossRef]

322. Anaki, A.; Tzror-Azankot, C.; Motiei, M.; Sadan, T.; Popovtzer, R. Impact of Synthesis Methods on the Functionality of Antibody-Conjugated Gold Nanoparticles for Targeted Therapy. *Nanoscale Adv.* **2024**, *6*, 5420–5429. [CrossRef] [PubMed]

323. Hirata, Y.; Tashima, R.; Mitsuhashi, N.; Yoneda, S.; Ozono, M.; Fukuta, T.; Majima, E.; Kogure, K. A Simple, Fast, and Orientation-Controllable Technology for Preparing Antibody-Modified Liposomes. *Int. J. Pharm.* **2021**, *607*, 120966. [CrossRef] [PubMed]

324. Kedmi, R.; Veiga, N.; Ramishetti, S.; Goldsmith, M.; Rosenblum, D.; Dammes, N.; Hazan-Halevy, I.; Nahary, L.; Leviatan-Ben-Arye, S.; Harlev, M.; et al. A Modular Platform for Targeted RNAi Therapeutics. *Nat. Nanotechnol.* **2018**, *13*, 214–219. [CrossRef] [PubMed]

325. Kampel, L.; Goldsmith, M.; Ramishetti, S.; Veiga, N.; Rosenblum, D.; Gutkin, A.; Chatterjee, S.; Penn, M.; Lerman, G.; Peer, D.; et al. Therapeutic Inhibitory RNA in Head and Neck Cancer via Functional Targeted Lipid Nanoparticles. *J. Control. Release* **2021**, *337*, 378–389. [CrossRef] [PubMed]

326. Karami, M.H.; Abdouss, M. Assessing Particle Size and Surface Charge in Drug Carrier Nanoparticles for Enhanced Cancer Treatment: A Comprehensive Review Utilizing DLS and Zeta Potential Characterization. *Polym. Sci. Peer Rev. J.* **2024**, *5*, 000615.

327. Munhoz, A.H.; de Paiva, H.; de Miranda, L.F.; de Oliveira, E.C.; Andrades, R.C.; Neto, A.C. Synthesis and Characterization of Pseudoboehmite and Gamma-Alumina. *Mater. Sci. Forum* **2015**, *820*, 131–136. [CrossRef]

328. Shukla, V.N.; Vikas; Mehata, A.K.; Setia, A.; Kumari, P.; Mahto, S.K.; Muthu, M.S.; Mishra, S.K. EGFR Targeted Albumin Nanoparticles of Oleanolic Acid: In Silico Screening of Nanocarrier, Cytotoxicity and Pharmacokinetics for Lung Cancer Therapy. *Int. J. Biol. Macromol.* **2023**, *246*, 125719. [CrossRef] [PubMed]

329. Shivanna, A.T.; Dash, B.S.; Lu, Y.-J.; Lin, W.-T.; Chen, J.-P. Magnetic Lipid-Poly(Lactic-Co-Glycolic Acid) Nanoparticles Conjugated with Epidermal Growth Factor Receptor Antibody for Dual-Targeted Delivery of CPT-11. *Int. J. Pharm.* **2024**, *667*, 124856. [CrossRef]

330. Li, X.; Zhang, L.; Guo, X.; Xie, F.; Shen, C.; Jun, Y.; Luo, C.; Liu, L.; Yu, X.; Zhang, Z.; et al. Self-Assembled RNA Nanocarrier-Mediated Chemotherapy Combined with Molecular Targeting in the Treatment of Esophageal Squamous Cell Carcinoma. *J. Nanobiotechnol.* **2021**, *19*, 388. [CrossRef]

331. Carolina Cruz de Sousa, A.; da Silva Santos, E.; da Silva Moreira, T.; Gabriela Araújo Mendes, M.; Rodrigues Arruda, B.; de Jesus Guimarães, C.; de Brito Vieira Neto, J.; Santiago de Oliveira, Y.; Pedro Ayala, A.; Rodrigues da Costa, M.D.; et al. Anti-EGFR Immunoliposomes for Cabazitaxel Delivery: From Formulation Development to in Vivo Evaluation in Prostate Cancer Xenograft Model. *Int. J. Pharm.* **2024**, *661*, 124439. [CrossRef] [PubMed]

332. Ruiz, A.L.; Arribas, E.V.; McEnnis, K. Poly(Lactic-Co-Glycolic Acid) Encapsulated Platinum Nanoparticles for Cancer Treatment. *Mater. Adv.* **2022**, *3*, 2858–2870. [CrossRef]

333. Eivazi, N.; Rahmani, R.; Paknejad, M. Specific Cellular Internalization and pH-Responsive Behavior of Doxorubicin Loaded PLGA-PEG Nanoparticles Targeted with Anti EGFRvIII Antibody. *Life Sci.* **2020**, *261*, 118361. [CrossRef] [PubMed]

334. Kielkopf, C.L.; Bauer, W.; Urbatsch, I.L. Sodium Dodecyl Sulfate-Polyacrylamide Gel Electrophoresis of Proteins. *Cold Spring Harb. Protoc.* **2021**, *12*, 494–504. [CrossRef] [PubMed]

335. Nowakowski, A.B.; Wobig, W.J.; Petering, D.H. Native SDS-PAGE: High Resolution Electrophoretic Separation of Proteins with Retention of Native Properties Including Bound Metal Ions. *Met. Integr. Biometal Sci.* **2014**, *6*, 1068. [CrossRef] [PubMed]

336. Lee, P.Y.; Costumbrado, J.; Hsu, C.-Y.; Kim, Y.H. Agarose Gel Electrophoresis for the Separation of DNA Fragments. *J. Vis. Exp. JoVE* **2012**, *62*, 3923. [CrossRef]

337. Saravanakumar, K.; Sathiyaseelan, A.; Mariadoss, A.V.A.; Jeevithan, E.; Hu, X.; Shin, S.; Wang, M.-H. Dual Stimuli-Responsive Release of Aptamer AS1411 Decorated Erlotinib Loaded Chitosan Nanoparticles for Non-Small-Cell Lung Carcinoma Therapy. *Carbohydr. Polym.* **2020**, *245*, 116407. [CrossRef] [PubMed]

338. Liu, Y.; Liu, R.; Dong, J.; Xia, X.; Yang, H.; Wei, S.; Fan, L.; Fang, M.; Zou, Y.; Zheng, M.; et al. Targeted Protein Degradation via Cellular Trafficking of Nanoparticles. *Nat. Nanotechnol.* **2024**, 1–7. [CrossRef] [PubMed]

339. Tanzadehpanah, H.; Mahaki, H.; Manoochehri, H.; Soleimani, M.; Najafi, R. AS1411 Aptamer Improves Therapeutic Efficacy of PEGylated Nanoliposomes Loaded with Gefitinib in the Mice Bearing CT26 Colon Carcinoma. *J. Nanopart. Res.* **2022**, *24*, 252. [CrossRef]

340. Bradford, M.M. A Rapid and Sensitive Method for the Quantitation of Microgram Quantities of Protein Utilizing the Principle of Protein-Dye Binding. *Anal. Biochem.* **1976**, *72*, 248–254. [CrossRef] [PubMed]

341. Smith, P.K.; Krohn, R.I.; Hermanson, G.T.; Mallia, A.K.; Gartner, F.H.; Provenzano, M.D.; Fujimoto, E.K.; Goeke, N.M.; Olson, B.J.; Klenk, D.C. Measurement of Protein Using Bicinchoninic Acid. *Anal. Biochem.* **1985**, *150*, 76–85. [CrossRef] [PubMed]

342. Menzel, C.; Bernkop-Schnürch, A. Enzyme Decorated Drug Carriers: Targeted Swords to Cleave and Overcome the Mucus Barrier. *Adv. Drug Deliv. Rev.* **2018**, *124*, 164–174. [CrossRef] [PubMed]

343. Cortés-Ríos, J.; Zárate, A.M.; Figueroa, J.D.; Medina, J.; Fuentes-Lemus, E.; Rodríguez-Fernández, M.; Aliaga, M.; López-Alarcón, C. Protein Quantification by Bicinchoninic Acid (BCA) Assay Follows Complex Kinetics and Can Be Performed at Short Incubation Times. *Anal. Biochem.* **2020**, *608*, 113904. [CrossRef]

344. Jha, A.; Goswami, P.; Kumar, M.; Bharti, K.; Manjit, M.; Satpute, A.P.; Gupta, A.; Moorkoth, S.; Koch, B.; Mishra, B. Cetuximab Functionalized Chitosan/Hyaluronic Acid-Based Nanoparticles Loaded with Cabazitaxel Enhances Anti-Tumor Efficacy in DMBA-Induced Breast Cancer Model in Rats through Spatial Targeting. *Chem. Phys. Impact* **2024**, *9*, 100750. [CrossRef]

345. Kumar, K.; Rawat, S.G.; Manjit; Mishra, M.; Rani, V.; Jadhav, A.P.; Priya; Kumar, A.; Chawla, R. Dual targeting pH responsive chitosan nanoparticles for enhanced active cellular internalization of gemcitabine in non-small cell lung cancer. *Int. J. Biol. Macromol.* **2023**; *249*, 126057. [CrossRef]

346. Bagheri, P.; Eremina, O.E.; Fernando, A.; Kamal, M.; Stegis, I.; Vazquez, C.; Shishido, S.N.; Kuhn, P.; Zavaleta, C. A Systematic Approach toward Enabling Maximal Targeting Efficiency of Cell Surface Proteins with Actively Targeted SERS Nanoparticles. *ACS Appl. Mater. Interfaces* **2024**, *16*, 15847–15860. [CrossRef] [PubMed]

347. Yang, Y.; Wang, F.; Li, Y.; Chen, R.; Wang, X.; Chen, J.; Lin, X.; Zhang, H.; Huang, Y.; Wang, R. Engineered Extracellular Vesicles with Polypeptide for Targeted Delivery of Doxorubicin against EGFR-positive Tumors. *Oncol. Rep.* **2024**, *52*, 154. [CrossRef] [PubMed]

348. Selvan, G.A.; Rachel, S.; Gajendran, T. Chapter 13—Several Assorted Characterization Methods of Nanoparticles. In *Nanomaterials*; Kumar, R.P., Bharathiraja, B., Eds.; Academic Press: Cambridge, MA, USA, 2021; pp. 301–308, ISBN 978-0-12-822401-4.

349. Abraham, J.; Jose, B.; Jose, A.; Thomas, S. Chapter 2—Characterization of Green Nanoparticles from Plants. In *Phytonanotechnology*; Thajuddin, N., Mathew, S., Eds.; Micro and Nano Technologies; Elsevier: Amsterdam, The Netherlands, 2020; pp. 21–39, ISBN 978-0-12-822348-2.

350. Zhang, Z.; Meng, X.; Cui, W.; Ahmad, S.S.; Kamal, M.A.; Zhang, J. NMR: From Molecular Mechanism to Its Application in Medical Care. *Med. Chem. Shariqah United Arab Emir.* **2020**, *16*, 1089–1098. [CrossRef]

351. López-Cebral, R.; Martín-Pastor, M.; Seijo, B.; Sanchez, A. Progress in the Characterization of Bio-Functionalized Nanoparticles Using NMR Methods and Their Applications as MRI Contrast Agents. *Prog. Nucl. Magn. Reson. Spectrosc.* **2014**, *79*, 1–13. [CrossRef]

352. Stevie, F.A.; Donley, C.L. Introduction to X-Ray Photoelectron Spectroscopy. *J. Vac. Sci. Technol. A* **2020**, *38*, 063204. [CrossRef]

353. Baer, D.R. Guide to Making XPS Measurements on Nanoparticles. *J. Vac. Sci. Technol. A* **2020**, *38*, 031201. [CrossRef]

354. Vikas; Viswanadh, M.K.; Mehata, A.K.; Sharma, V.; Priya, V.; Varshney, N.; Mahto, S.K.; Muthu, M.S. Bioadhesive Chitosan Nanoparticles: Dual Targeting and Pharmacokinetic Aspects for Advanced Lung Cancer Treatment. *Carbohydr. Polym.* **2021**, *274*, 118617. [CrossRef]

355. Dongargaonkar, A.A.; Clogston, J.D. Quantitation of Surface Coating on Nanoparticles Using Thermogravimetric Analysis. In *Characterization of Nanoparticles Intended for Drug Delivery*; McNeil, S.E., Ed.; Springer: New York, NY, USA, 2018; pp. 57–63, ISBN 978-1-4939-7352-1.

356. Mansfield, E.; Tyner, K.M.; Poling, C.M.; Blacklock, J.L. Determination of Nanoparticle Surface Coatings and Nanoparticle Purity Using Microscale Thermogravimetric Analysis. *Anal. Chem.* **2014**, *86*, 1478–1484. [CrossRef] [PubMed]

357. Wang, J.T.-W.; Spinato, C.; Klippstein, R.; Costa, P.M.; Martincic, M.; Pach, E.; Ruiz de Garibay, A.P.; Ménard-Moyon, C.; Feldman, R.; Michel, Y.; et al. Neutron-Irradiated Antibody-Functionalised Carbon Nanocapsules for Targeted Cancer Radiotherapy. *Carbon* **2020**, *162*, 410–422. [CrossRef]

358. Johnson, K.K.; Koshy, P.; Kopecky, C.; Devadason, M.; Biazik, J.; Zheng, X.; Jiang, Y.; Wang, X.; Liu, Y.; Holst, J.; et al. ROS-Mediated Anticancer Effects of EGFR-Targeted Nanoceria. *J. Biomed. Mater. Res. A* **2024**, *112*, 754–769. [CrossRef] [PubMed]